Neocarzilin A is a potent inhibitor of cancer cell motility targeting VAT-1 controlled pathways

Carolin M.-L. Gleissner[†‡], Carolin L. Pyka[§‡], Wolfgang Heydenreuter[†‡], Thomas F. Gronauer[†], Carina Atzberger[§], Vadim S. Korotkov[†], Weiting Cheng[§], Stephan M. Hacker[⊥], Angelika M. Vollmar[§], Simone Braig[§*] and Stephan A. Sieber[†*]

[†] Center for Integrated Protein Science at the Department of Chemistry, Technische Universität München, Lichtenbergstrasse 4, Garching, D-85747, Germany.

[§] Department of Pharmacy, Pharmaceutical Biology, Ludwig-Maximilians-University of Munich (LMU), Butenandtstrasse 5-13, Munich, D-81377, Germany.

[⊥]Department of Chemistry, Technische Universität München, Lichtenbergstrasse 4, Garching, D-85747, Germany

[‡] These authors contributed equally to this work.

-Supporting Information -

Table of contents

1. Supplementary Figures S1-S7

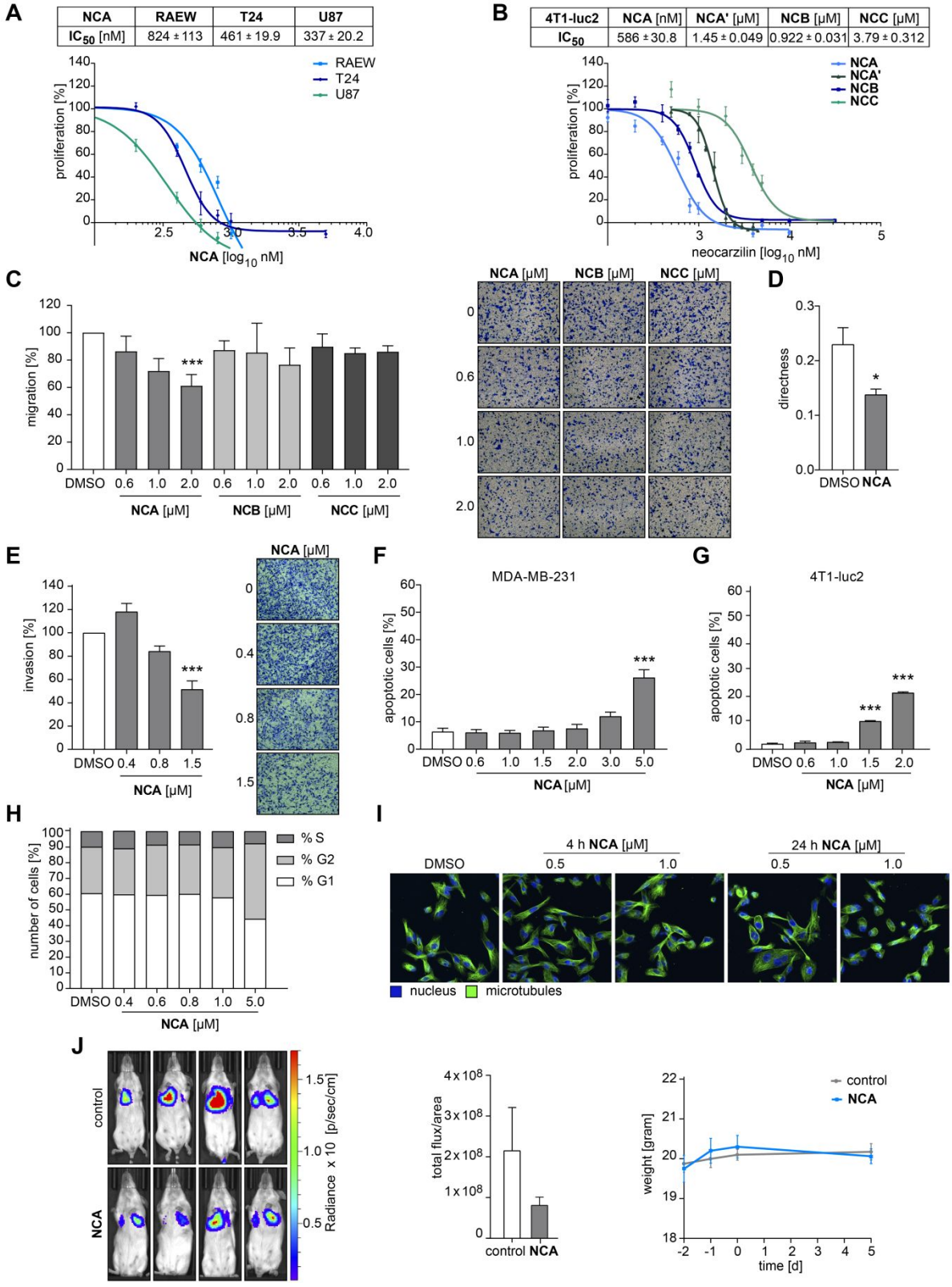

Figure S1: Anti-cancer effects of neocarzilins. A, The anti-proliferative effect of **NCA** on T24 human bladder carcinoma cells and the glioblastoma cell lines RAEW and U87 was determined by crystal violet staining after 72 h. **B**, Proliferative capacity of 4T1-luc2 murine breast carcinoma cells treated with **NCA**, **NCA'**; **NCB** and **NCC** was determined by crystal violet staining after 72 h. **C**, Transwell migration of 4T1-luc2 cells treated with **NCA**, **NCB** or

NCC determined by Boyden Chamber assay. **A-C**, Bars always represent the mean ± SEM of at least three independent experiments performed in duplicates/triplicates, one-way ANOVA, Dunnett's test, ***P < 0.001 compared with DMSO control (**C**). **D**, Effect of **NCA** on the directness of migrating MDA-MB-231 cells determined via chemotaxis assay. 30 cells per condition were monitored over 20 hours. Bars represent the mean ±SEM of 4 independent experiments, two-tailed unpaired Student's *t* test, *P < 0.033. **E**, The effect of **NCA** on the invasiveness of MDA-MB-231 cells was determined via Boyden Chamber assay using Matrigel-coated membrane inserts. The bar diagram shows the number of invasive cells normalized to the control. **F-G**, MDA-MB-231 (**F**) or 4T1-luc2 cells (**G**) were treated with indicated concentrations of **NCA**. Cells were permeabilized and stained with propidiumiodide using the method described by Nicoletti *et al*.[1]. The percentage of dying cells was determined by flow cytometry. **E-G**, Bars always represent the mean ± SEM of at least three independent experiments performed in duplicates/triplicates, one-way ANOVA, Dunnett's test, ***P < 0.001 compared with DMSO control. **H**, The effect of **NCA** on the cell cycle progression of MDA-MB-231 cells was determined by propidiumiodide staining using the method described by Nicoletti *et al*.[1].The cell cycle analysis was performed with the FlowJo 7.4 program using the Watson pragmatic model. **I**, MDA-MB-231 cells were seeded in eight-well microscopic slides and stimulated with **NCA** or DMSO as indicated. α-Tubulin (green) and nuclei (blue) were visualized by immunocytochemistry. Representative images out of 3 independent experiments are shown. **J**, Dissemination of 4T1-luc2 cells injected into the tail vein of control and NCA-treated Balb/c mice into the lungs and bodyweight changes in control and **NCA**-treated mice. Representative in vivo bioluminescent images of 4 out of 8 mice on day 5 are shown. Bar diagram shows corresponding signal intensities with bars representing the mean ± SEM of 8 mice, two-tailed unpaired Student's t test, not significant.

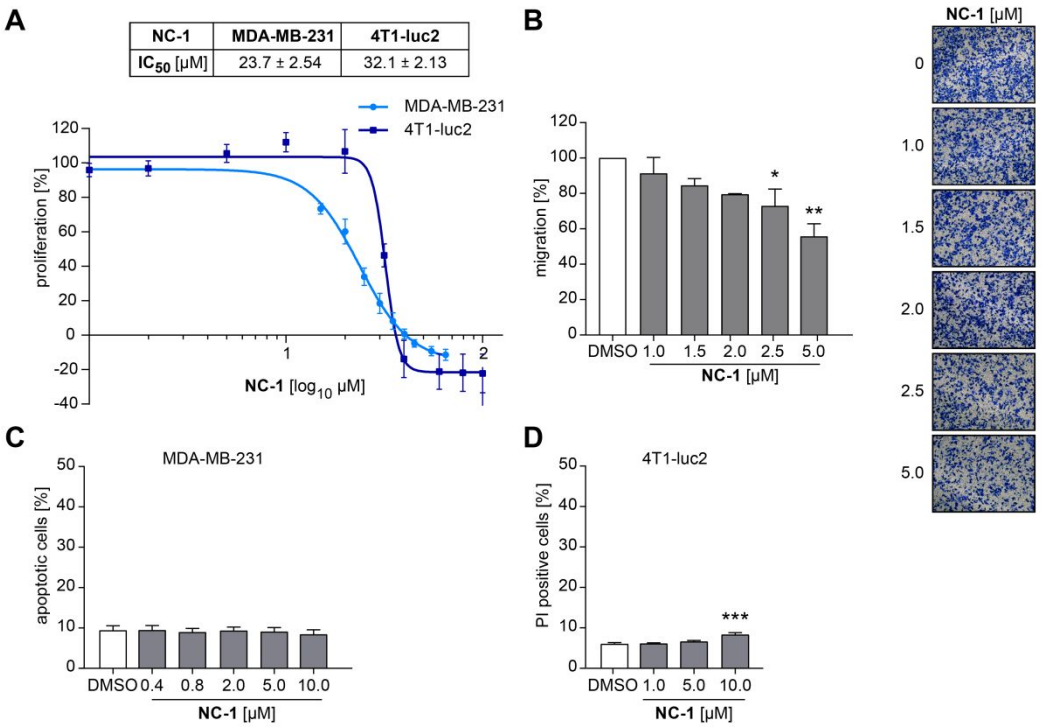

Figure S2: Anti-cancer effects of probe NC-1. A, Proliferative capacity of human MDA-MB-231 and murine 4T1-luc2 breast cancer cells treated with the activity-based probe **NC-1** determined by crystal violet staining after 72 h. **B**, Transwell migration of MDA-MB-231 cells treated with **NC-1** determined by Boyden Chamber assay. Bar diagram showing the number of migrated cells normalized to the control is presented. **C-D**, MDA-MB-231 (**C**) and 4T1-luc2 cells (**D**) treated with indicated concentrations of **NC-1**. Cells were either permeabilized and stained with propidiumiodide using the method described by Nicoletti *et al*.[1] (**C**) or stained with propidiumiodide (**D**). The percentage of dying cells was determined by flow cytometry. **A-D**, Bars represent the mean ± SEM of three independent experiments performed in duplicates/triplicates, one-way ANOVA, Dunnett's test, *P < 0.033, **P < 0.002, ***P < 0.001 compared with DMSO control (**B**-**D**).

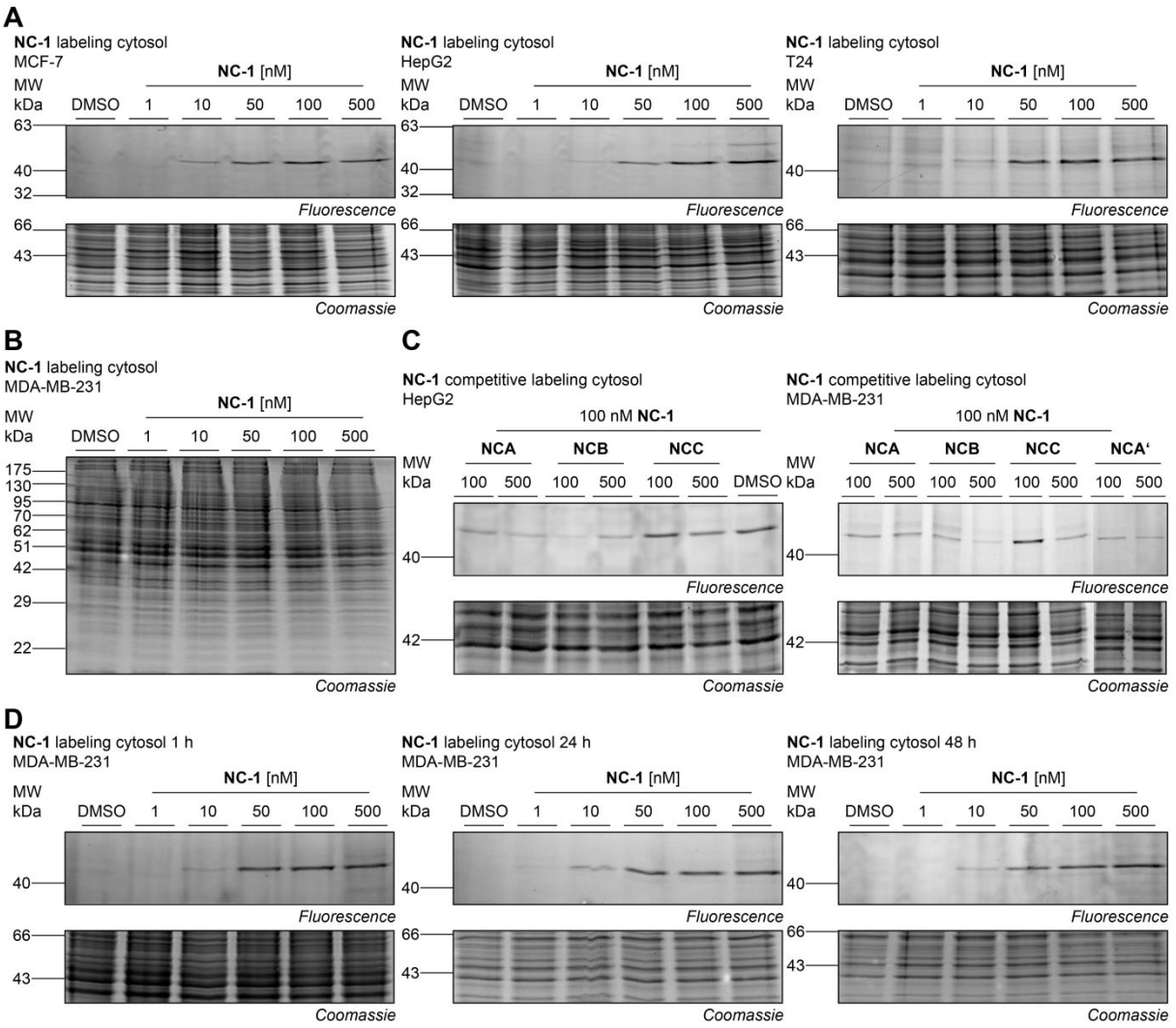

Figure S3: Analytical *in situ* labeling and competitive labeling in different cell lines and time dependent labeling. A, SDS-PAGE analysis of cytosolic fraction of analytical *in situ* labeling with **NC-1** (0.1% DMSO) in three different cell lines for 1 h. **B**, Coomassie stained gel of analytical *in situ* labeling with increasing concentrations of **NC-1** in MDA-MB-231 cells. The corresponding fluorescence gel is shown in Figure 2B. **C**, SDS-PAGE of competitive analytical labeling for 1 h in HepG2 cells with natural products **NCA**, **NCB**, **NCC** and DMSO control and in MDA-MB-231 cells with natural products **NCA**, **NCA'**, **NCB**, **NCC** and probe **NC-1** in concentration ratios 1:1 and 5:1 (natural product:probe). **D**, SDS-PAGE of time dependent analytical *in situ* labeling with **NC-1** for 1 h, 24 h and 48 h in MDA-MB-231 cells.

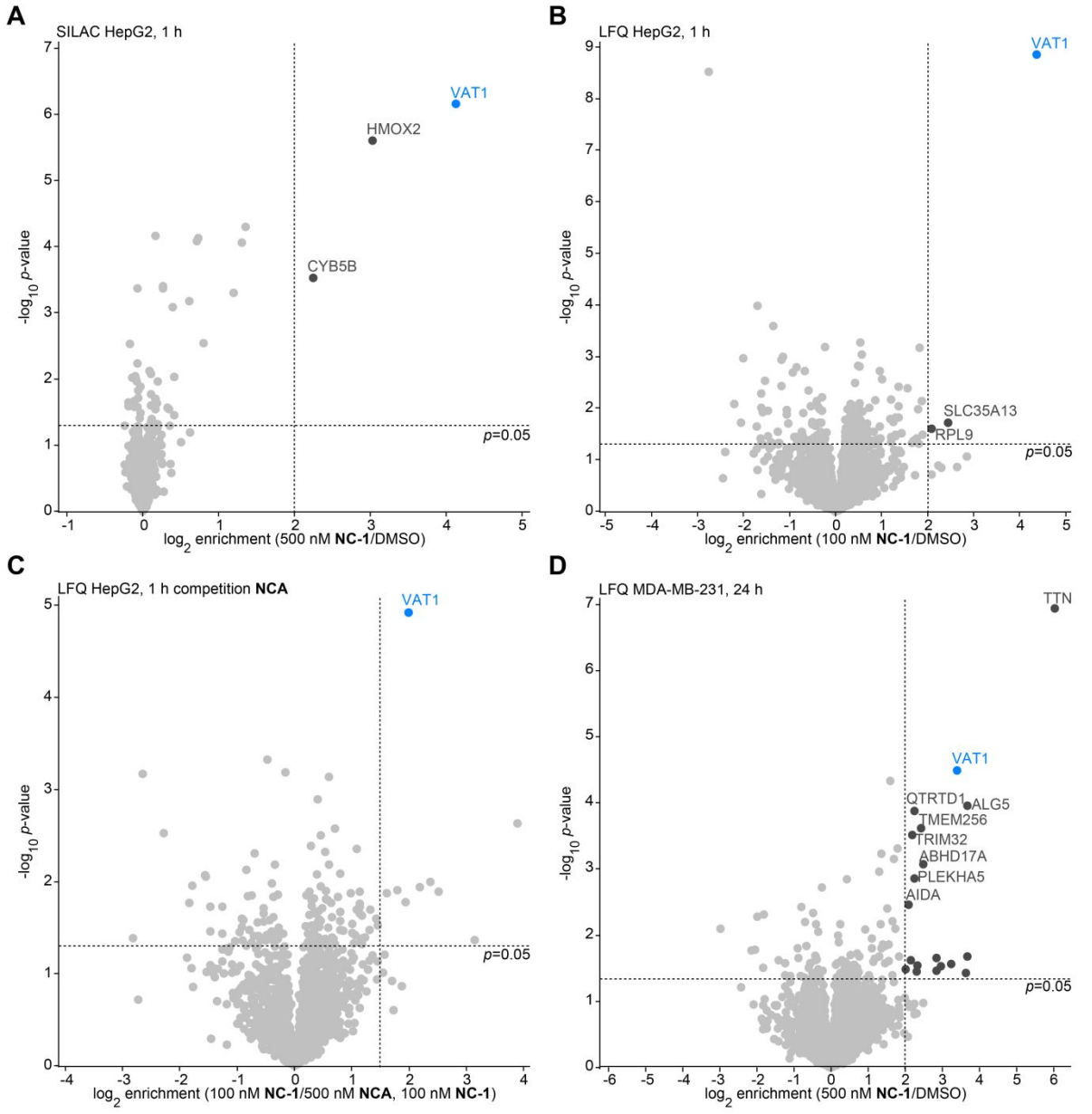

Figure S4: Identification of VAT-1 as cellular target protein of neocarzilin A by competitive LC-MS/MS-based ABPP in HepG2 cells and time dependent stability of labeling in MDA-MB-231 cells. A, Volcano plot of *in situ* SILAC ABPP experiment in HepG2 cells with 500 nM **NC-1**. Two tailed t-test on n=6 biological independent samples for each group was performed. Hits matching the criteria ((log_2(enrichment) > 2, p-value < 0.05) are highlighted in dark grey (Table S11) and the protein with the highest enrichment factor (VAT-1) is shown in blue. **B**, Volcano plot of *in situ* label-free ABPP experiment in HepG2 cells with 100 nM **NC-1** (n=6) (Table S12). **C**, Volcano plot of *in situ* competitive label-free ABPP experiment in HepG2 cells which were pretreated with 500 nM **NCA** before labeling with 100 nM **NC-1** (n=6). Hits matching the criteria ((log_2(enrichment) > 1.5, p-value < 0.05) shown in light grey were not found among enriched proteins in **B** and are shown in Table S12. **D**, Volcano plot of *in situ* label-free ABPP experiment in MDA-MB-231 cells which were incubated for 24 h with 500 nM **NC-1** (n=4). Hits matching the criteria ((log_2(enrichment) > 2, p-value < 0.05) highlighted in dark grey are listed in Table S13.

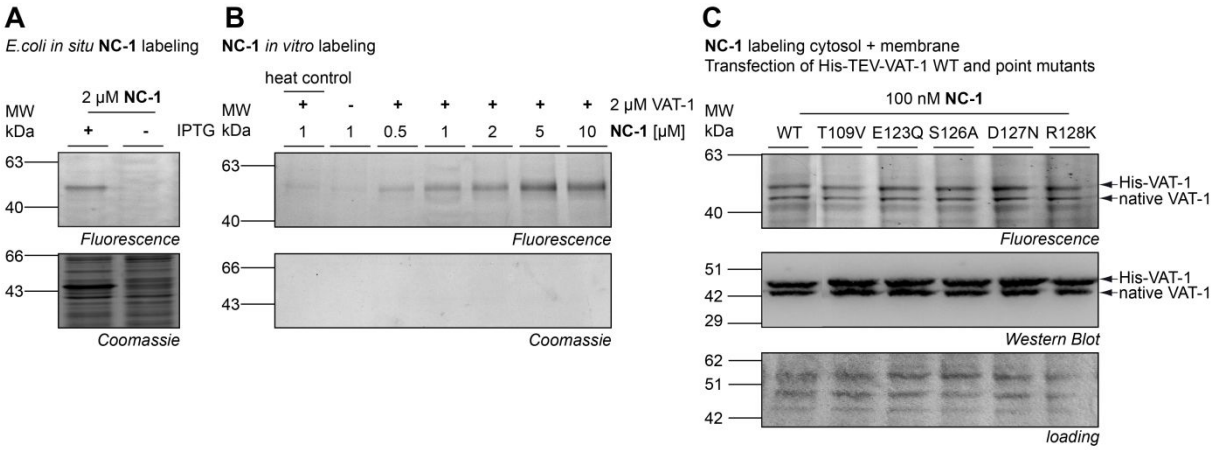

Figure S5: VAT-1 and VAT-1 point mutant labeling for verification of the target protein. **A**, SDS-PAGE of *E. coli* cell lysate of i*n situ* labeling with **NC-1** after VAT-1 overexpression induced by IPTG. **B**, SDS-PAGE of *in vitro* labeling of recombinant *E. coli* VAT-1 with increasing **NC-1** concentrations. Heat control and no enzyme control are included. **C**, SDS-PAGE of *in situ* labeling of transfected VAT-1 wildtype (WT) and point mutants with an additional HIS-TEV tag compared to native VAT-1 in MDA-MB-231 cells for binding site identification. Labeling pattern of transfected point mutants was detected for all five constructs.

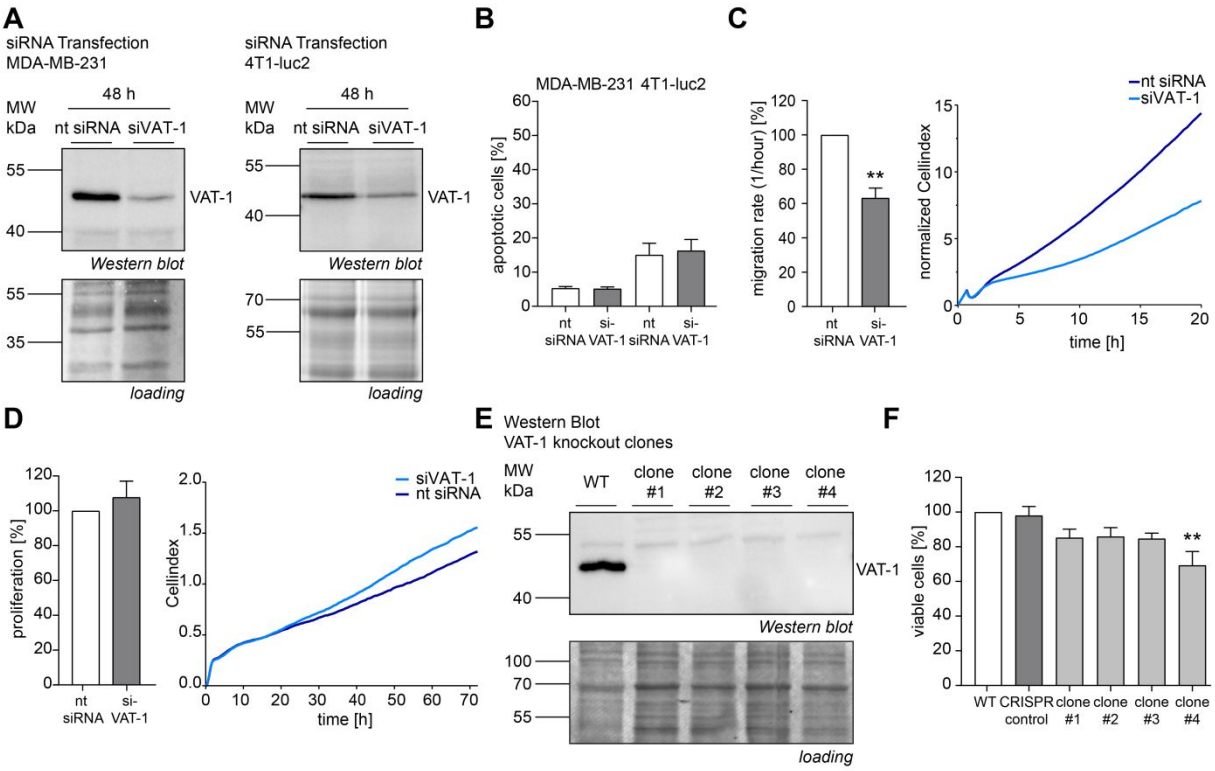

Figure S6: Effects of VAT-1 silencing and knockout on migration and proliferation capacity. A, Western Blot showing VAT-1 protein levels in non-targeting (nt) and VAT-1 siRNA MDA-MB-231 and 4T1-luc2 cells after 48 h of siRNA transfection. **B**, MDA-MB-231 or 4T1-luc2 cells were transfected with siRNA targeting VAT-1 for 48 h. Cells were permeabilized and stained with propidiumiodide using the method described by Nicoletti *et al.*[1]. The percentage of dying cells was determined by flow cytometry. **C**, Dynamic real time monitoring of migration of nt and VAT-1 siRNA transfected MDA-MB-231 cells using the xCELLigence migration assay. Representative graph out of three independent experiments is shown. Diagram showing the migration rate per hour of siVAT-1 cells normalized to nt siRNA cells is presented. **D**, Proliferation of nt and VAT-1 siRNA transfected MDA-MB-231 cells determined by crystal violet staining after 72 h (left) and dynamic real time xCELLigence proliferation assay (right). Bar diagram showing the proliferation capacity of siVAT-1 cells normalized to nt siRNA cells is presented. Representative xCELLigence graph out of three independent experiments is shown. **E**, Western Blot showing VAT-1 protein levels in Hek293 WT cells and Hek293 VAT-1 knockout clones generated via the CRISPR-Cas9 method. **F**, Proliferative capacity of WT and VAT-1 knockout clones was determined by measuring metabolic activity using CellTiter-Blue® Cell Viability Assay after 72h. As additional control WT cells which were subjected to the complete CRISPR-Cas9 procedure but did not result in successful knockout of VAT-1 were included in the experiment (*CRISPR control*). **B-D** and **F**, Bars represent the mean ± SEM of three independent experiments performed in triplicates, two-tailed unpaired Student's *t* test, **P < 0.002 (**B**-**D**), one-way ANOVA, Dunnett's test, **P < 0.002 compared with DMSO control (**F**).

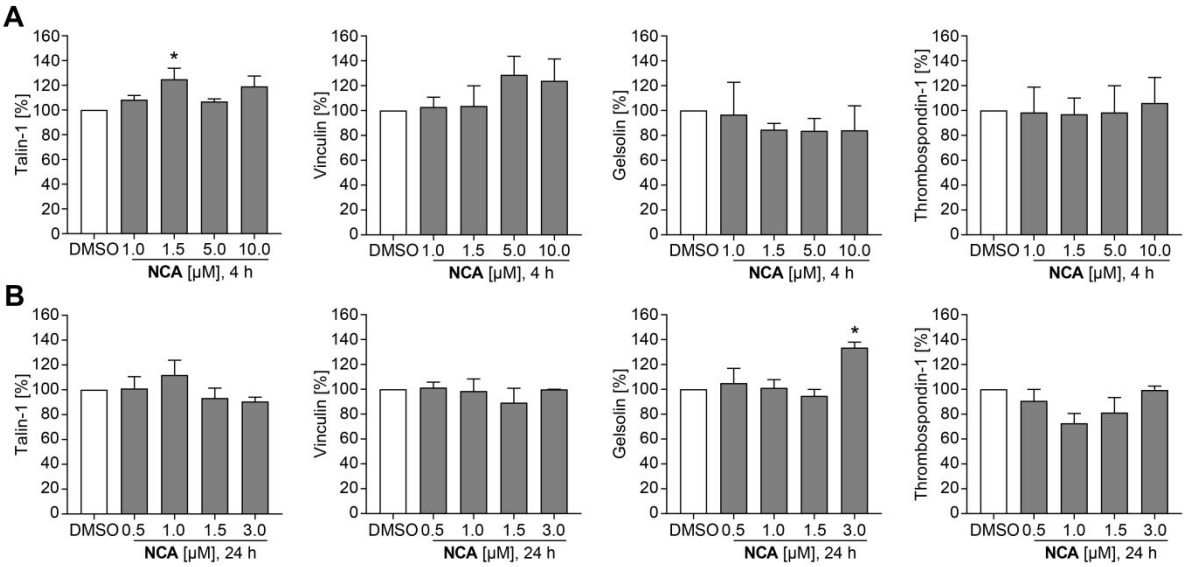

Figure S7: Effect of NCA on the cellular level of selected interaction partners of VAT-1. **A-B**, MDA-MB-231 cells were treated with the indicated concentrations of **NCA** or DMSO for 4 h (**A**) or 24 h (**B**), respectively. Cellular protein levels were detected by Western blot analysis and results normalized to DMSO treated cells. Bars represent the mean ± SEM of three independent experiments, one-way ANOVA, Dunnett's test, *P < 0.033 compared with DMSO control.

2. Methods

2.1. Cell culture and cell lines

For proteomics experiments, HepG2 cells were purchased from DSMZ and cultured in RPMI-1640 media (Sigma Aldrich) supplemented with 10% (v/v) heat-inactivated fetal bovine serum (FBS) (Sigma Aldrich) and 2 mM L-glutamine (PAA). Urinary bladder cells T24 (DSMZ, kindly provided by the LMU) and adenocarcinoma cells MDA-MB-231 (ATCC) and MCF-7 (Bayer) were all cultured in Dulbecco´s Modified Eagle´s Medium (DMEM) (Sigma Aldrich) supplemented with 10% FBS and 2 mM L-glutamine. Cells were grown at 37 °C and 5% CO_2.
For SILAC experiments, MDA-MB-231 and HepG2 cells were passaged at least six times in SILAC-DMEM (gibco, Life Technologies) or respectively SILAC-RPMI (gibco, Life Technologies) supplemented with 10% dialyzed FBS and 2 mM L-glutamine as well as 214 µM [13C6,15N4] L-arginine HCl (Arg10) and 419 µM [13C6,15N2] L-lysine 2 HCl (Lys8) (Cambridge Isotope Laboratories) resulting in “heavy” cells or with 214 µM [13C6] L-arginine HCl (Arg6) and 419 µM [4,4,5,5-D4]L-lysine 2 HCl (Lys4) (Cambridge Isotope Laboratories) resulting in “light” cells.
For biological experiments, MDA-MB-231, T24 and HEK293 cells were obtained from DSMZ and cultured in Dulbecco´s Modified Eagle´s Medium (DMEM) (PAA) supplemented with 10% FBS and 1% penicillin/streptomycin (P/S). The murine breast carcinoma cell line 4T1-luc2 was purchased from PerkinElmer and maintained in RPMI 1640 medium (PAA). RAEW glioblastoma multiforme cells established from a patient isolate in Linz were kindly provided by the MedUni Vienna and cultivated in RPMI 1640 medium (PAA) supplemented with 10% FBS and 1% P/S. U87 human primary glioblastoma cells were kindly provided by the Weatherall Institute of Molecular Medicine of the University of Oxford and cultivated in RPMI 1640 medium (PAA) supplemented with 10% FBS and 1% P/S. All cells were routinely tested for mycoplasma contamination.

2.2. MS-based proteomics procedures

2.2.1. *In situ* labeling in human cells

Cells were seeded in 6-well plates for analytical and in 15 cm plates for preparative labeling and treated at 90% confluence for 1 h with varying concentrations (1-500 nM) of probe **NC-1** (stock solution in DMSO, 0.1 % end concentration of DMSO for all compounds) or respectively DMSO diluted in PBS at 37 °C and 5% CO_2. For competition experiments, cells were preincubated for 1 h with 100 nM or respectively 500 nM of the natural products **NCA**, **NCB**, **NCC** diluted in PBS before addition of 100 nM **NC-1** for 1 h. Labeling experiments were performed as described before.[2] Briefly, cells were scraped off, pelletized for 3 min at 800xg and washed with PBS. Cell lysis was performed with 0.1 mL for analytical or respectively 1 mL lysis buffer for preparative labeling (1% (v/v) NP40 and 1% (w/v) sodium deoxycholate) at 4 °C for 15 min.

2.2.1.1. Analytical *in situ* labeling

For some experiments, soluble and insoluble fractions were not separated and whole cell lysate was applied for click chemistry. Otherwise, soluble and insoluble fractions were separated by centrifugation at 20,000xg and membrane fraction was washed with PBS and resuspended in 100 µL PBS supplemented with 0.2% SDS. Click chemistry was performed with 0.20 mM rhodamine-azide (10 mM stock in DMSO; base click; Rh-N_3), 1.0 mM TCEP (52 mM stock in ddH_2O), 0.10 mM TBTA ligand (1.667 mM stock) and 1.0 mM $CuSO_4$ (50 mM stock in ddH_2O). The reaction was incubated at rt for 1 h and stopped by addition of 100 µL 2x SDS loading buffer (63 mM Tris-HCl, 2% (v/v) glycerol, 139 mM sodium dodecylsulfate (SDS), 0.0025% (v/v) Bromophenol blue, 5% (v/v) 2-mercaptoethanol). For gel electrophoresis, 50 µL were applied per gel-lane on a SDS−PAGE gel (12.5% acrylamide). Fluorescence was recorded using a Fujifilm LAS 4000 luminescent image analyzer with a Fujinon VRF43LMD3 lens and a 575DF20 filter.

2.2.1.2. *In situ* preparative labeling SILAC

Both heavy and light labeled HepG2 or MDA-MB-231 respectively cells were treated with 500 nM probe **NC-1** or DMSO, respectively. Soluble and insoluble cell fractions were not separated after cell lysis. After BCA assay (Roti Quant, Roth), equal protein amounts resulting from “heavy” or “light” cells incubated with the probe and the corresponding DMSO control of the opposite label were pooled and adjusted to a final volume of 1880 µL with lysis buffer (approximately 2 µg). Samples were supplemented with 0.20 mM azide-PEG_3-biotin conjugate (10 mM stock in DMSO; Jena Bioscience), 0.52 mM TCEP (52 mM stock in ddH_2O), 0.050 mM TBTA ligand (1.67 mM stock) and 0.50 mM $CuSO_4$ (50 mM stock in ddH_2O). Click reaction was performed at rt for 1 h and MS sample preparation was performed as described before.[2] Briefly, proteins were precipitated in 4-fold volume access ice-cold acetone (MS-grade) at -80 °C, washed with MeOH (MS-grade) and enriched on 50 µL avidin-agarose beads in PBS supplemented with 0.2% SDS at rt for 1 h. Beads were washed three times with 0.2% SDS in PBS, twice with 6 M urea, three times with PBS and were supplemented with 200 µL denaturation buffer (7 M urea, 2 M thiourea in 20 mM Hepes, pH 8.0). Reduction and alkylation were performed at rt with 1 mM DTT for 45 min, 5.5 mM IAA for 30 min and 4 mM DTT for 30 min. Proteins were digested with 1 µL Lys-C (0.5 mg/mL) at 25 °C for 3 h, diluted in 600 µL 50 mM TEAB buffer and digested with 2 µL Trypsin (0.5 mg/mL, Promega) at 37 °C overnight. Digestion was stopped with a final concentration of 0.75% formic acid (FA) and peptides were desalted with Sep-Pak C18 1 cc Vac cartridges (Waters Corp.). Therefore, C18 material was washed with acetonitrile (MeCN, MS grade), elution buffer (80% MeCN, 0.5% FA in H_2O) and 0.1% TFA in H_2O. Peptides were loaded on the cartridges and were washed with 0.1% trifluoroacetic acid (TFA) in H_2O, 0.5% FA in H_2O and eluted in elution buffer. Peptides were lyophilized, stored at -80 °C and reconstituted in 30 µL 1% FA for MS/MS measurements.

2.2.2.3. *In situ* preparative labeling label-free quantification

Cells were incubated with 100 nM **NC-1** for 1 h or respectively 500 nM **NC-1** for 24 h. For competition experiments, cells were preincubated with 500 nM **NCA** or DMSO for 1 h. Soluble and insoluble fractions of MDA-MB-231 or HepG2 cells respectively were not separated. Protein amount was adjusted after BCA assay to a final concentration of 1 µg in 1 mL and LFQ samples were further processed separately. Click chemistry and MS sample preparation was performed according to the SILAC labeling with one modification. Beads were only washed three times with 0.2% SDS in PBS and five times with PBS.

2.2.1.4. *In situ* preparative labeling LFQ for binding site peptide identification

In situ labeling in MDA-MB-231 cells with 100 nM **NC-1** was performed as described before with the following modifications: Azide-PEG_3-Desthiobiotin (Jena Bioscience) was used for click chemistry and proteins were digested before enrichment. For click chemistry, 150 µg cell lysate of MDA-MB-231 cells was incubated with 0.20 mM azide-PEG_3-Desthiobiotin conjugate (5 mM stock in DMSO), 0.52 mM TCEP (52 mM stock in ddH_2O), 0.050 mM TBTA ligand (1.67 mM stock) and 0.50 mM $CuSO_4$ (50 mM stock in ddH_2O). After protein precipitation, proteins were resuspended in 300 µL 0.1 M TEAB supplemented with 8 M urea and digested 1:200 (w/w) with LysC at rt, diluted with 900 µL 0.1 M TEAB and digested 1:150 (w/w) Trypsin overnight at 37 °C. After digestion, samples were supplemented 1:1 (v/v) with 0.2% NP40 in PBS and enriched for 1 h on 50 µL avidin agarose beads, which were pre-washed with 0.1% NP40. Peptides were washed twice with 0.1% NP40, three times with PBS and twice with H_2O. Peptides were eluted twice with 100 µL 80% MeCN, 0.5% FA in ddH_2O, were lyophilized and reconstituted in 30 µL 1% FA for MS/MS measurements.

2.2.2. Whole proteome analysis

Cells were seeded in 15 cm plates and were treated at 80% confluence with 500 nM **NCA** or DMSO respectively diluted in DMEM supplemented with FBS for 24 h at 37 °C. Cells were scraped off and pelletized for 3 min at 800xg. The pellets were washed with PBS and lysed in 1 ml lysis buffer at 4 °C for 15 min. Membrane fraction was separated at 20,000xg at 4°C for 20 min. Protein concentration of cytosolic fraction was adjusted after BCA assay to 500 µg and proteins were precipitated in 4-fold volume access acetone. Proteins were washed with cold methanol and resuspended in 300 µL denaturation buffer. Reduction and alkylation of disulfides was performed as described for ABPP experiments. Whole proteome was predigested 1:200 (w/w) with LysC at rt, diluted with 900 µL 50 mM TEAB and digested 1:150 (w/w) Trypsin overnight at 37°C. Protein digestion was stopped with a final concentration of 0.75% formic acid peptides were desalted with Sep-Pak C18 1 cc Vac cartridges (Waters Corp.). Peptides were lyophilized and were reconstituted in 1% FA in ddH_2O to a final concentration of 2 µg/µL.

2.2.3. Co-Immunoprecipitation (co-IP)

Cells were seeded in 15 cm plates and were applied at 90% confluence for co-IP using disuccinimidyl sulfoxide (DSSO) crosslinker. Co-IP with MS sample preparation was performed as described before.[3] Synthesis of DSSO and crosslinking was carried out as described previously.[4] Briefly, cells were washed with PBS, scraped off in PBS and pelletized. Crosslinking reaction was performed with 2 mM DSSO in 1 mL PBS at 37 °C and 250 rpm for 1 h. Crosslinking reaction was quenched with 50 mM Tris-HCl pH 8.0 and cells were lysed in co-IP lysis buffer (50 mM Tris-HCl, 150 mM NaCl, 10% glycerol, 1% NP40, pH 8.0). Membrane fraction was pelleted at 21,000xg and 4 °C for 20 min. Protein concentration of cytosolic fraction was adjusted after BCA assay to 500 µg. 30 µL of Protein AG beads (Pierce) were equilibrated with 1 mL wash buffer (50 mM Tris-HCl, 150 mM NaCl, 10% glycerol, 0.05% NP40, pH 8.0) and were incubated with 500 µg protein lysate and approximately 5 µg of VAT-1 antibody (1:100, antibodies.online, ABIN2443750) or the corresponding amount of rabbit IgG isotype control (Cell signaling, #3900) for 3 h at 4 °C Beads were washed twice with wash buffer and twice with basic buffer (50 mM Tris-HCl, 150 mM NaCl, 10% glycerol pH 8.0). For MS sample preparation, 25 µL of elution buffer I (50 mM Tris-HCl, 2 M urea, 1 mM DTT, 0.5 ng/µL trypsin) was added to the beads for 30 min at rt. Subsequently, the beads were treated with 100 µL elution buffer II (50 mM Tris-HCl, 2 M urea, 5 mM IAA) overnight at 37°C. Protein digestion was stopped with a final concentration of 0.75% TFA and peptides were desalted using stage-tips (self-made pipette tips containing two layers of C18 disks) according to the standard protocol.[5] Therefore, C18 materials was washed with 70 µL MeOH, three times with 70 µL 0.5% FA in ddH_2O, samples were loaded, again washed three times with 70 µL 0.5% FA in ddH_2O and peptides were eluted with 80% MeCN, 0.5% FA in ddH_2O.

2.2.4. MS/MS measurement Orbitrap Fusion

For MS measurements, peptide samples were first dissolved 1% FA in H_2O, sonicated for 15 min and filtered with 0.22 µm Ultrafree-MC® centrifugal filters (Merck, UFC30GVNB) equilibrated with 1% FA in H_2O.
Samples were analyzed by LC-MS/MS using an UltiMate 3000 nano HPLC system (Dionex) equipped with an Acclaim C18 PepMap100 75 µm ID x 2 cm trap and an Acclaim Pepmap RSLC C18 separation column (75 µm ID x 50 cm) in an EASY-spray setting coupled to an Orbitrap Fusion (Thermo Fisher Scientific Inc.). Approximately 8 µg were loaded on the trap column with a flow rate of 5 µL/min with 0.1% TFA buffer and then transferred onto the separation column at a flow rate of 0.3 µL/min. Samples were separated using a 152 min gradient (buffer A: H_2O with 0.1% FA, buffer B: MeCN with 0.1% FA, gradient: to 5% buffer B in 7 min, from 5% to 22% buffer B in 105 min, then to 32% buffer B in 10 min, to 90% buffer B in 10 min and hold at 90% buffer B for 10 min, then to 5% buffer B in 0.1 min and hold 5% buffer B for 9.9 min). Peptides were ionized using a nanospray source at 1.7-1.9 kV and a capillary temperature of 275 °C. The instrument was operated in a top speed data dependent mode with a cycle time between master scans of 3 s. MS full scans were performed in the orbitrap with quadrupole isolation at a resolution of R = 120,000 and an automatic gain control (AGC) ion target value of 2e5 in a scan range of 300 – 1500 m/z with a maximum injection time of 50 ms. Internal calibration was performed using the ion signal of fluoranthene cations (EASY-ETD/IC source). Besides two experiments, all samples were measured on the Orbitrap Fusion instrument for the publication.
Dynamic exclusion time was set to 60 s with a mass tolerance of 10 ppm (low/high). Precursors with intensities higher than 5e3 and charge states 2 – 7 were selected for fragmentation with HCD (30%). MS^2 scans were recorded in the ion trap operating in a rapid mode with an isolation window of 1.6 m/z. For enriched samples, the AGC target was set to 1.0e4 with a maximum injection time of 100 ms and the “inject ions for all available parallelizable time” was enabled. For complex samples, AGC target of 1.0e4 with a maximum injection time of 35 ms was applied.

2.2.5. MS/MS measurement Q Exactive

Samples clicked to the desthiobiotin-linker and 24 h labeling in HepG2 were analyzed via an UltiMate 3000 nano HPLC system (Dionex) using Acclaim C18 PepMap100 75 µm ID x 2 cm trap and Acclaim PepMap RSLC C18 (75 µm ID x 50 cm) separation columns in an EASY-spray setting coupled to a Q Exactive Plus (Thermo Fisher). After reconstitution of the samples in 1% FA in ddH_2O and filtering, 5 µL peptide samples were loaded on the trap column with a flow rate 5 µL/min in 0.1% TFA, and were subsequently transferred to the separation column at a flow rate of 0.3 µL/min. Separation was performed with a 152 min gradient (buffer A: H_2O with 0.1% FA, buffer B: MeCN with 0.1% FA) increasing buffer B to 5% within 7 min, to 22% the next 105 min, to 32% the next 10 min and to 90% the next ten min. Buffer b was held another 10 min at 90% and was then decreased to 5% in 0.1 min and held until end of the run. Peptide samples were ionized at spray voltage of 1.6 kV and a capillary temperature of 275 °C. Q Exactive Plus was operated in a TopN data dependent mode of 12. Full scans were performed in the orbitrap mass analyzer with a resolution of R=140,000 and an AGC target of 3.0 e6 with a maximum injection time of 80 ms. The scan range was set to 300-15000 m/z. Peptide fragments were generated by HCD with a normalized collision energy of 27%.
MS^2 scans were recorded in the orbitrap at a resolution of 17,500 with an AGC target of 1e5 and a maximum injection time of 100 ms scan range. Isolation was performed in the quadrupole using a window of 1.6 m/z. Dynamic exclusion duration was set to 60 s. Precursors with charge states >1, intensities higher than 1e4 and a minimum AGC target of 1.00e3 were selected for fragmentation.

2.2.6. Bioinformatics and statistics

MS data was processed with the software MaxQuant version 1.6.0.1. For peptide identification, MS/MS spectra were searched against the Uniprot database for *homo sapiens* (taxon identifier: 9606, canonical version, reviewed and unreviewed proteome downloaded on 05.04.2018) using the Andromeda search engine.[6]
MaxQuant was run using mostly default settings (trypsin/P set as the digest enzyme, max. 2 missed cleavages, oxidation (M) and protein N-term acetylation as variable modifications, carbamidomethylation (C) as fixed modification, min. peptide length 7, 4.5 ppm for precursor mass tolerance (FTMS MS/MS match tolerance) and 0.5 Da for fragment mass tolerance (ITMS MS/MS match tolerance)). For protein identification the following settings were used: PSM FDR 0.01, Protein FDR 0.01, min. razor + unique peptides: 2, razor protein FDR enabled, second peptides enabled. The match between run option with a matching window of 0.7 min and alignment time window of 20 min was enabled for all experiments. LFQ samples were processed using the built-in label-free quantification algorithm in the MaxQuant software (MaxLFQ)[7] with a minimal ratio count of 2.
For SILAC experiments, multiplicity was set to 2, parameter groups were defined and corresponding labels were selected: For light labels, Arg6 and Lys4 was selected for samples which have been treated with probe **NC-1** in Arg10 Lys8 medium and heavy labels were set to Arg10 Lys8. For samples which have been treated with **NC-1** in Arg6 Lys4 medium, light labels were set to Arg10 Lys8 and heavy labels to Arg6 Lys4. The re-quantify option was enabled for SILAC samples. The mass spectrometry proteomics data have been deposited to the ProteomeXchange Consortium[8] via the PRIDE[9] partner repository with the dataset identifier PXD012952.

Resulting data was statistically analyzed further with Perseus software[10] (version 1.6.2.3). The *protein groups* table in the *txt* folder was selected and the rows containing the normalized ratios were filtered by “filtering by categorical columns”, namely the columns “identified by site”, “reverse” and “contaminants”. Ratios were $\log_2$ transformed and categorical annotation of treated samples and control was performed for LFQ samples. Matrices were further filtered against 70% of valid values in at least one group and missing values were imputed from normal distribution (width 0.3, down shift 0.9, for the total matrix. For LFQ experiments, two-sided

student's *t*-tests with background as single control group and Benjamini-Hochberg false discovery rate correction (FDR 0.05) were applied. Volcano plots were generated by plotting student's t-test difference (treated/control) against t-test p-value (treated/control).
For SILAC experiments, rows were filtered against 70% of valid values in total after $\log_2$ transformation and a one-sample Student's *t*-test was performed

2.2.7. Gene ontology enrichment analysis

Gene Ontology enrichment analysis was performed in Cytoscape[11] version 3.7.1. using the BiNGO app[12] 3.0.3. Human gene association (.gaf) and ontology (.obo) files were downloaded from http://www.geneontology.org/ (31/01/2019). An overrepresentation among the proteins of interest was selected and a hypergeometric test with a significance level of 0.05 and Benjamini & Hochberg False Discovery Rate (FDR) correction was performed. Biological process name space was used to select the terms molecular function, biological process and cellular compartment. Whole annotations were used as reference set.

2.3. Cell-based and *in vivo* assays

2.3.1. Proliferation assay

5.000 (MDA-MB-231, 4T1-luc2, T24) or 10.000 (RAEW, U87) cells were incubated in triplicates for 72 h with the indicated concentrations of compounds and stained with crystal violet/methanol [(0.5% crystal violet (w/v), 20% methanol (v/v)] for 10 min. Crystal violet was redissolved with 50% ethanol (v/v), 50% 0.1 M sodium citrat (w/v) to measure absorption at 550 nm at a microplate reader (Tecan SunriseTM Microplate Absorbance Reader). For statistical analysis, values of the day zero control were subtracted, and results of each biological replicate were normalized to the corresponding DMSO control which was set to 100% proliferation.

2.3.2. Proliferation assay using xCELLigence system

Cellular growth was investigated using xCELLigence real-time impedance based measurements from OLS Omni Life Sciences GmbH according to the manufacturer's instructions. MDA-MB-231 cells were transfected with non-targeting control siRNA or siRNA targeting VAT-1 (Dharmacon™, GE Healthcare) for 48 h using DharmaFECT™ transfection reagent according to manufacturer's protocol (Dharmacon™, GE Healthcare). 5.000 cells were seeded in triplicates in culture medium per 100 µL in equilibrated E plates. Proliferation was monitored over 72 h. For statistical analysis, results of each biological replicate were normalized to the corresponding nt siRNA control which was set to 100% proliferation.

2.3.3. Migration assays using xCELLigence system

Real-time impedance based monitoring of migrating cells was analyzed by using the xCELLigence system from OLS Omni Life Sciences GmbH according to the manufacturer's instructions. MDA-MB-231 cells were transfected with non-targeting control siRNA or siRNA targeting VAT-1 (Dharmacon™, GE Healthcare) for 48 h using DharmaFECT™ transfection reagent according to manufacturer's protocol (Dharmacon™, GE Healthcare). Cells were starved overnight, resuspended in media without FBS and 40.000 cells were seeded in triplicates per 100 µL in equilibrated CIM plates and migration towards culture medium containing 10% FBS as chemoattractant was monitored over 16 h. For statistical analysis, results of each biological replicate were normalized to the corresponding nt siRNA control which was set to 100% migration.

2.3.4. Boyden chamber assay

For trans-well migration/invasion assays using Boyden chamber inserts cells were treated with indicated concentrations of compounds for 24 h or silenced with siRNA targeting VAT-1 and starved overnight. HEK293 CRISPR-Cas9 VAT-1 k.o. clones were additionally treated with 10 µg/mL mitomycin for 2 h prior to harvest to inhibit proliferation. 1.6 x 10^5 cells (MDA-MB-231, 4T1-luc2) or 1.4 x 10^5 cells (HEK293, CRISPR-Cas9 VAT-1 k.o. clones) were resuspended in media without FBS and added on top of the Boyden chamber membrane (8 µm, Corning) in duplicates. Culture medium containing 10% FBS (MDA-MB-231, 4T1-luc2) or fibroblast-conditioned medium (HEK293, CRISPR-Cas9 VAT-1 k.o. clones) was used as chemoattractant. After 4 h (MDA-MB-231), 6 h (4T1-luc2) or 42 h (HEK293, CRISPR-Cas9 VAT-1 k.o. clones) migrated cells were fixed and stained with crystal violet/methanol [(0.5% crystal violet (w/v), 20% methanol (v/v)] for 10 min. Non-migrated cells on top of the membrane were removed with a cotton swab. For invasion assays, membranes were coated with Matrigel (VWR) according to manufacturer's instructions. Pictures were taken with an Axiovert 25 microscope (Zeiss) and a Canon EOS 450 C camera (Canon). For statistical analysis, results of each biological replicate were normalized to the corresponding DMSO control which was set to 100% migration.

2.3.5. Chemotaxis assay

For chemotaxis assay, MDA-MB-231 cells were treated with 1 µM **NCA** for 24 h in serum-free DMEM medium. Afterwards cells were seeded in ibidi™ Chemotaxis µ-Slides (ibidi, Munich, Germany) in DMEM medium containing FCS for better adhesion. After cell attachment, channels were washed with serum-free DMEM medium and a FCS-gradient was established by filling one reservoir of the slide with FCS negative medium and the other with medium containing 10% FCS. Images were taken every ten minutes for 20 h using a Nikon Eclipse Ti inverted microscope (Nikon, Düsseldorf, Germany) and the indicated migration parameters were calculated using the chemotaxis and migration tool Qt Open Source Edition version 4.3.2 (ibidi, Munich, Germany).

2.3.6. Apoptosis and cell cycle analysis

MDA-MB-231 and 4T1-luc2 cells were treated with **NCA** for 24 h or transfected with non-targeting control siRNA or siRNA targeting VAT-1 (Dharmacon™, GE Healthcare) in triplicates for 48 h using DharmaFECT™ transfection reagent according to manufacturer's protocol (Dharmacon™, GE Healthcare). Cells were harvested on ice and permeabilized in fluorochrome solution [0.1% (v/v) Triton X-100, 0.1% (w/v) sodium citrate, in PBS], supplemented with 50 µg/mL propidium iodide for at least 30 min at 4 °C. Flow cytometric measurements were made on a FACSCanto II instrument (Becton Dickinson) using FACSDiva Software (Becton Dickinson) and the flow cytometry analysis software FlowJo 7.6 using the Watson pragmatic model for cell cycle analysis (Tree Star). Apoptosis was determined according to Nicoletti *et al.*[1] by analyzing cells at subG1 phase.

2.3.7. PI exclusion assay

4T1-luc2 cells were treated with **NC-1** in triplicates for 24 h and harvested on ice. Cell death was analyzed by staining of cells with 50 µg/µL propidium iodide in PBS and subsequent measurement on a FACSCalibur flow cytometer (Becton Dickinson) using Cell Quest Pro Software (Becton Dickinson) and the flow cytometry analysis software FlowJo 7.6 (Tree Star).

2.3.8. *In vivo* dissemination assay

Animal experiments were approved by the District Government of Upper Bavaria in accordance with the German animal welfare and institutional guidelines. 16 female Balb/c "Balb/cOlaHsd" mice, six weeks old, purchased from Envigo were used. The mice were pretreated intraperitoneally with 10 mg/kg **NCA** or solvent (5% DMSO, 10% Solutol, 85% PBS) three times (48, 24, and 0.5 h) before the cell injection. 1 x 10^5 4T1-luc2 cells were injected into the tail vein. Imaging of the mice after intraperitoneal injection of 6 mg luciferin/mouse was performed on day five and on day eight after the cell injection using the IVIS Lumina system (PerkinElmer). The tumour signal per defined region of interest was calculated with the Living Image 4.4 software (PerkinElmer) as photons/second/cm^2 (total flux/area).

2.3.9. Statistical analysis

Results of at least three independent experiments (biological replicates, each performed in two or three technical replicates) are expressed as mean ± SEM or as percentage value. Statistical analysis was performed using GraphPad Prism 7 (GraphPad Software) using either two-tailed unpaired Student's *t* test, or one-way ANOVA, Dunnett's test, *P < 0.033, **P < 0.002, ***P < 0.001 compared with DMSO control.

2.4. Immunological-based procedures

2.4.1. Antibodies

The following primary antibodies were used: anti-Gelsolin (Cell Signaling; 12953) rabbit IgG monoclonal, anti-Rac1 (Upstate; 05-389) mouse IgG_{2b} monoclonal, anti-Talin-1 (Chemicon International, MAB1676) mouse IgG_1 monoclonal, anti-Talin-1 (Cell Signaling; 4021) rabbit polyclonal, anti-Thrombospondin-1 (Cell Signaling; 37879) rabbit IgG monoclonal, anti-α-tubulin (abcam; ab18251) rabbit polyclonal, anti-VAT-1 (abcam; ab89138) mouse IgG_{2a} monoclonal, anti-VAT-1 (Santa Cruz; sc-515705) mouse IgG_{2b} monoclonal, anti-VAT-1 (Sigma Aldrich; SAB1100727) rabbit polyclonal, anti-VAT-1 (Santa Cruz; sc-107348) goat polyclonal, anti-VAT-1 (antibodies online, ABIN2443750) rabbit polyclonal, anti-Vinculin (Santa Cruz; sc-25336) mouse IgG_{2a} monoclonal.

2.4.2. Rac1 staining

T24 cells were pretreated with 1.5 µM **NCA** for 24 h. Confluent cells were wounded with a pipette tip, washed and treated as indicated for additional 8 h. Afterwards cells were fixed with 4% (w/w) PFA in PBS for 10 min, permeabilized with 0.2% (v/v) Triton X-100 in PBS for 10 min, blocked with 1% BSA in PBS for 2 h at rt and incubated over night with anti-Rac1. Cells were washed with PBS, incubated with secondary antibody and Rhodamine phalloidin and mounted with FluorSave Reagent mounting medium (Merck). Nuclei were stained with Hoechst 33342 (Invitrogen; H3750). Images were taken on the inverted confocal laser scanning microscope LSM510 (Zeiss).

2.4.3. Co-Immunostaining

T24 cells were pretreated with 1.5 µM **NCA** for 24 h. Confluent cells were wounded with a pipette tip, washed and treated as indicated for additional 8 h. Afterwards cells were fixed with 4% (w/w) PFA in PBS for 10 min, permeabilized with 0.2% (v/v) Triton X-100 in PBS for 10 min, blocked with 1% BSA in PBS for 2 h at rt and incubated over night with anti-VAT-1 and anti-Talin-1. Cells were washed with PBS, incubated with secondary antibody and Rhodamine phalloidin and mounted with FluorSave Reagent mounting medium (Merck). Nuclei were stained with Hoechst 33342 (Invitrogen; H3750). Images were taken on the inverted confocal laser scanning microscope SP8 (Leica).

2.4.4. Microtubule staining

Microtubule staining was performed according to Braig *et al*..[13] In brief, MDA-MB-231 cells were treated with **NCA** as indicated, incubated with Brinkley Buffer 1980 for 2 min and fixed with glutaraldehyde. Following treatment with 0.1% $NaBH_4$ solution to quench unreacted glutaraldehyde, washing steps and blocking with 0.2% BSA in PBS, cells were incubated with anti-α-tubulin antibody for 30 min at rt. An appropriate secondary antibody and Hoechst dye was added to stain microtubules and nuclei, respectively. Images were taken on the inverted confocal laser scanning microscope LSM510 (Zeiss).

2.4.5. Rac1 activation assay

MDA-MB-231 cells were treated with 1.5 µM **NCA** for 24 h. Rac1 activation was induced by adding epidermal growth factor (EGF 100 ng/mL) for 5 min prior to harvest. GTP-bound Rac1 was enriched and detected by using the active Rac1 pull-down and detection kit according to the manufacturer's instructions (Thermo Fisher Scientific). For statistical analysis, results of each biological replicate were normalized to the corresponding DMSO control which was set to 1.0-fold Rac1 activation.

2.4.6. Co-Immunoprecipitation (co-IP)

MDA-MB-231 cells were treated with 1.5 µM **NCA** for 24 h, washed with PBS, harvested, and lysed with co-IP lysis buffer (50 mM Tris-HCl, 150 mM NaCl, 1% Triton-X, 1% NP40, pH 8.0). VAT-1 was precipitated using protein A/G PLUS-Agarose (Santa Cruz; sc-2003) according to the manufacturer's instructions using PBS for washing. A specific isotype control antibody served as control of heavy and light chains (Cell Signaling; 2729). The amount of VAT-1 and Talin-1 in pull-down fractions was analyzed via SDS-gel electrophoresis and Western blot. For statistical analysis, results of each biological replicate were normalized to the corresponding DMSO control which was set to 1.0-fold VAT-1:Talin-1 ratio.

2.4.7. Western blot analysis

Western blotting was performed according to standard procedures after separation of proteins via SDS-gel electrophoresis. Protein amount was quantified by Uptima BC Assay Kit (Interchim). Cell lysates were transferred onto a Roti®-PVDF 2.0 pore size 0.2 µm membrane (Carl Roth) with blotting buffer (48 mM Tris base, 39 mM glycine, 20% (v/v) MeOH, ddH2O) in a Trans-Blot® SD Semi-Dry Transfer cell (Bio-Rad) for 50 min at 20 V. Membranes were blocked with 5% milk powder (Carl Roth) in PBS-T (PBS buffer with 0.5% Tween-20®, pH 7.4) for 1 h and incubated overnight at 4 °C 1:1000 with the respective primary antibody. Afterwards, membranes were washed with PBS-T and incubated with the corresponding horseradish peroxidase (HRP)-conjugated secondary antibody 1:10.000 for 1 h at rt. Protein bands were visualized using enhanced luminol/enhancer and peroxide solution (Clarity TM Western ECL Substrate, Bio-Rad,) with a Fujifilm LAS 4000 luminescent image analyser with a Fujinon VRF43LMD3 lens or with a Chemidoc Touch Imaging system (Bio-Rad) in chemiluminescence mode. Protein amount was verified by 0.1% Ponceau S solution in 5% acetic acid or by stainfree detection using Chemidoc Touch Imaging system (Bio-Rad).

2.5. Cloning procedures

2.5.1. Cloning of VAT-1 for overexpression in *E.coli*

The gene sequence encoding human VAT-1 (hVAT-1) was inserted in the expression vector pET300 by using the Invitrogen™ Gateway® Technology (Life Technologies Corp.). The target gene was amplified from the corresponding cDNA (GeneCopoeia, GC-T3028) by PCR with a Phusion® HF DNA Polymerase. For Gateway® Technology, *att*B1 forward primer and *att*B2 reverse primer were designed to yield *att*B-PCR products. Primers are listed in the table below. The expression construct for hVAT1 (uniprot-ID: Q99536) with protein purification tags was N-Start-His-attB1-TEV-Start-VAT1-Stop-attB2-C.

Table S1: Primer for Gateway Cloning

Primer	Sequence
for_attB1_VAT1	5'-ggggacaagtttgtacaaaaaagcaggctttgagaatctttattttcagggctccgac gagagagaggtagc-3'
rev_attB1_VAT1	5'-ggggaccactttgtacaagaaagctgggtgctagttctccttctctggccc-3'

PCR was performed in a CFX96™ Real-Time PCR System (Bio-Rad) according to Phusion® HF DNA Polymerase (NEB) manufacturer´s PCR protocol and thermocycling conditions for a routine PCR. PCR products were extracted with an E.Z.N.A.® Gel Extraction Kit (Omega Bio-Tek Inc.) and DNA concentrations were measured using an Infinite® M200 Pro multiplate reader (Tecan Group Ltd.). Purified *att*B-PCR product (100 fmol) and *att*P-containing donor vector pDONR™ 207 (50 fmol) in TE buffer (10 mM Tris Base, 1 mM EDTA, pH 8.0) were used for *in vitro* BP recombination reaction with BP Clonase™ II enzyme mix to yield the appropriate *att*L-containing entry clone. After transformation in chemically competent One Shot® TOP10 *E. coli* (Life Technologies Corp.), cells were plated on LB agar plates containing 7.5 µg/mL gentamycin. Clones of transformed cells were selected and grown in gentamycin 15 µg/mL LB medium. Plasmids were isolated using an E.Z.N.A.® Plasmid Mini Kit I (Omega Bio-Tek Inc.). The corresponding *att*B-containing expression clone was generated by *in vitro* LR recombination reaction of the *att*L-containing entry clone (50 fmol) and the *att*R-containing destination vector pET300 (50 fmol) using LR Clonase™ II enzyme mix in TE buffer. The expression clone was transformed in chemically competent *E. coli* BL21 (DE3) (Sigma Aldrich) and selected on LB agar plates containing 100 µg/mL ampicillin. Validity of the clone sequence was confirmed by plasmid sequence analysis by GATC Biotech AG. Sequence is shown in Table S14.

2.5.2. Cloning of VAT-1 and point mutants in human vector

The gene of interest His-TEV-tagged VAT-1 was cloned in the human vector pRK5SV40 with a bearing an ampicillin resistance and the restriction sites Xho1 and HindIII, which was generously provided by the MPI of Psychiatry (Munich). The vector pET300 encoding His-TEV-tagged VAT-1 (section 2.5.1.) was applied as a template for PCR according to Phusion® HF DNA Polymerase (New England Biolabs) manufacturer´s PCR protocol. Applied primers are listed in the table below. PCR product and vector were digested with the restriction enzyme XhoI (New England Biolabs) and HindIII (New England Biolabs) according to the manufacturer´s protocol. The digested vector was extracted from a 1% agarose gel by E.Z.N.A.® Gel Extraction Kit (Omega Bio-Tek Inc.) and the gene of interest was purified by E.Z.N.A. MicroElute Cycle Pure Kit (Omega Bio-Tek Inc.). Vector and gene were ligated with Quick Ligation Kit (New England Biolabs), transformed in *E.coli* Top10 and grown on LB agar plates supplemented with ampicillin (100 µg/mL).
QuikChange™ PCR was applied for the creation of the humane VAT-1 mutants. Primers are listed in the table below. Mutants are named corresponding to the location in the native VAT-1 protein (Table S2, sequence Table S14). Location in the His-TEV-VAT-1 construct is always shifted 23 residues to the c-terminus and is shown in brackets (Table S2, sequence Table

S14). After PCR according to Phusion DNA polymerase (New England Biolabs) manufacturer´s instructions, constructs were digested with DpnI (Promega) according to the manufacturer´s protocol, transformed in *E.coli* XL1-blue cells and grown on LB agar plates with ampicillin. Clones were isolated, grown in LB media with ampicillin and purified using an E.Z.N.A.® Plasmid Mini Kit I (Omega Bio-Tek Inc.). After sequencing, constructs were transformed in *E.coli* Top10 cells and were purified by QIAGEN Plasmid Midi Kit according to the manufacturer´s protocol. Sequencing services, sequencing primers, and PCR primers were provided by Eurofins Genomics GmbH (Ebersberg).

Table S2: Primer for human VAT-1 expression construct

Primer	Sequence
Xho1_TEV_VAT-1_fwd	5'-ccgctcgagatgcatcatcatcatcacatcacaagttt-3'
HindIII_VAT-1_rev	5'-gggaagcttctagttctccttctctggccctg-3'
T109V fwd (T132V)	5'-cgcctctgcctgtcgttccgggcatggagg-3'
T109V rev (T132V)	5'-cctccatgcccggaacgacaggcagaggcg-3'
E113Q fwd (E136Q)	5'-acccgcgccctgcatgcccggag-3'
E113Q rev (E136Q)	5'-ctccgggcatgcagggcgcgggt-3'
E123Q fwd (E146Q)	5'-cgctgactccctggcccactgcgat-3'
E123Q rev (E146Q)	5'-atcgcagtgggccagggagtcagcg-3'
S126A fwd (S149A)	5'-tgccttgcggtcggcgactccctcgccc-3'
S126A rev (S149A)	5'-gggcgagggagtcgccgaccgcaaggca-3'
D127N fwd (D150N)	5'-cctgccttgcggttgctgactccctcg-3'
D127N rev (D150N)	5'-cgagggagtcagcaaccgcaaggcagg-3'
R128K fwd (R128K)	5'-ccggtctcctgccttcttgtcgctgactccctc-3'
R128K rev (R128K)	5'-gagggagtcagcgacaagaaggcaggagaccgg-3'

2.5.3. Genome engineering using the CRISPR-Cas9 System

The CRISPR-Cas9 system was used to knock out VAT-1 in HEK293 cells as described by Ran *et al.*.[14] In brief, exon 2 of VAT-1 was removed leading to loss of function of the protein. For this purpose, single guide RNAs (sgRNAs) were designed as described by Haeussler *et al.*..[15] For experiments, the two highest ranked sgRNAs were used and ligated into the austriaeCas9_Puro2.0 plasmid using the T4 DNA ligase according to the manufacturer's protocol (New England BioLabs). Following transformation into competent DH5α-*E.coli*, plasmids were isolated using the QIAGEN Plasmid Maxiprep Kit (Qiagen) as described by the manufacturer. Two validated correct insertion plasmids were sequenced starting from the U6 promotor. HEK293 cells were transfected with respective plasmids using Lipofectamin™ 3000 reagent (Invitrogen) according to the manufacturer's protocol. Transfected cells were selected with puromycin and blasticidin S and genome targeting efficiency of different sgRNAs was investigated using T7 DNA endonuclease I according to the manufacturer's protocol (New England BioLabs). Cells were transfected with two sgRNA pairs respectively and diluted for selection of clones. Successful deletion of exon 2 was verified by PCR product size analysis using primer pairs in which either both primers anneal outside of the deleted region or one primer anneals outside and one within the deleted region.

Table S3: Primer for Genome engineering using the CRISPR-Cas9 System

sgRNA/Primer	Sequence
sgRNA-5'_1 top	5'-CACCGAAAGCACTTGAAATCGGGCT-3'
sgRNA-5'_1 bottom	5'-AAACAGCCCGATTTCAAGTGCTTTC-3'
sgRNA-5'_2 top	5'-CACCGTAGGGCAGCATGAAGTATTG-3'
sgRNA-5'_2 bottom	5'-AAACCGGCAACTACACAGCAGAGGC-3'
sgRNA-3' top	5'-CACCGCCTCTGCTGTGTAGTTGCCG-3'
sgRNA-3' bottom	5'-AAACCGGCAACTACACAGCAGAGGC-3'
out-fwd primer	5'-GCTCAAACACACTTCTCCCG-3'
out-rev primer	5'-CTCCCTACCCCCTCCCATAT-3'
in-fwd primer	5'-ATGTGGCAGGAAGAGGTGAC-3'
out-rev primer	5'-CCATTCTCCTTCAGTGCCTC- 3'

Knockout of VAT-1 in identified clones was confirmed by sequencing and Western blot. Sequencing services, sequencing primers, cloning oligomers and PCR primers were provided by Eurofins Genomics GmbH. Additionally, to HEK293 WT cells, the clone cell line *CRISPR control* was isolated which was subjected to the complete CRISPR-Cas9 procedure but did not result in successful knockout of VAT-1 and used as control in all experiments.

2.6. Transfection of cells

MDA-MB-231 and 4T1-luc2 cells were transfected with non-targeting control siRNA or siRNA targeting VAT-1 (Dharmacon™, GE Healthcare) for 48 h using DharmaFECT™ transfection reagent according to manufacturer's protocol (Dharmacon™, GE Healthcare).
For plasmid transfection, MDA-MB-231 were seeded in 12-well plates and were transfected at 90% confluence. Cells were transfected with Lipofectamin3000 (ThermoFisher Scientific) according to the manufacturer's instructions. 1 µg of plasmid DNA which was purified by QUIAGEN MidiPrep Kit was applied for complex formation in serum-fee Opti-MEM medium (ThermoFisher Scientific) per well. Transfection was performed at 37 °C for 48 h in DMEM supplemented with FBS. Expressed VAT-1 constructs were labeled with **NC-1** according to section 2.1.

2.7. Protein expression of VAT-1 in *E.coli*

2.7.1. Protein expression and analytical labeling in *E.coli*

E.coli BL21 (DE3) cells transformed with pET300-TEV-VAT-1 were grown in LB medium supplemented with ampicillin (100 µg/mL) and target gene expression was induced with 500 µM isopropyl β-D-thiogalactopyranoside (IPTG) at 22 °C for 3 h. Cells were harvested at 6000xg for 15 min at 4 °C. The cells were resuspended in PBS to a theoretical OD_{600} of 40 and 200 µL were labelled with 5 µM probe **NC-1** (1% DMSO) for 1 h at rt. A control with no induction of protein expression was additionally added to each experiment. Cells were pelletized, washed with 800 µL PBS and lysed by sonication on ice (3 x 20 sec, 85% of maximal intensity). Membrane and cytosol fraction were separated by centrifugation at 21,000xg for 30 min at 4 °C and membrane fraction was additionally washed with 800 µL PBS. Membrane fraction was resuspended in 100 µL PBS. For click reaction, 50 µl of membrane or respectively cytosolic fraction were incubated with 0.1 mM 5-TAMRA-N_3 (5 mM in DMSO), 1 mM TCEP (50 mM in ddH_2O), 0.1 mM TBTA ligand (1.667 mM in 80% tBuOH and 20% DMSO)) and 1 mM $CuSO_4$ (50 mM in ddH_2O). Reaction was carried at rt for 1 h and was quenched by addition of 50 µL 2 x SDS loading buffer. For SDS-PAGE, 50 µL were applied on an analytical 12.5% SDS gel.

2.7.2. Recombinant protein purification and intact protein MS

E.coli BL21 (DE3) cells were transformed with a pET300 expression vector encoding the human VAT-1 with a N-terminal His-TEV tag. The cells were grown in two liters of LB medium supplemented with ampicillin (100 µg/mL) at 37 °C to OD_{600} ~ 0.6 and protein expression was induced with 500 µM IPTG for 3 h at 22 °C. Cells were harvested at 6000xg for 15 min at 4 °C, washed in PBS (140 mM NaCl, 10 mM Na_2HPO_4, 2.7 mM KCl, 1.8 mM KH_2PO_4, pH 7.6), resuspended in His-binding buffer (20 mM Tris, 150 mM NaCl, 10% glycerin, 1 mM DTT, 10 mM imidazole, pH 8.0) and lysed on ice by ultrasonication (20 min in total, 80% of maximal intensity) (Bandolin sonupuls). Cell debris was pelletized at 18,000 rpm (30 min, 4 °C) for 30 min at 4 °C and cell lysates were loaded onto a HisTrap HP (5 mL, GE Healthcare) by an Äkta system (GE Healthcare). The protein of interest was washed with 20 mM and 40 mM imidazole and was eluted in His-elution buffer (20 mM Tris, 150 mM NaCl, 10% glycerin, 1 mM DTT, 500 mM imidazole, pH 8.0). Protein containing fractions were loaded onto a Superose6 prep grade column (130 mL, GE Healthcare) with gel filtration buffer (20 mM Tris, 150 mM NaCl, 1 mM DTT, 10% glycerol, pH 8.0). Fractions containing VAT-1 were pooled and concentrated using centrifugal filter tubes with a molecular weight cut-off of 30 kDa. Protein concentration was determined by absorbance measurement at 280 nm with a Nanoquant plate in an Infinite F200 Pro reader (Tecan). Proteins were stored at -80 °C for further use. Protein size was verified by intact protein mass spectrometry measurements.

2.7.3. Intact protein MS

LC-MS analysis of intact proteins was performed on a Dionex UltiMate 3000 HPLC system coupled to a Thermo LTQ-FT Ultra mass spectrometer with an electrospray ionization source (capillary temp 275 °C, spray voltage 4.0 kV, tube lens 110 V, capillary voltage 48 V, sheath gas 60 arb, aux gas 10 arb, sweep gas 0.2 arb). Desalting was carried out with Massprep online desalting cartridges (Waters Corp.). Briefly, proteins were loaded in 1% FA and eluted in a 5 min gradient from 6 to 95% acetonitrile, 1% FA. The mass spectrometer was operated in positive mode collecting full scans at high resolution (R = 200,000) from m/z = 600 to m/z = 2000. Data analysis and deconvolution was performed using *Thermo Xcalibur Xtract* software.

2.7.4. VAT-1 *in vitro* labeling

For validation of covalent binding, 2 µM of recombinant TEV-VAT-1 were labeled in a final volume of 50 µL PBS with 1 µL of the probe **NC-1** (DMSO stock) at various concentrations for 1 h at rt. Heat control and no enzyme control were included. Click chemistry was performed with 0.2 mM Rh-N_3 (10 mM in DMSO), 1 mM TCEP (52 mM in ddH_2O), 0.1 mM TBTA ligand (1.667 mM in 80% tBuOH and 20% DMSO)), 1.0 mM $CuSO_4$ (50 mM in ddH_2O) for 1h at rt. Reaction was quenched with 50 µL 2x SDS loading buffer and SDS PAGE was performed as described before.

3. Supplementary Tables

Table S4: Hits matching the criteria ($(\log_2(\text{enrichment}) > 2$, p-value < 0.05) of SILAC targetID with 500 nM **NC-1** in MDA-MB-231

protein name	gene name	enrichment	p-value	sequence coverage [%]
Synaptic vesicle membrane protein VAT-1 homolog	VAT1	4.49	5.19	57
Reticulon	RTN3	4.23	3.16	22
Heme oxygenase 2	HMOX2	3.68	3.85	66.8
Redox-regulatory protein FAM213A	FAM213A	2.97	3.37	29.3
Transcriptional enhancer factor TEF-1	TEAD1	2.65	4.65	23
Glutathione S-transferase omega-1	GSTO1	2.55	4.36	49
Endonuclease domain-containing 1 protein	ENDOD1	2.55	4.76	16.2
Cytochrome b5 type B	CYB5B	2.29	4.13	50.7

Table S5: Hits matching the criteria ($(\log_2(\text{enrichment}) > 2$, p-value < 0.05) of LFQ targetID with 100 nM **NC-1** and hits matching the criteria ($(\log_2(\text{enrichment}) > 1.5$, p-value < 0.05) for competition with 500 nM **NCA** in MDA-MB-231

protein name	gene name	enrichment	p-value	sequence coverage [%]
Synaptic vesicle membrane protein VAT-1 homolog	VAT1	5.77	5.00	27
Heme oxygenase 2	HMOX2	5.07	4.67	34.5
Cytochrome b5 type B	CYB5B	2.58	3.00	18
Mitochondrial antiviral-signaling protein	MAVS	2.52	2.32	19.8
competition				
Synaptic vesicle membrane protein VAT-1 homolog	VAT1	2.98	2.23	27
Heme oxygenase 2	HMOX2	1.82	2.16	34.5

Table S6: Hits matching the criteria ((log_2(enrichment) > 1, p-value < 0.05) of VAT-1 co-IP with DSSO crosslinker in MDA-MB-231

protein name	gene name	enrichment	p-value	sequence coverage [%]
Synaptic vesicle membrane protein VAT-1 homolog	VAT1	10.03	3.33	70.5
Gelsolin	GSN	9.17	2.89	37.2
Talin-1	TLN1	7.19	3.32	44.6
Complement C5	C5	7.13	2.24	5.4
Alpha-2-macroglobulin	A2M	7.11	2.31	6
Aspartate--tRNA ligase, mitochondrial	DARS2	7.10	2.32	44.7
Complement C4-A	C4A	7.01	2.20	7.5
Thrombospondin-1	THBS1	6.67	2.01	15.9
Inter-alpha-trypsin inhibitor heavy chain H2	ITIH2	6.62	2.33	9.4
Serum paraoxonase/arylesterase 1	PON1	6.34	2.20	8.5
UTP--glucose-1-phosphate uridylyltransferase	UGP2	6.33	2.39	46.7
L-lactate dehydrogenase	LDHA	6.13	2.62	74.7
Peroxisomal multifunctional enzyme type 2	HSD17B4	6.02	2.08	53.4
Complement C3	C3	5.60	1.99	4.6
Heat shock protein 75 kDa, mitochondrial	TRAP1	5.52	3.16	27.5
Histidine-rich glycoprotein	HRG	5.52	1.83	1.9
Fibronectin	FN1	5.44	1.86	6.4
Succinate dehydrogenase [ubiquinone] flavoprotein subunit, mitochondrial	SDHA	5.33	3.11	47.9
L-lactate dehydrogenase	LDHB	5.32	3.34	46.4
Complement component 1 Q subcomponent-binding protein, mitochondrial	C1QBP	5.27	4.12	33.7
Inter-alpha-trypsin inhibitor heavy chain H1	ITIH1	5.25	1.81	3.6

Ceruloplasmin	CP	5.20	2.00	14.1
Glutathione peroxidase	GPX3	5.20	1.78	10.7
Cofilin-1	CFL1	5.20	2.29	61.4
Endoplasmin	TRA1	5.16	1.92	67
Inter-alpha-trypsin inhibitor heavy chain H3	ITIH3	4.93	1.62	13.4
Serpin H1	SERPINH1	4.78	1.62	40.2
Polyribonucleotide nucleotidyltransferase 1, mitochondrial	PNPT1	4.69	2.09	32.6
Monofunctional C1-tetrahydrofolate synthase, mitochondrial	MTHFD1L	4.63	2.44	23.7
Complement component C8 beta chain	C8B	4.44	2.09	14.4
Vinculin	VCL	4.22	2.95	17.8
Filamin-A	FLNA	4.21	1.99	39.6
Cytochrome b-c1 complex subunit 2, mitochondrial	UQCRC2	4.17	1.55	44.2
Pyruvate carboxylase	PC	4.12	1.91	40.7
Nucleoside diphosphate kinase	NME2	4.10	3.33	55.1
Malate dehydrogenase	MDH2	4.06	1.85	64.6
Alkyldihydroxyacetonephosphate synthase, peroxisomal	AGPS	4.03	3.10	34.5
	MYL6	4.01	2.19	65.1
Complement factor B	CFB	3.96	1.59	4.8
Procollagen galactosyltransferase 1	COLGALT1	3.88	2.03	17.7
Leucine-rich PPR motif-containing protein, mitochondrial	LRPPRC	3.87	1.39	49
Fructose-bisphosphate aldolase;Fructose-bisphosphate aldolase A	ALDOA	3.87	1.80	54.4
Glutaminase kidney isoform, mitochondrial	GLS	3.78	1.91	39.5
Ras-related protein Rab-1B	RAB1B	3.78	2.58	66.2

Procollagen-lysine,2-oxoglutarate 5-dioxygenase 3	PLOD3	3.65	1.57	33.9
Transmembrane protein 33	TMEM33	3.63	2.42	26.3
Plastin-2	LCP1	3.54	1.90	15.6
Tropomyosin alpha-4 chain	TPM4	3.46	2.46	52.4
Serum paraoxonase/lactonase 3	PON3	3.46	1.99	11
Succinate dehydrogenase [ubiquinone] iron-sulfur subunit, mitochondrial	SDHB	3.45	1.77	20
GDP-fucose protein O-fucosyltransferase 1	POFUT1	3.45	1.51	11.9
Acyl-coenzyme A thioesterase 8	ACOT8	3.42	1.84	25.7
Aconitate hydratase, mitochondrial	ACO2	3.41	2.51	18.8
Aldehyde dehydrogenase, mitochondrial	ALDH2	3.32	1.56	29.8
Medium-chain specific acyl-CoA dehydrogenase, mitochondrial	ACADM	3.31	3.21	30.9
Serotransferrin	TF	3.26	1.33	7.5
Proteasome subunit alpha type	PSMA5	3.15	2.61	17
Mitochondrial import receptor subunit TOM70	TOMM70A	3.02	1.84	20.7
Mitochondrial dicarboxylate carrier	SLC25A10	2.99	2.67	16.7
60S ribosomal protein L28	RPL28	2.87	1.31	32.9
Adipocyte plasma membrane-associated protein	APMAP	2.82	1.77	21.8
Proteasome subunit alpha type	PSMA7	2.78	1.80	28.2
Cell division control protein 42 homolog	CDC42	2.60	1.56	52.4
Sodium/potassium-transporting ATPase subunit alpha-1	ATP1A1	2.60	1.84	34.6
60S ribosomal protein L27	RPL27	2.59	1.69	22.2
CD44 antigen	CD44	2.57	1.74	29.1
Acetyl-CoA acetyltransferase, mitochondrial	ACAT1	2.56	2.26	25.1

Solute carrier family 2, facilitated glucose transporter member 1	SLC2A1	2.53	2.30	8.4
Tyrosine-protein phosphatase non-receptor type	PTPN1	2.49	1.47	16.8
ATP-dependent Clp protease ATP-binding subunit clpX-like, mitochondrial	CLPX	2.48	2.53	22.7
Ras-related C3 botulinum toxin substrate 2	RAC2	2.44	2.75	31.2
Procollagen-lysine,2-oxoglutarate 5-dioxygenase 1	PLOD1	2.38	1.53	18.2
Glutamate dehydrogenase	GLUD1	2.26	1.64	52.3
Elongation factor Tu, mitochondrial	TUFM	2.21	1.73	43.6
Integrin beta-1	ITGB1	2.20	2.95	8.3
Isoleucine--tRNA ligase, mitochondrial	IARS2	2.19	1.97	13.6
Ras-related protein Rab-11B	RAB11B	2.16	1.31	50
Voltage-dependent anion-selective channel protein 1	VDAC1	2.12	1.32	67.5
Hypoxia up-regulated protein 1	HYOU1	1.84	2.89	20.4
Neutral alpha-glucosidase AB	GANAB	1.83	1.97	32.8
Microtubule-associated protein RP/EB family member 1	MAPRE1	1.77	1.61	31.5
Transferrin receptor protein 1	TFRC	1.75	2.16	33.2
10 kDa heat shock protein, mitochondrial	HSPE1	1.74	1.54	55.9
Protein disulfide-isomerase A6	PDIA6	1.52	1.73	35.5
Endoplasmic reticulum resident protein 29	HEL-S-107	1.49	1.84	14.6
60 kDa heat shock protein, mitochondrial	HSPD1	1.43	2.90	79.8
Protein disulfide-isomerase	PDIA3	1.19	2.90	51.2

Table S7: Hits matching the criteria ($(\log_2$(t-test difference) > 1, p-value < 0.05) of LFQ global proteome with 500 nM **NCA** in MDA-MB-231

protein name	gene name	enrichment	p-value	sequence coverage [%]
depleted				
Prostaglandin reductase 2	PTGR2	-6.01	3.02	26.5
Proteasome subunit beta type-10	PSMB10	-3.64	1.96	23.4
Tetratricopeptide repeat protein 17	TTC17	-5.41	2.78	3.8
Prenylated Rab acceptor protein 1	RABAC1	-8.35	3.80	19.2
Vacuolar protein sorting-associated protein 37C	VPS37C	-2.56	1.37	33.8
Tubulin beta-4A chain	TUBB4A	-2.62	1.40	57
[3-methyl-2-oxobutanoate dehydrogenase [lipoamide]] kinase, mitochondrial	BCKDK	-2.63	1.41	19.2
Guanine nucleotide exchange factor MSS4	RABIF	-3.80	2.05	29.3
Delta-like protein	JAG1	-2.79	1.50	4.5
WD repeat-containing protein 43	WDR43	-2.55	1.36	8.3
Bcl2-associated agonist of cell death	BAD	-4.47	2.37	69.1
28S ribosomal protein S18c, mitochondrial	MRPS18C	-2.68	1.44	16.8
Molybdenum cofactor sulfurase	MOCOS	-2.52	1.34	8.7
Mannose-P-dolichol utilization defect 1 protein	MPDU1	-3.78	2.04	20.6
enriched				
Rab GTPase-binding effector protein 1	RABEP1	1.64	1.32	10.7
cAMP-dependent protein kinase catalytic subunit beta	PRKACB	1.33	1.80	40.7
Ribonuclease T2	RNASET2	1.29	1.59	17.9
Cytosolic Fe-S cluster assembly factor NUBP1	NUBP1	1.21	2.08	11.2
Suppressor of tumorigenicity 7 protein-like	ST7	1.17	1.62	7.1
Protein Njmu-R1	C17orf75	1.17	2.52	12.6

Rho-related GTP-binding protein RhoF	RHOF	1.05	1.49	46

Table S8: Cytoscape GO enrichment analysis of VAT-1 co-IP: Biological process

GO-ID	description	corr p-value	co-IP [%]	global [%]
19752	carboxylic acid metabolic process	2.47E-13	5.04	33.33
43436	oxoacid metabolic process	1.52E-12	5.54	33.33
6082	organic acid metabolic process	1.75E-12	5.66	33.33
44281	small molecule metabolic process	1.95E-11	10.20	41.38
55114	oxidation-reduction process	1.38E-09	5.40	28.74
8152	metabolic process	1.03E-07	47.49	80.46
52547	regulation of peptidase activity	1.03E-07	2.43	18.39
2576	platelet degranulation	2.12E-07	0.72	11.49
71704	organic substance metabolic process	1.18E-06	44.94	75.86
44237	cellular metabolic process	1.33E-06	42.72	73.56
52548	regulation of endopeptidase activity	2.25E-06	2.27	16.09
10951	negative regulation of endopeptidase activity	5.98E-06	1.36	12.64
10466	negative regulation of peptidase activity	8.01E-06	1.41	12.64
1901564	organonitrogen compound metabolic process	1.15E-05	30.67	58.62
6986	response to unfolded protein	1.43E-05	0.89	10.34
44283	small molecule biosynthetic process	2.71E-05	3.34	17.24
43687	post-translational protein modification	2.71E-05	2.02	13.79
45055	regulated exocytosis	2.80E-05	3.86	18.39
97435	supramolecular fiber organization	2.94E-05	2.47	14.94
35966	response to topologically incorrect protein	3.27E-05	1.02	10.34
30162	regulation of proteolysis	3.27E-05	3.95	18.39
6957	complement activation, alternative pathway	4.43E-05	0.07	4.60
30029	actin filament-based process	4.71E-05	3.08	16.09
17144	drug metabolic process	6.25E-05	3.66	17.24
43648	dicarboxylic acid metabolic process	7.94E-05	0.58	8.05

32787	monocarboxylic acid metabolic process	8.23E-05	2.80	14.94
32940	secretion by cell	8.23E-05	5.46	20.69
44238	primary metabolic process	8.23E-05	43.08	68.97
46903	secretion	8.23E-05	6.09	21.84
45861	negative regulation of proteolysis	8.23E-05	1.94	12.64
6887	exocytosis	8.23E-05	4.36	18.39
30449	regulation of complement activation	1.00E-04	0.63	8.05
72350	tricarboxylic acid metabolic process	1.00E-04	0.22	5.75
7015	actin filament organization	1.63E-04	1.31	10.34
30036	actin cytoskeleton organization	2.50E-04	2.67	13.79
16999	antibiotic metabolic process	2.54E-04	0.73	8.05
2920	regulation of humoral immune response	2.54E-04	0.73	8.05
46395	carboxylic acid catabolic process	2.70E-04	1.42	10.34
16054	organic acid catabolic process	2.70E-04	1.42	10.34
6810	transport	3.01E-04	24.70	47.13
46394	carboxylic acid biosynthetic process	3.02E-04	1.85	11.49
16053	organic acid biosynthetic process	3.03E-04	1.85	11.49
44282	small molecule catabolic process	3.44E-04	2.33	12.64
51179	localization	5.34E-04	31.29	54.02
51234	establishment of localization	5.48E-04	25.37	47.13
44419	interspecies interaction between organisms	5.65E-04	4.05	16.09
51346	negative regulation of hydrolase activity	5.94E-04	2.49	12.64
6950	response to stress	6.41E-04	19.10	39.08
6457	protein folding	6.50E-04	1.23	9.20
43062	extracellular structure organization	6.74E-04	2.07	11.49
9987	cellular process	7.51E-04	80.82	96.55
30212	hyaluronan metabolic process	7.71E-04	0.17	4.60
5975	carbohydrate metabolic process	8.26E-04	2.62	12.64
1901135	carbohydrate derivative metabolic process	1.03E-03	6.20	19.54
6732	coenzyme metabolic process	1.03E-03	1.75	10.34
6090	pyruvate metabolic process	1.03E-03	0.39	5.75

6099	tricarboxylic acid cycle	1.03E-03	0.19	4.60
44248	cellular catabolic process	1.04E-03	9.76	25.29
34976	response to endoplasmic reticulum stress	1.04E-03	1.35	9.20
6091	generation of precursor metabolites and energy	1.05E-03	2.23	11.49
44403	symbiont process	1.05E-03	3.80	14.94
6101	citrate metabolic process	1.05E-03	0.20	4.60
9060	aerobic respiration	1.05E-03	0.40	5.75
30198	extracellular matrix organization	1.22E-03	1.82	10.34
16192	vesicle-mediated transport	1.23E-03	10.70	26.44
6826	iron ion transport	1.23E-03	0.41	5.75
6807	nitrogen compound metabolic process	1.25E-03	40.26	62.07
16051	carbohydrate biosynthetic process	1.25E-03	0.69	6.90
51336	regulation of hydrolase activity	1.33E-03	7.13	20.69
43650	dicarboxylic acid biosynthetic process	1.50E-03	0.08	3.45
10033	response to organic substance	1.77E-03	15.93	33.33
2252	immune effector process	1.80E-03	5.96	18.39
42398	cellular modified amino acid biosynthetic process	2.06E-03	0.24	4.60
10810	regulation of cell-substrate adhesion	2.32E-03	1.15	8.05
6094	gluconeogenesis	2.32E-03	0.25	4.60
1902743	regulation of lamellipodium organization	2.32E-03	0.25	4.60
2697	regulation of immune effector process	2.32E-03	2.53	11.49
51246	regulation of protein metabolic process	2.32E-03	15.39	32.18
46946	hydroxylysine metabolic process	2.32E-03	0.02	2.30
46947	hydroxylysine biosynthetic process	2.32E-03	0.02	2.30
72512	trivalent inorganic cation transport	2.32E-03	0.02	2.30
42060	wound healing	2.75E-03	2.59	11.49
19319	hexose biosynthetic process	2.81E-03	0.27	4.60
55086	nucleobase-containing small molecule metabolic process	3.05E-03	3.75	13.79
72521	purine-containing compound metabolic process	3.81E-03	2.71	11.49

30968	endoplasmic reticulum unfolded protein response	3.99E-03	0.56	5.75
46364	monosaccharide biosynthetic process	4.12E-03	0.30	4.60
960	regulation of mitochondrial RNA catabolic process	4.12E-03	0.02	2.30
21943	formation of radial glial scaffolds	4.12E-03	0.02	2.30
2001027	negative regulation of endothelial cell chemotaxis	4.12E-03	0.02	2.30
7161	calcium-independent cell-matrix adhesion	4.12E-03	0.02	2.30
51186	cofactor metabolic process	4.28E-03	2.78	11.49
36498	IRE1-mediated unfolded protein response	4.28E-03	0.31	4.60
9056	catabolic process	4.42E-03	11.09	25.29
16032	viral process	4.60E-03	3.38	12.64
6635	fatty acid beta-oxidation	4.76E-03	0.32	4.60
50776	regulation of immune response	4.87E-03	5.96	17.24
9150	purine ribonucleotide metabolic process	5.90E-03	2.37	10.34
72329	monocarboxylic acid catabolic process	5.90E-03	0.63	5.75
19835	cytolysis	6.37E-03	0.14	3.45
6956	complement activation	6.39E-03	1.00	6.90
42981	regulation of apoptotic process	6.72E-03	8.34	20.69
10811	positive regulation of cell-substrate adhesion	7.21E-03	0.66	5.75
2443	leukocyte mediated immunity	7.21E-03	4.22	13.79
42221	response to chemical	7.21E-03	24.16	41.38
9259	ribonucleotide metabolic process	7.21E-03	2.46	10.34
43067	regulation of programmed cell death	7.37E-03	8.44	20.69
6605	protein targeting	7.46E-03	1.96	9.20
6163	purine nucleotide metabolic process	7.50E-03	2.48	10.34
34620	cellular response to unfolded protein	7.90E-03	0.68	5.75
41	transition metal ion transport	8.13E-03	0.69	5.75
6537	glutamate biosynthetic process	8.31E-03	0.03	2.30
30155	regulation of cell adhesion	8.34E-03	3.70	12.64
1901607	alpha-amino acid biosynthetic process	8.34E-03	0.39	4.60

9611	response to wounding	8.34E-03	3.10	11.49
1902905	positive regulation of supramolecular fiber organization	8.34E-03	1.08	6.90
43086	negative regulation of catalytic activity	8.61E-03	4.35	13.79
19693	ribose phosphate metabolic process	8.83E-03	2.57	10.34
5996	monosaccharide metabolic process	9.74E-03	1.12	6.90
16064	immunoglobulin mediated immune response	9.74E-03	1.12	6.90
2682	regulation of immune system process	9.91E-03	8.74	20.69
19724	B cell mediated immunity	1.00E-02	1.13	6.90
1901575	organic substance catabolic process	1.00E-02	9.54	21.84
51702	interaction with symbiont	1.01E-02	0.41	4.60
2000427	positive regulation of apoptotic cell clearance	1.03E-02	0.04	2.30
1903896	positive regulation of IRE1-mediated unfolded protein response	1.03E-02	0.04	2.30
1902235	regulation of endoplasmic reticulum stress-induced intrinsic apoptotic signaling pathway	1.05E-02	0.18	3.45
71702	organic substance transport	1.05E-02	12.05	25.29
9117	nucleotide metabolic process	1.05E-02	3.24	11.49
7596	blood coagulation	1.08E-02	1.62	8.05
19395	fatty acid oxidation	1.10E-02	0.43	4.60
50817	coagulation	1.10E-02	1.63	8.05
10591	regulation of lamellipodium assembly	1.10E-02	0.18	3.45
6753	nucleoside phosphate metabolic process	1.10E-02	3.28	11.49
34440	lipid oxidation	1.13E-02	0.44	4.60
9058	biosynthetic process	1.13E-02	16.51	31.03
7599	hemostasis	1.14E-02	1.65	8.05
50878	regulation of body fluid levels	1.16E-02	2.72	10.34
2001233	regulation of apoptotic signaling pathway	1.17E-02	2.17	9.20
3012	muscle system process	1.18E-02	1.66	8.05
17185	peptidyl-lysine hydroxylation	1.22E-02	0.04	2.30
51248	negative regulation of protein metabolic process	1.22E-02	6.01	16.09

1900026	positive regulation of substrate adhesion-dependent cell spreading	1.22E-02	0.20	3.45
1905897	regulation of response to endoplasmic reticulum stress	1.22E-02	0.45	4.60
9892	negative regulation of metabolic process	1.22E-02	15.76	29.89
35967	cellular response to topologically incorrect protein	1.22E-02	0.80	5.75
45785	positive regulation of cell adhesion	1.22E-02	2.21	9.20
15980	energy derivation by oxidation of organic compounds	1.27E-02	1.23	6.90
33572	transferrin transport	1.28E-02	0.20	3.45
10941	regulation of cell death	1.30E-02	9.10	20.69
9205	purine ribonucleoside triphosphate metabolic process	1.31E-02	1.24	6.90
6631	fatty acid metabolic process	1.32E-02	1.72	8.05
71705	nitrogen compound transport	1.40E-02	9.99	21.84
72594	establishment of protein localization to organelle	1.40E-02	2.28	9.20
8652	cellular amino acid biosynthetic process	1.40E-02	0.48	4.60
33622	integrin activation	1.40E-02	0.05	2.30
2000425	regulation of apoptotic cell clearance	1.40E-02	0.05	2.30
6105	succinate metabolic process	1.40E-02	0.05	2.30
19538	protein metabolic process	1.42E-02	24.51	40.23
9199	ribonucleoside triphosphate metabolic process	1.42E-02	1.27	6.90
9144	purine nucleoside triphosphate metabolic process	1.44E-02	1.28	6.90
33036	macromolecule localization	1.53E-02	13.46	26.44
45333	cellular respiration	1.53E-02	0.86	5.75
9062	fatty acid catabolic process	1.53E-02	0.50	4.60
65008	regulation of biological quality	1.58E-02	21.79	36.78
32268	regulation of cellular protein metabolic process	1.58E-02	14.42	27.59
2001242	regulation of intrinsic apoptotic signaling pathway	1.58E-02	0.88	5.75

19318	hexose metabolic process	1.58E-02	0.88	5.75
70486	leukocyte aggregation	1.58E-02	0.06	2.30
21932	hindbrain radial glia guided cell migration	1.58E-02	0.06	2.30
51918	negative regulation of fibrinolysis	1.58E-02	0.06	2.30
2836	positive regulation of response to tumor cell	1.58E-02	0.06	2.30
2839	positive regulation of immune response to tumor cell	1.58E-02	0.06	2.30
1903897	regulation of PERK-mediated unfolded protein response	1.58E-02	0.06	2.30
6520	cellular amino acid metabolic process	1.60E-02	1.82	8.05
22603	regulation of anatomical structure morphogenesis	1.61E-02	5.60	14.94
34613	cellular protein localization	1.63E-02	8.62	19.54
71622	regulation of granulocyte chemotaxis	1.68E-02	0.24	3.45
70727	cellular macromolecule localization	1.71E-02	8.66	19.54
34329	cell junction assembly	1.74E-02	0.91	5.75
6958	complement activation, classical pathway	1.74E-02	0.91	5.75
2001243	negative regulation of intrinsic apoptotic signaling pathway	1.75E-02	0.53	4.60
1903018	regulation of glycoprotein metabolic process	1.75E-02	0.24	3.45
51235	maintenance of location	1.76E-02	0.91	5.75
70527	platelet aggregation	1.86E-02	0.25	3.45
98657	import into cell	1.86E-02	3.67	11.49
2455	humoral immune response mediated by circulating immunoglobulin	1.86E-02	0.93	5.75
19058	viral life cycle	1.86E-02	0.93	5.75
6936	muscle contraction	1.86E-02	1.38	6.90
6959	humoral immune response	1.88E-02	1.90	8.05
9141	nucleoside triphosphate metabolic process	1.88E-02	1.39	6.90
1901566	organonitrogen compound biosynthetic process	1.90E-02	8.01	18.39

50778	positive regulation of immune response	2.00E-02	4.39	12.64
30199	collagen fibril organization	2.00E-02	0.26	3.45
35722	interleukin-12-mediated signaling pathway	2.00E-02	0.26	3.45
51130	positive regulation of cellular component organization	2.03E-02	6.55	16.09
2000377	regulation of reactive oxygen species metabolic process	2.03E-02	0.96	5.75
1903894	regulation of IRE1-mediated unfolded protein response	2.03E-02	0.07	2.30
1775	cell activation	2.04E-02	5.82	14.94
19637	organophosphate metabolic process	2.09E-02	5.84	14.94
2449	lymphocyte mediated immunity	2.09E-02	1.43	6.90
71349	cellular response to interleukin-12	2.19E-02	0.27	3.45
2253	activation of immune response	2.23E-02	3.16	10.34
7010	cytoskeleton organization	2.27E-02	5.91	14.94
70671	response to interleukin-12	2.27E-02	0.27	3.45
2834	regulation of response to tumor cell	2.27E-02	0.07	2.30
2837	regulation of immune response to tumor cell	2.27E-02	0.07	2.30
36109	alpha-linolenic acid metabolic process	2.27E-02	0.07	2.30
1900103	positive regulation of endoplasmic reticulum unfolded protein response	2.27E-02	0.07	2.30
1903510	mucopolysaccharide metabolic process	2.28E-02	0.59	4.60
7159	leukocyte cell-cell adhesion	2.35E-02	0.28	3.45
1900024	regulation of substrate adhesion-dependent cell spreading	2.35E-02	0.28	3.45
2684	positive regulation of immune system process	2.37E-02	5.97	14.94
2460	adaptive immune response based on somatic recombination of immune receptors built from immunoglobulin superfamily domains	2.43E-02	1.50	6.90
32655	regulation of interleukin-12 production	2.45E-02	0.29	3.45
71345	cellular response to cytokine stimulus	2.45E-02	5.27	13.79

2688	regulation of leukocyte chemotaxis	2.45E-02	0.61	4.60
19439	aromatic compound catabolic process	2.46E-02	2.62	9.20
8104	protein localization	2.46E-02	11.64	22.99
60009	Sertoli cell development	2.46E-02	0.08	2.30
51917	regulation of fibrinolysis	2.46E-02	0.08	2.30
19372	lipoxygenase pathway	2.46E-02	0.08	2.30
44794	positive regulation by host of viral process	2.46E-02	0.08	2.30
43170	macromolecule metabolic process	2.46E-02	35.06	50.57
10952	positive regulation of peptidase activity	2.51E-02	1.04	5.75
2000378	negative regulation of reactive oxygen species metabolic process	2.60E-02	0.30	3.45
51128	regulation of cellular component organization	2.60E-02	13.46	25.29
1901576	organic substance biosynthetic process	2.64E-02	16.18	28.74
6006	glucose metabolic process	2.65E-02	0.63	4.60
33540	fatty acid beta-oxidation using acyl-CoA oxidase	2.72E-02	0.08	2.30
21535	cell migration in hindbrain	2.72E-02	0.08	2.30
71801	regulation of podosome assembly	2.72E-02	0.08	2.30
46034	ATP metabolic process	2.72E-02	1.06	5.75
32880	regulation of protein localization	2.85E-02	5.42	13.79
70887	cellular response to chemical stimulus	2.92E-02	15.42	27.59
34109	homotypic cell-cell adhesion	2.92E-02	0.31	3.45
6886	intracellular protein transport	3.01E-02	5.46	13.79
34975	protein folding in endoplasmic reticulum	3.02E-02	0.09	2.30
32695	negative regulation of interleukin-12 production	3.02E-02	0.09	2.30
50922	negative regulation of chemotaxis	3.02E-02	0.32	3.45
43065	positive regulation of apoptotic process	3.06E-02	3.40	10.34
50790	regulation of catalytic activity	3.06E-02	12.82	24.14
44092	negative regulation of molecular function	3.11E-02	6.25	14.94
6165	nucleoside diphosphate phosphorylation	3.11E-02	0.33	3.45

6626	protein targeting to mitochondrion	3.11E-02	0.33	3.45
43068	positive regulation of programmed cell death	3.12E-02	3.42	10.34
2366	leukocyte activation involved in immune response	3.12E-02	3.42	10.34
22617	extracellular matrix disassembly	3.22E-02	0.33	3.45
2263	cell activation involved in immune response	3.23E-02	3.44	10.34
71711	basement membrane organization	3.25E-02	0.10	2.30
7597	blood coagulation, intrinsic pathway	3.25E-02	0.10	2.30
6839	mitochondrial transport	3.27E-02	1.13	5.75
9888	tissue development	3.30E-02	9.52	19.54
46939	nucleotide phosphorylation	3.30E-02	0.34	3.45
1666	response to hypoxia	3.30E-02	1.65	6.90
48584	positive regulation of response to stimulus	3.36E-02	12.98	24.14
50920	regulation of chemotaxis	3.42E-02	1.15	5.75
43281	regulation of cysteine-type endopeptidase activity involved in apoptotic process	3.45E-02	1.15	5.75
72522	purine-containing compound biosynthetic process	3.45E-02	1.15	5.75
7160	cell-matrix adhesion	3.45E-02	0.71	4.60
34755	iron ion transmembrane transport	3.48E-02	0.10	2.30
43649	dicarboxylic acid catabolic process	3.48E-02	0.10	2.30
34330	cell junction organization	3.48E-02	1.16	5.75
32269	negative regulation of cellular protein metabolic process	3.60E-02	5.66	13.79
32963	collagen metabolic process	3.63E-02	0.35	3.45
48523	negative regulation of cellular process	3.70E-02	25.53	39.08
36293	response to decreased oxygen levels	3.77E-02	1.71	6.90
9084	glutamine family amino acid biosynthetic process	3.80E-02	0.11	2.30
48519	negative regulation of biological process	3.80E-02	28.65	42.53
6879	cellular iron ion homeostasis	3.88E-02	0.36	3.45
31532	actin cytoskeleton reorganization	3.88E-02	0.36	3.45

51495	positive regulation of cytoskeleton organization	3.88E-02	1.20	5.75
2009	morphogenesis of an epithelium	3.90E-02	2.31	8.05
51641	cellular localization	3.95E-02	13.23	24.14
34097	response to cytokine	3.95E-02	5.76	13.79
2376	immune system process	4.00E-02	15.06	26.44
6952	defense response	4.01E-02	7.32	16.09
1902236	negative regulation of endoplasmic reticulum stress-induced intrinsic apoptotic signaling pathway	4.01E-02	0.11	2.30
10592	positive regulation of lamellipodium assembly	4.01E-02	0.11	2.30
60008	Sertoli cell differentiation	4.01E-02	0.11	2.30
97242	amyloid-beta clearance	4.01E-02	0.11	2.30
46683	response to organophosphorus	4.17E-02	0.76	4.60
2001234	negative regulation of apoptotic signaling pathway	4.17E-02	1.23	5.75
6625	protein targeting to peroxisome	4.17E-02	0.38	3.45
72663	establishment of protein localization to peroxisome	4.17E-02	0.38	3.45
72662	protein localization to peroxisome	4.17E-02	0.38	3.45
1901605	alpha-amino acid metabolic process	4.17E-02	1.24	5.75
140053	mitochondrial gene expression	4.17E-02	0.77	4.60
30168	platelet activation	4.17E-02	0.77	4.60
9749	response to glucose	4.17E-02	0.77	4.60
2001026	regulation of endothelial cell chemotaxis	4.17E-02	0.12	2.30
1903020	positive regulation of glycoprotein metabolic process	4.17E-02	0.12	2.30
6897	endocytosis	4.17E-02	3.02	9.20
10942	positive regulation of cell death	4.17E-02	3.70	10.34
43574	peroxisomal transport	4.17E-02	0.39	3.45
19674	NAD metabolic process	4.17E-02	0.39	3.45
45223	regulation of CD4 biosynthetic process	4.17E-02	0.01	1.15
45225	negative regulation of CD4 biosynthetic process	4.17E-02	0.01	1.15

1905000	regulation of membrane repolarization during atrial cardiac muscle cell action potential	4.17E-02	0.01	1.15
90616	mitochondrial mRNA 3'-end processing	4.17E-02	0.01	1.15
70145	mitochondrial asparaginyl-tRNA aminoacylation	4.17E-02	0.01	1.15
1902860	propionyl-CoA biosynthetic process	4.17E-02	0.01	1.15
1902858	propionyl-CoA metabolic process	4.17E-02	0.01	1.15
2368	B cell cytokine production	4.17E-02	0.01	1.15
72019	proximal convoluted tubule development	4.17E-02	0.01	1.15
72229	metanephric proximal convoluted tubule development	4.17E-02	0.01	1.15
97017	renal protein absorption	4.17E-02	0.01	1.15
2842	positive regulation of T cell mediated immune response to tumor cell	4.17E-02	0.01	1.15
97222	mitochondrial mRNA polyadenylation	4.17E-02	0.01	1.15
48291	isotype switching to IgG isotypes	4.17E-02	0.01	1.15
1903906	regulation of plasma membrane raft polarization	4.17E-02	0.01	1.15
1904237	positive regulation of substrate-dependent cell migration, cell attachment to substrate	4.17E-02	0.01	1.15
1904235	regulation of substrate-dependent cell migration, cell attachment to substrate	4.17E-02	0.01	1.15
71310	cellular response to organic substance	4.27E-02	12.58	22.99
72655	establishment of protein localization to mitochondrion	4.28E-02	0.40	3.45
48729	tissue morphogenesis	4.30E-02	3.05	9.20
34404	nucleobase-containing small molecule biosynthetic process	4.31E-02	0.80	4.60
30031	cell projection assembly	4.31E-02	2.42	8.05
51223	regulation of protein transport	4.31E-02	3.74	10.34
43603	cellular amide metabolic process	4.31E-02	4.44	11.49
80134	regulation of response to stress	4.36E-02	7.52	16.09
2000116	regulation of cysteine-type endopeptidase activity	4.36E-02	1.28	5.75

9746	response to hexose	4.36E-02	0.80	4.60
10605	negative regulation of macromolecule metabolic process	4.39E-02	14.45	25.29
70482	response to oxygen levels	4.47E-02	1.84	6.90
6928	movement of cell or subcellular component	4.51E-02	8.38	17.24
9067	aspartate family amino acid biosynthetic process	4.52E-02	0.13	2.30
6541	glutamine metabolic process	4.52E-02	0.13	2.30
90023	positive regulation of neutrophil chemotaxis	4.52E-02	0.13	2.30
22607	cellular component assembly	4.72E-02	13.65	24.14
34284	response to monosaccharide	4.78E-02	0.83	4.60
10770	positive regulation of cell morphogenesis involved in differentiation	4.78E-02	0.83	4.60
44260	cellular macromolecule metabolic process	4.83E-02	28.34	41.38
90505	epiboly involved in wound healing	4.83E-02	0.13	2.30
44319	wound healing, spreading of cells	4.83E-02	0.13	2.30
14074	response to purine-containing compound	4.84E-02	0.83	4.60
30203	glycosaminoglycan metabolic process	4.99E-02	0.85	4.60
7265	Ras protein signal transduction	4.99E-02	1.34	5.75
46907	intracellular transport	4.99E-02	8.54	17.24
70585	protein localization to mitochondrion	4.99E-02	0.44	3.45
7266	Rho protein signal transduction	4.99E-02	0.44	3.45
90504	epiboly	4.99E-02	0.14	2.30
70129	regulation of mitochondrial translation	4.99E-02	0.14	2.30
34394	protein localization to cell surface	4.99E-02	0.14	2.30
18126	protein hydroxylation	4.99E-02	0.14	2.30
71624	positive regulation of granulocyte chemotaxis	4.99E-02	0.14	2.30
43032	positive regulation of macrophage activation	4.99E-02	0.14	2.30
10499	proteasomal ubiquitin-independent protein catabolic process	4.99E-02	0.14	2.30

10758	regulation of macrophage chemotaxis	4.99E-02	0.14	2.30
1900101	regulation of endoplasmic reticulum unfolded protein response	4.99E-02	0.14	2.30
44788	modulation by host of viral process	4.99E-02	0.14	2.30

Table S9: Cytoscape GO enrichment analysis of VAT-1 co-IP: molecular function

GO-ID	description	corr p-value	co-IP [%]	global [%]
42802	identical protein binding	2.56E-06	32.18	9.61
61134	peptidase regulator activity	2.88E-06	12.64	1.25
16491	oxidoreductase activity	2.88E-06	20.69	4.18
4866	endopeptidase inhibitor activity	2.66E-05	10.34	1.00
30414	peptidase inhibitor activity	2.66E-05	10.34	1.04
61135	endopeptidase regulator activity	2.66E-05	10.34	1.04
44877	protein-containing complex binding	4.09E-05	21.84	5.87
51087	chaperone binding	4.30E-05	8.05	0.57
48037	cofactor binding	8.01E-05	14.94	2.91
50662	coenzyme binding	8.41E-05	11.49	1.64
3824	catalytic activity	8.58E-05	57.47	32.81
36094	small molecule binding	8.58E-05	34.48	14.34
4064	arylesterase activity	9.36E-05	3.45	0.03
50839	cell adhesion molecule binding	1.42E-04	13.79	2.70
43168	anion binding	1.58E-04	35.63	15.75
5515	protein binding	2.23E-04	87.36	66.35
4867	serine-type endopeptidase inhibitor activity	2.43E-04	6.90	0.54
3723	RNA binding	2.88E-04	25.29	9.24
5518	collagen binding	4.72E-04	5.75	0.37
4063	aryldialkylphosphatase activity	6.18E-04	2.30	0.01
45296	cadherin binding	6.18E-04	10.34	1.78
166	nucleotide binding	6.48E-04	28.74	12.20
1901265	nucleoside phosphate binding	6.48E-04	28.74	12.21
51082	unfolded protein binding	9.69E-04	6.90	0.73
97367	carbohydrate derivative binding	1.01E-03	28.74	12.59

50211	procollagen galactosyltransferase activity	1.16E-03	2.30	0.02
8475	procollagen-lysine 5-dioxygenase activity	1.16E-03	2.30	0.02
51538	3 iron, 4 sulfur cluster binding	1.16E-03	2.30	0.02
46573	lactonohydrolase activity	1.16E-03	2.30	0.02
102007	acyl-L-homoserine-lactone lactonohydrolase activity	1.16E-03	2.30	0.02
15091	ferric iron transmembrane transporter activity	1.16E-03	2.30	0.02
72510	trivalent inorganic cation transmembrane transporter activity	1.16E-03	2.30	0.02
8177	succinate dehydrogenase (ubiquinone) activity	1.16E-03	2.30	0.02
4857	enzyme inhibitor activity	1.50E-03	10.34	2.12
1848	complement binding	1.89E-03	3.45	0.11
104	succinate dehydrogenase activity	2.01E-03	2.30	0.02
70815	peptidyl-lysine 5-dioxygenase activity	2.01E-03	2.30	0.02
16635	oxidoreductase activity, acting on the CH-CH group of donors, quinone or related compound as acceptor	2.01E-03	2.30	0.02
8092	cytoskeletal protein binding	2.72E-03	16.09	5.34
3779	actin binding	2.88E-03	10.34	2.37
51015	actin filament binding	3.93E-03	6.90	1.04
31406	carboxylic acid binding	4.31E-03	6.90	1.07
4459	L-lactate dehydrogenase activity	4.31E-03	2.30	0.03
16885	ligase activity, forming carbon-carbon bonds	4.31E-03	2.30	0.03
5102	signaling receptor binding	4.63E-03	21.84	9.41
5178	integrin binding	4.90E-03	5.75	0.72
43177	organic acid binding	5.34E-03	6.90	1.14
48029	monosaccharide binding	5.67E-03	4.60	0.42
43167	ion binding	6.37E-03	52.87	35.35
16787	hydrolase activity	6.37E-03	28.74	14.77
4457	lactate dehydrogenase activity	6.77E-03	2.30	0.05
1849	complement component C1q binding	6.77E-03	2.30	0.05
43394	proteoglycan binding	6.78E-03	3.45	0.20

19900	kinase binding	8.14E-03	12.64	4.09
52689	carboxylic ester hydrolase activity	8.18E-03	5.75	0.84
32553	ribonucleotide binding	8.32E-03	22.99	10.86
16874	ligase activity	9.15E-03	5.75	0.87
5381	iron ion transmembrane transporter activity	1.18E-02	2.30	0.06
32555	purine ribonucleotide binding	1.82E-02	21.84	10.78
1846	opsonin binding	1.87E-02	2.30	0.08
17076	purine nucleotide binding	1.93E-02	21.84	10.86
16829	lyase activity	1.93E-02	5.75	1.05
15037	peptide disulfide oxidoreductase activity	2.05E-02	2.30	0.08
51287	NAD binding	2.07E-02	3.45	0.31
19899	enzyme binding	2.07E-02	24.14	12.72
16864	intramolecular oxidoreductase activity, transposing S-S bonds	2.19E-02	2.30	0.09
3756	protein disulfide isomerase activity	2.19E-02	2.30	0.09
42803	protein homodimerization activity	2.21E-02	12.64	4.77
5525	GTP binding	2.29E-02	8.05	2.19
16616	oxidoreductase activity, acting on the CH-OH group of donors, NAD or NADP as acceptor	2.35E-02	4.60	0.69
32550	purine ribonucleoside binding	2.35E-02	8.05	2.21
16627	oxidoreductase activity, acting on the CH-CH group of donors	2.35E-02	3.45	0.34
32549	ribonucleoside binding	2.35E-02	8.05	2.23
1883	purine nucleoside binding	2.35E-02	8.05	2.23
16788	hydrolase activity, acting on ester bonds	2.35E-02	11.49	4.17
35639	purine ribonucleoside triphosphate binding	2.35E-02	20.69	10.41
1882	nucleoside binding	2.50E-02	8.05	2.26
19001	guanyl nucleotide binding	2.59E-02	8.05	2.30
32561	guanyl ribonucleotide binding	2.59E-02	8.05	2.30
16614	oxidoreductase activity, acting on CH-OH group of donors	2.59E-02	4.60	0.75
31418	L-ascorbic acid binding	2.59E-02	2.30	0.11

30234	enzyme regulator activity	2.59E-02	13.79	5.83
5539	glycosaminoglycan binding	2.59E-02	5.75	1.24
5540	hyaluronic acid binding	2.59E-02	2.30	0.12
33823	procollagen glucosyltransferase activity	2.59E-02	1.15	0.01
33882	choloyl-CoA hydrolase activity	2.59E-02	1.15	0.01
33919	glucan 1,3-alpha-glucosidase activity	2.59E-02	1.15	0.01
33989	3alpha,7alpha,12alpha-trihydroxy-5beta-cholest-24-enoyl-CoA hydratase activity	2.59E-02	1.15	0.01
18733	3,4-dihydrocoumarin hydrolase activity	2.59E-02	1.15	0.01
50560	aspartate-tRNA(Asn) ligase activity	2.59E-02	1.15	0.01
8609	alkylglycerone-phosphate synthase activity	2.59E-02	1.15	0.01
16843	amine-lyase activity	2.59E-02	1.15	0.01
16844	strictosidine synthase activity	2.59E-02	1.15	0.01
46554	malate dehydrogenase (NADP+) activity	2.59E-02	1.15	0.01
90600	alpha-1,3-glucosidase activity	2.59E-02	1.15	0.01
51748	UTP-monosaccharide-1-phosphate uridylyltransferase activity	2.59E-02	1.15	0.01
4654	polyribonucleotide nucleotidyltransferase activity	2.59E-02	1.15	0.01
44594	17-beta-hydroxysteroid dehydrogenase (NAD+) activity	2.59E-02	1.15	0.01
4736	pyruvate carboxylase activity	2.59E-02	1.15	0.01
3983	UTP:glucose-1-phosphate uridylyltransferase activity	2.59E-02	1.15	0.01
31714	C5a anaphylatoxin chemotactic receptor binding	2.59E-02	1.15	0.01
31715	C5L2 anaphylatoxin chemotactic receptor binding	2.59E-02	1.15	0.01
4298	threonine-type endopeptidase activity	2.92E-02	2.30	0.13
70003	threonine-type peptidase activity	2.92E-02	2.30	0.13
1901681	sulfur compound binding	3.43E-02	5.75	1.36
71813	lipoprotein particle binding	3.61E-02	2.30	0.15
71814	protein-lipid complex binding	3.61E-02	2.30	0.15

50660	flavin adenine dinucleotide binding	3.69E-02	3.45	0.46
5506	iron ion binding	3.69E-02	4.60	0.89
1968	fibronectin binding	4.05E-02	2.30	0.16
5488	binding	4.08E-02	94.25	85.53
35250	UDP-galactosyltransferase activity	4.08E-02	2.30	0.17
34986	iron chaperone activity	4.08E-02	1.15	0.01
34988	Fc-gamma receptor I complex binding	4.08E-02	1.15	0.01
4329	formate-tetrahydrofolate ligase activity	4.08E-02	1.15	0.01
4352	glutamate dehydrogenase (NAD+) activity	4.08E-02	1.15	0.01
4353	glutamate dehydrogenase [NAD(P)+] activity	4.08E-02	1.15	0.01
30984	kininogen binding	4.08E-02	1.15	0.01
70052	collagen V binding	4.08E-02	1.15	0.01
52815	medium-chain acyl-CoA hydrolase activity	4.08E-02	1.15	0.01
4772	sterol O-acyltransferase activity	4.08E-02	1.15	0.01
32427	GBD domain binding	4.08E-02	1.15	0.01
4815	aspartate-tRNA ligase activity	4.08E-02	1.15	0.01
4822	isoleucine-tRNA ligase activity	4.08E-02	1.15	0.01
33570	transferrin transmembrane transporter activity	4.08E-02	1.15	0.01
32557	pyrimidine ribonucleotide binding	4.08E-02	1.15	0.01
46922	peptide-O-fucosyltransferase activity	4.08E-02	1.15	0.01
4998	transferrin receptor activity	4.08E-02	1.15	0.01
34736	cholesterol O-acyltransferase activity	4.08E-02	1.15	0.01
30246	carbohydrate binding	4.59E-02	5.75	1.54

Table S10: Cytoscape GO enrichment analysis of VAT-1 co-IP: cellular compartment

GO-ID	description	corr p-value	co-IP [%]	global [%]
70062	extracellular exosome	1.16E-33	67.82	11.09
1903561	extracellular vesicle	1.16E-33	67.82	11.21
43230	extracellular organelle	1.16E-33	67.82	11.22
5615	extracellular space	5.15E-25	70.11	17.62
44421	extracellular region part	8.66E-24	70.11	18.61
31982	vesicle	5.17E-23	71.26	20.09
5576	extracellular region	6.92E-19	70.11	23.01

43227	membrane-bounded organelle	1.04E-14	100.00	66.11
44444	cytoplasmic part	1.06E-14	91.95	51.30
72562	blood microparticle	1.47E-13	16.09	0.76
5759	mitochondrial matrix	8.71E-13	22.99	2.47
44429	mitochondrial part	1.98E-12	31.03	5.47
43226	organelle	9.82E-12	100.00	71.90
5788	endoplasmic reticulum lumen	1.98E-11	18.39	1.63
43233	organelle lumen	4.10E-10	62.07	27.57
31974	membrane-enclosed lumen	4.10E-10	62.07	27.57
70013	intracellular organelle lumen	4.10E-10	62.07	27.57
5925	focal adhesion	6.17E-10	18.39	2.08
5924	cell-substrate adherens junction	6.55E-10	18.39	2.09
30055	cell-substrate junction	7.23E-10	18.39	2.12
44446	intracellular organelle part	8.40E-10	82.76	48.73
42470	melanosome	9.95E-10	11.49	0.56
48770	pigment granule	9.95E-10	11.49	0.56
5737	cytoplasm	1.30E-09	91.95	61.27
5739	mitochondrion	3.34E-09	32.18	8.37
44422	organelle part	4.56E-09	82.76	50.36
60205	cytoplasmic vesicle lumen	6.18E-09	16.09	1.78
31983	vesicle lumen	6.19E-09	16.09	1.79
44432	endoplasmic reticulum part	1.55E-08	28.74	7.17
5912	adherens junction	2.59E-08	18.39	2.78
70161	anchoring junction	3.75E-08	18.39	2.86
43229	intracellular organelle	1.20E-07	93.10	67.48
12505	endomembrane system	1.36E-07	51.72	23.56
5783	endoplasmic reticulum	1.57E-07	32.18	10.07
34774	secretory granule lumen	3.03E-07	13.79	1.70
16020	membrane	4.96E-07	79.31	51.03
31410	cytoplasmic vesicle	5.11E-07	34.48	12.11
97708	intracellular vesicle	5.13E-07	34.48	12.12
30054	cell junction	2.14E-06	24.14	6.71
99503	secretory vesicle	9.41E-05	18.39	5.21
31093	platelet alpha granule lumen	1.40E-04	5.75	0.36
34663	endoplasmic reticulum chaperone complex	1.40E-04	3.45	0.06
44424	intracellular part	1.40E-04	94.25	77.11

5622	intracellular	1.40E-04	94.25	77.11
43231	intracellular membrane-bounded organelle	2.10E-04	79.31	58.08
30141	secretory granule	2.18E-04	16.09	4.40
62023	collagen-containing extracellular matrix	2.53E-04	10.34	1.82
5740	mitochondrial envelope	2.61E-04	14.94	3.90
44433	cytoplasmic vesicle part	2.87E-04	21.84	7.84
98805	whole membrane	3.39E-04	22.99	8.67
32587	ruffle membrane	3.39E-04	5.75	0.45
9295	nucleoid	3.44E-04	4.60	0.23
42645	mitochondrial nucleoid	3.44E-04	4.60	0.23
31091	platelet alpha granule	4.46E-04	5.75	0.48
46930	pore complex	5.37E-04	3.45	0.10
31966	mitochondrial membrane	5.54E-04	13.79	3.67
30863	cortical cytoskeleton	5.59E-04	5.75	0.51
31967	organelle envelope	5.59E-04	18.39	6.23
31975	envelope	5.59E-04	18.39	6.23
14704	intercalated disc	5.98E-04	4.60	0.27
31256	leading edge membrane	6.74E-04	6.90	0.86
1726	ruffle	6.74E-04	6.90	0.86
98798	mitochondrial protein complex	1.27E-03	8.05	1.38
5829	cytosol	1.49E-03	44.83	26.92
15629	actin cytoskeleton	1.49E-03	10.34	2.41
31090	organelle membrane	1.49E-03	31.03	15.67
44291	cell-cell contact zone	1.74E-03	4.60	0.37
45257	succinate dehydrogenase complex (ubiquinone)	1.74E-03	2.30	0.03
45273	respiratory chain complex II	1.74E-03	2.30	0.03
45281	succinate dehydrogenase complex	1.74E-03	2.30	0.03
45283	fumarate reductase complex	1.74E-03	2.30	0.03
5749	mitochondrial respiratory chain complex II, succinate dehydrogenase complex (ubiquinone)	1.74E-03	2.30	0.03
2102	podosome	1.75E-03	3.45	0.15
31012	extracellular matrix	1.88E-03	10.34	2.52
30139	endocytic vesicle	1.94E-03	8.05	1.52
31252	cell leading edge	2.24E-03	9.20	2.06

5579	membrane attack complex	2.27E-03	2.30	0.04
42175	nuclear outer membrane-endoplasmic reticulum membrane network	2.27E-03	16.09	5.78
1990712	HFE-transferrin receptor complex	2.90E-03	2.30	0.04
5577	fibrinogen complex	2.90E-03	2.30	0.04
19773	proteasome core complex, alpha-subunit complex	3.67E-03	2.30	0.05
9986	cell surface	3.85E-03	13.79	4.73
44448	cell cortex part	4.19E-03	5.75	0.85
31253	cell projection membrane	4.19E-03	8.05	1.77
55037	recycling endosome	5.25E-03	5.75	0.90
5789	endoplasmic reticulum membrane	5.47E-03	14.94	5.66
31907	microbody lumen	7.67E-03	3.45	0.27
5782	peroxisomal matrix	7.67E-03	3.45	0.27
30027	lamellipodium	7.67E-03	5.75	0.99
98554	cytoplasmic side of endoplasmic reticulum membrane	8.23E-03	2.30	0.07
98796	membrane protein complex	8.31E-03	14.94	5.97
5938	cell cortex	8.79E-03	6.90	1.51
32991	protein-containing complex	9.28E-03	42.53	27.78
98588	bounding membrane of organelle	1.01E-02	21.84	10.94
31968	organelle outer membrane	1.03E-02	5.75	1.07
19867	outer membrane	1.05E-02	5.75	1.08
1904813	ficolin-1-rich granule lumen	1.05E-02	4.60	0.66
101002	ficolin-1-rich granule	1.05E-02	4.60	0.66
5793	endoplasmic reticulum-Golgi intermediate compartment	1.05E-02	4.60	0.66
45121	membrane raft	1.05E-02	6.90	1.59
98857	membrane microdomain	1.05E-02	6.90	1.59
19866	organelle inner membrane	1.07E-02	9.20	2.76
45335	phagocytic vesicle	1.07E-02	4.60	0.67
5905	clathrin-coated pit	1.14E-02	3.45	0.33
44449	contractile fiber part	1.16E-02	5.75	1.13
71682	endocytic vesicle lumen	1.16E-02	2.30	0.10
16323	basolateral plasma membrane	1.17E-02	5.75	1.13
98589	membrane region	1.19E-02	6.90	1.65
30016	myofibril	1.22E-02	5.75	1.15

42383	sarcolemma	1.25E-02	4.60	0.71
30864	cortical actin cytoskeleton	1.44E-02	3.45	0.37
43292	contractile fiber	1.44E-02	5.75	1.20
31258	lamellipodium membrane	1.57E-02	2.30	0.12
5839	proteasome core complex	1.57E-02	2.30	0.12
45274	plasma membrane respiratory chain complex II	1.57E-02	1.15	0.01
45282	plasma membrane succinate dehydrogenase complex	1.57E-02	1.15	0.01
9841	mitochondrial endopeptidase Clp complex	1.57E-02	1.15	0.01
34677	integrin alpha7-beta1 complex	1.57E-02	1.15	0.01
30867	rough endoplasmic reticulum membrane	1.68E-02	2.30	0.12
5743	mitochondrial inner membrane	1.81E-02	8.05	2.44
5791	rough endoplasmic reticulum	2.07E-02	3.45	0.43
98803	respiratory chain complex	2.11E-02	3.45	0.43
5746	mitochondrial respirasome	2.11E-02	3.45	0.43
98590	plasma membrane region	2.31E-02	13.79	6.18
44464	cell part	2.54E-02	97.70	90.40
9368	endopeptidase Clp complex	2.73E-02	1.15	0.01
17177	glucosidase II complex	2.73E-02	1.15	0.01
31523	Myb complex	2.73E-02	1.15	0.01
70470	plasma membrane respirasome	2.73E-02	1.15	0.01
34665	integrin alpha1-beta1 complex	2.73E-02	1.15	0.01
34667	integrin alpha3-beta1 complex	2.73E-02	1.15	0.01
35692	macrophage migration inhibitory factor receptor complex	2.73E-02	1.15	0.01
34680	integrin alpha10-beta1 complex	2.73E-02	1.15	0.01
34681	integrin alpha11-beta1 complex	2.73E-02	1.15	0.01
45025	mitochondrial degradosome	2.73E-02	1.15	0.01
5741	mitochondrial outer membrane	2.74E-02	4.60	0.94
70469	respirasome	2.75E-02	3.45	0.50
51233	spindle midzone	2.92E-02	2.30	0.18
5790	smooth endoplasmic reticulum	2.92E-02	2.30	0.18
5623	cell	2.93E-02	97.70	90.74
44438	microbody part	3.14E-02	3.45	0.53

44439	peroxisomal part	3.14E-02	3.45	0.53
30175	filopodium	3.20E-02	3.45	0.54
30665	clathrin-coated vesicle membrane	3.44E-02	3.45	0.55
30017	sarcomere	3.57E-02	4.60	1.04
98797	plasma membrane protein complex	3.65E-02	8.05	2.92
30981	cortical microtubule cytoskeleton	3.65E-02	1.15	0.02
17087	mitochondrial processing peptidase complex	3.65E-02	1.15	0.02
34666	integrin alpha2-beta1 complex	3.65E-02	1.15	0.02
34678	integrin alpha8-beta1 complex	3.65E-02	1.15	0.02
98858	actin-based cell projection	3.65E-02	4.60	1.06
16324	apical plasma membrane	3.65E-02	5.75	1.63
1990204	oxidoreductase complex	4.04E-02	3.45	0.60
5911	cell-cell junction	4.16E-02	6.90	2.33
45202	synapse	4.65E-02	12.64	6.18
5757	mitochondrial permeability transition pore complex	4.65E-02	1.15	0.02
5862	muscle thin filament tropomyosin	4.65E-02	1.15	0.02
30478	actin cap	4.65E-02	1.15	0.02
44455	mitochondrial membrane part	4.98E-02	4.60	1.18

Table S11: Hits matching the criteria ((log_2(enrichment) > 2, p-value < 0.05) of SILAC targetID with 500 nM **NC-1** in HEPG2

protein name	gene name	enrichment	p-value	sequence coverage [%]
Synaptic vesicle membrane protein VAT-1 homolog	VAT1	4.13	6.16	56.2
Heme oxygenase 2	HMOX2	3.03	5.60	57.6
Cytochrome b5 type B	CYB5B	2.25	3.53	50.7

Table S12: Hits matching the criteria ((log_2(enrichment) > 2, p-value < 0.05) of LFQ targetID with 100 nM **NC-1** and hits matching the criteria ((log_2(enrichment) > 1.5, p-value < 0.05) for competition with 500 nM **NCA** in HEPG2

protein name	gene name	enrichment	p-value	sequence coverage [%]
Synaptic vesicle membrane protein VAT-1 homolog	VAT1	4.37	8.86	36.1
Calcium-binding mitochondrial carrier protein Aralar2	SLC25A13	2.44	1.72	7.9
60S ribosomal protein L9	RPL9	2.08	1.61	16
competition				
60S ribosomal protein L10a	RPL10A	3.90	2.63	12.4
Adenylate kinase 2, mitochondrial	AK2	2.52	1.89	57.1
Peroxisomal 2,4-dienoyl-CoA reductase	DECR2	2.37	2.00	7.1
Actin, gamma-enteric smooth muscle	ACTA2	2.18	1.94	28.4
Synaptic vesicle membrane protein VAT-1 homolog	VAT1	1.99	4.92	36.1
F-box only protein 22	FBXO22	1.94	1.77	8.4
Helicase SKI2W	SKIV2L	1.79	1.91	4.4
Secernin-1	SCRN1	1.61	1.87	11.1

Table S13: Hits matching the criteria ((log_2(enrichment) > 2, p-value < 0.01) of LFQ targetID with 500 nM **NC-1** for 24 hs in HEPG2

protein name	gene name	enrichment	p-value	sequence coverage [%]
Titin	TTN	6.05	6.95	0.2
Dolichyl-phosphate beta-glucosyltransferase	ALG5	3.69	3.96	18.3
Splicing factor U2AF 26 kDa subunit	U2AF1L4	3.68	1.68	44.4
Protein transport protein Sec61 subunit gamma	SEC61G	3.64	1.43	23.5
Synaptic vesicle membrane protein VAT-1 homolog	VAT1	3.41	4.49	45.5
Hyccin	FAM126A	3.26	1.57	6.5
Vesicular integral-membrane protein VIP36	LMAN2	2.97	1.53	11.2
Tubulin alpha-4A chain	TUBA4A	2.85	1.66	43.8
RAD50-interacting protein 1	RINT1	2.84	1.46	5.7
Alpha/beta hydrolase domain-containing protein 17A	ABHD17A	2.50	3.08	6.1
Transmembrane protein 256	TMEM256	2.43	3.62	22
Signal peptidase complex subunit 1	SPCS1	2.35	1.55	26.5
Metalloproteinase inhibitor 2	TIMP2	2.32	1.45	11.7
Pleckstrin homology domain-containing family A member 5	PLEKHA5	2.26	2.86	9.5
Queuine tRNA-ribosyltransferase subunit QTRTD1	QTRTD1	2.26	3.88	8.4
E3 ubiquitin-protein ligase TRIM32	TRIM32	2.20	3.51	5.1
Peptidyl-prolyl cis-trans isomerase	PPIF	2.16	1.62	32.4
Axin interactor, dorsalization-associated protein	AIDA	2.10	2.46	23
39S ribosomal protein L24, mitochondrial	MRPL24	2.02	1.48	28.7

Table S14: VAT-1 sequences with binding site peptide and mutated residues

gene	protein sequence
VAT-1 uniprot Q99536	MSDEREVAEAATGEDASSPPPKTEAASDPQHPAASEGAAAAAASPPLL RCLVLTGFGGYDKVKLQSRPAAPPAPGPGQLTLRLRACGLNFADLMAR QGLYDR**LPPLPVTPGMEGAGVVIAVGEGVSDR**KAGDRVMVLNRSGM WQEEVTVPSVQTFLIPEAMTFEEAAALLVNYITAYMVLFDFGNLQPGHS VLVHMAAGGVGMAAVQLCRTVENVTVFGTASASKHEALKENGVTHPID YHTTDYVDEIKKISPKGVDIVMDPLGGSDTAKGYNLLKPMGKVVTYGMA NLLTGPKRNLMALARTWWNQFSVTALQLLQANRAVCGFHLGYLDGEV ELVSGVVARLLALYNQGHIKPHIDSVWPFEKVADAMKQMQEKKNVGKV LLVPGPEKEN
His-TEV-VAT-1 (*E.coli* and human)	MHHHHHHITSLYKKAGFENLYFQGSDEREVAEAATGEDASSPPPKTEA ASDPQHPAASEGAAAAAASPPLLRCLVLTGFGGYDKVKLQSRPAAPPA PGPGQLTLRLRACGLNFADLMARQGLYDR**LPPLPVTPGMEGAGVVIA VGEGVSDR**KAGDRVMVLNRSGMWQEEVTVPSVQTFLIPEAMTFEEAA ALLVNYITAYMVLFDFGNLQPGHSVLVHMAAGGVGMAAVQLCRTVENV TVFGTASASKHEALKENGVTHPIDYHTTDYVDEIKKISPKGVDIVMDPLG GSDTAKGYNLLKPMGKVVTYGMANLLTGPKRNLMALARTWWNQFSVT ALQLLQANRAVCGFHLGYLDGEVELVSGVVARLLALYNQGHIKPHIDSV WPFEKVADAMKQMQEKKNVGKVLLVPGPEKEN

4. Supplementary schemes

Neocarzilin A and C

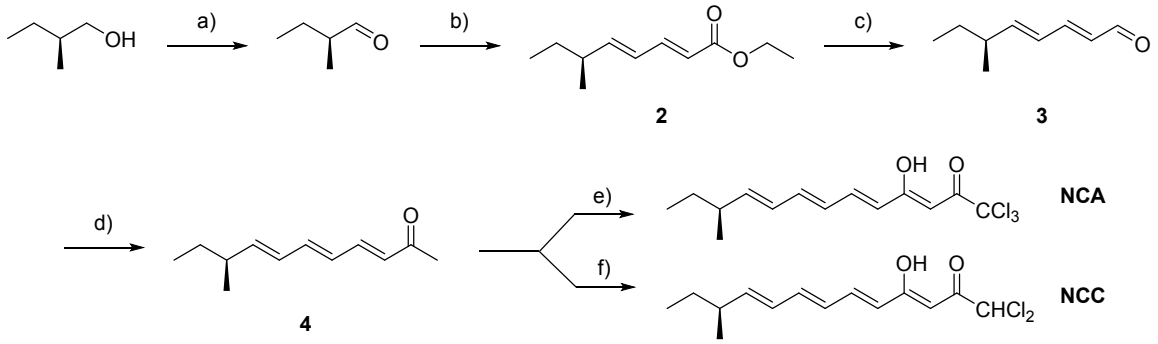

Scheme S1: Synthesis of **Neocarzilins A** and **C**: a) TEMPO (1 mol-%), KBr (0.10 eq), NaOCl (2.00 eq), CH_2Cl_2/carbonate-buffer pH = 8.6, 0 °C, 45 min, 85%; b) 1. LiHMDS (1.00 eq), 2. ethyl (E)-4-(diethoxyphosphoryl)-but-2-enoate (1.00 eq), THF, -78 °C → -40 °C, 3 h, 76%; c) DIBAL-H (2.10 eq) MnO_2 (20.0 eq), THF, hexane, -78 °C → rt, 5 h, 72% over 2 steps; d) 1-(Triphenylphosphoranylidene)-2-propanone (2.00 eq), toluene, 100 °C, 16 h, 59%; e) 1. LiHMDS (1.05 eq); 2. Trichloroacetic anhydride (2.00 eq), THF, -78 °C, 3 h, 71%; f) 1. LiHMDS (1.05 eq), 2. Dichloroacetic anhydride (2.00 eq), THF, -78 °C, 3 h, 44%.

Neocarzilin A'

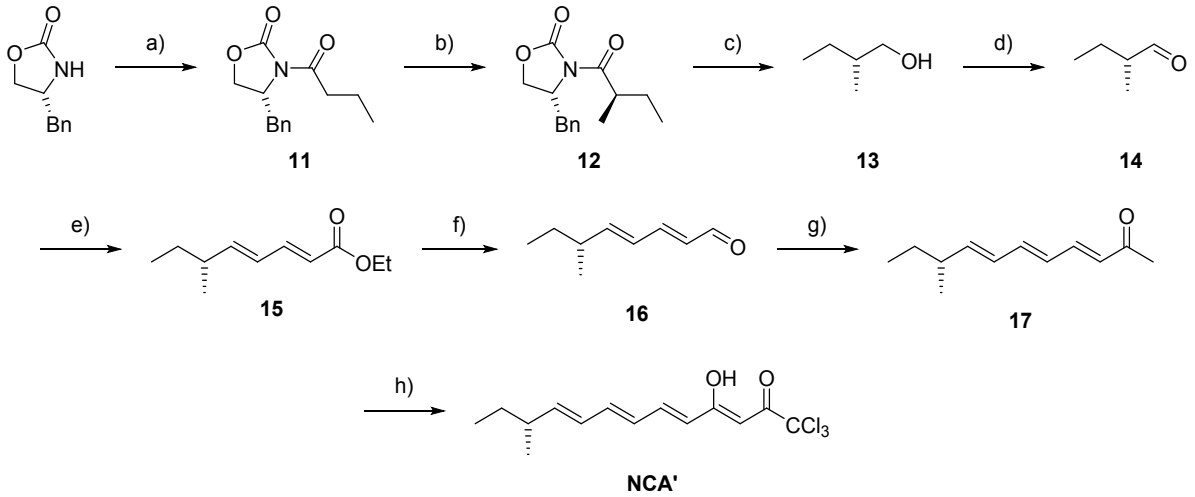

Scheme S2: Synthesis of **Neocarzilin A'**: a) 1.) *n*-BuLi (1.10 eq), THF, -78 °C, 0.5 h, 2.) butyryl chloride, -78 °C, 0.5 h, -78 °C – rt, 0.5 h, 68%; b) 1.) NaHMDS (1.20 eq), THF, -78 °C, 1 h, 2.) MeI (2.50 eq), -78 °C, 2.5 h, 77%; c) $LiBH_4$ (0.70 eq), MeOH (1.48 eq), Et_2O, -20 °C → rt, 5 h, 66%; d) $(COCl)_2$ (1.50 eq), DMSO (2.50 eq), NEt_3 (5.00 eq), CH_2Cl_2, -78 °C, 0.5 h, rt, 2 h, 56%; e) 1. LiHMDS (1.50 eq), 2. ethyl (E)-4-(diethoxyphosphoryl)-but-2-enoate (1.50 eq), THF, -78 °C → -40 °C, 3 h, 30%; f) DIBAL-H (2.50 eq) MnO_2 (20.0 eq), THF, hexane, -78 °C → rt, 5 h, 78% over 2 steps; g) 1-(Triphenylphosphoranylidene)-2-propanone (2.00 eq), toluene, 100 °C, 16 h, 77%; h) 1. LiHMDS (1.10 eq); 2. Trichloroacetic anhydride (2.00 eq), THF, -78 °C, 3 h, 60%.

Neocarzilin B

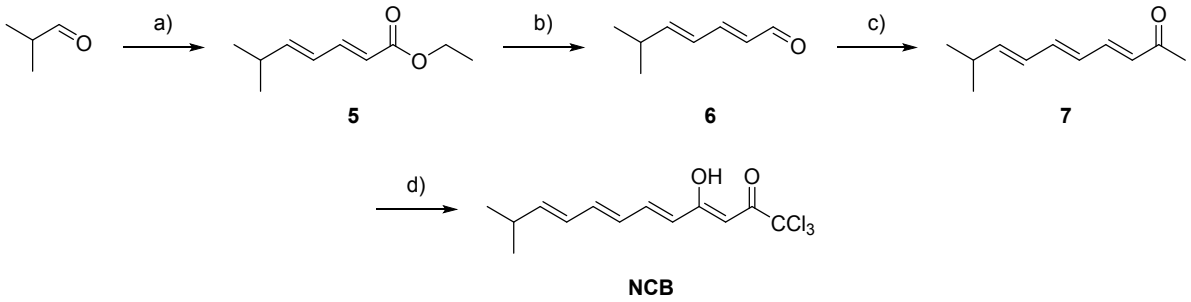

Scheme S3: Synthesis of **Neocarzilin B**: a) LiHMDS (1.00 eq) ethyl (E)-4-(diethoxyphosphoryl)-but-2-enoate (1.00 eq), THF, -78 °C → rt, 4 h, 51%; b) DIBAL-H (2.10 eq), MnO_2 (20.0 eq), THF, hexane, -78 °C → rt, 5 h, 83% over 2 steps; c) 1-(Triphenylphosphoranylidene)-2-propanone (2.00 eq), toluene,100 °C, 16 h, 60%; d) 1. LiHMDS (1.00 eq), 2. trichloroacetic anhydride (2.00 eq), THF, -78 °C, 3 h, 83%.

5. Synthetic procedures

5.1. General Methods and Materials

All used reagents and solvents were purchased reagent grade or higher from commercial sources (Sigma-Aldrich, Thermo Fisher Scientific Inc., Merck KGaA, Alfa Aesar, Roth, VWR International, Fluka, Acros Chemicals) and were used without further purification. Technical grade solvents were always distilled prior to use. All reactions were conducted using oven dried glassware whereas reactions containing oxygen or water sensitive reagents were carried under argon atmosphere.
For reaction control, analytical thin-layer chromatography (TLC) was carried out on Merck silica-gel 60 F254 plates, using short wave UV light (λ=254 nm and 366 nm) or $KMnO_4$-stain (1.50 g $KMnO_4$, 10.0 g K_2CO_3, 1.25 mL $NaOH_{aq}$ (10 wt-%), 200 mL ddH_2O) to visualize single components. Preparative TLC was performed using TLC Silica gel 60 F_{254} (20 x 20 cm) plates from Merck KGaA or pre-coated TLC plates DIL G-200 from MACHEREY-NAGEL GmbH & Co. KG or Silica gel 60 (particle size = 40–63 µM) from *VWR* with compressed air.

^{1}H-NMR experiments were recorded on *Avance-III* (AV-HD300, AV-HD400 or AV-HD500) NMR systems (*Bruker Co.*) at room temperature with $CDCl_3$ or DMSO-d_6 as solvents and referenced to the residual proton signal of the corresponding deuterated solvent ($CDCl_3$: δ = 7.26 ppm, DMSO-d_6: δ = 2.50 ppm). Chemical shifts are reported in parts per million (ppm). Coupling constants (*J*) are reported in hertz (Hz) and for the assignment of multiplicity to the signals the following abbreviations were used: s = singlet, br s = broad singlet, d = doublet, t = triplet, q = quartet, m = multiplet or unresolved.
^{13}C-NMR spectra were collected on *Avance-III* NMR systems (*Bruker Co.*) at 75, 101 or 126 MHz with $CDCl_3$ or DMSO-d_6 as solvents. Chemical shifts were referenced to the residual solvent peak as an internal standard ($CDCl_3$: δ = 77.16 ppm, DMSO-d_6: δ = 39.52 ppm).

Reversed high performance liquid chromatography (RP-HPLC) for analytical purposes was performed on a Waters 2695 separations module with a Waters 2996 Photodiode Array Detector at wavelengths between 210 and 600 nm with mobile phases A: H_2O + 0.5% TFA, B: MeCN + 0.5% TFA, C: H_2O, or D: MeCN. Separation was performed on a C18 column (Waters XBridge C18, 3.5 µm, 4.6 x 100 mm).
Preparative reversed phase HPLC runs were conducted on a Waters system with a Waters 2545 Quaternary Gradient Module, a Waters 2998 Photodiode Array Detector and a Waters Fraction Collector III with the same mobile phases as in the analytical setup. As stationary phases different C18 columns were used: P1: YMC-Triart C18, 10 x 250 mm, 5 µm; P2: Waters XBridge prep C18 OBD™, 30 x 150 mm, 5 µm; P3: Waters XBridge prep C18 OBD™, 50 x 250 mm, 10 µm.

High resolution mass spectra were recorded using an *LTQ-FT Ultra* (*Thermo Fisher Scientific Inc.*) coupled with a Dionex UltiMate 3000 HPLC system and an ESI or APCI ion source.

5.2. Synthesis

Ethyl (*E*)-4-(diethoxyphosphoryl)but-2-enoate (1)

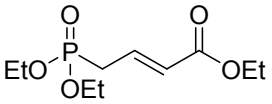

Chemical Formula: $C_{10}H_{19}O_5P$
Molecular Weight: 250.23

12.2 g (73.7 mmol, 1.13 eq) triethylphosphite and 16.7 g (65.0 mmol, 1.00 eq) ethyl 4-bromocrotonate (75% purity) were heated to 125 °C for 4 h. The crude product was purified via vacuum destillation (113-116 °C, 0.04 mbar). 16.2 g (64.8 mmol, 88%) desired product were obtained as a slightly yellow oil.

^{1}H NMR (500 MHz, $CDCl_3$, 300 K): δ (ppm) = 6.92 – 6.83 (dq, *J* = 7.7, 15.4 Hz, 1H), 5.99 – 5.92 (dd, *J* = 4.9, 15.6 Hz, 1H), 4.23 – 4.17 (q, *J* = 7.1 Hz, 2H), 4.17 – 4.06 (*virt*. dddt, *J* = 3.2, 7.1, 10.3, 14.6 Hz, 4H), 2.78 – 2.69 (dd, *J* = 7.8, 22.9 Hz, 2H), 1.35 – 1.31 (t, *J* = 7.1 Hz, 6H), 1.35 – 1.31 (t, *J* = 7.1 Hz, 3H).
^{13}C NMR (91 MHz, $CDCl_3$, 300 K): δ (ppm) = 165.8, 165.8, 137.6, 137.5, 126.07, 125.9, 62.5, 62.4, 60.6, 31.6, 30.0, 16.6, 16.5, 14.4.

Ethyl (*S*,2*E*,4*E*)-6-methylocta-2,4-dienoate (2)

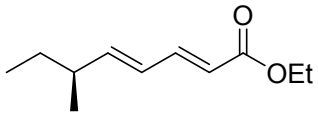

Chemical Formula: $C_{11}H_{18}O_2$
Molecular Weight: 182.26

To a solution of 6.55 g (26.1 mmol, 1.50 eq) Ethyl (*E*)-4-(diethoxyphosphoryl)but-2-enoate in 20 mL THF was added 26.1 mL (26.1 mmol, 1 M in THF, 1.50 eq) LiHMDS at -78 °C. The solution was stirred at that temperature for 1 h and then 1.50 g (17.4 mmol, 1.00 eq) aldehyde in 10 mL THF were added. The mixture was stirred for 1h at -78 °C and then at -40 °C for 3 h. The reaction was quenched by addition of saturated NH_4Cl solution (30 mL) and the mixture was extracted with Et_2O (2 x 50 mL). The combined organic fractions were dried, filtered and the solvent evaporated under reduced pressure. Purification via flash chromatography (hexanes/Et_2O 15:1 → 5:1) yielded 1.56 g (8.56 mmol, 49%) ester as a yellow oil.

R_f = 0.79 (hexanes/Et_2O 6:1) [UV, $KMnO_4$]
^{1}H NMR (300 MHz, $CDCl_3$, 300 K): δ (ppm) = 7.26 (dd, *J* = 15.4, 10.6 Hz, 1H), 6.23 – 5.94 (m, 2H), 5.86 – 5.72 (m, 1H), 4.19 (q, *J* = 7.1 Hz, 2H), 2.16 (*virt.* p, *J* = 6.9 Hz, 1H), 1.44 – 1.32 (m, 2H), 1.29 (t, *J* = 7.1 Hz, 3H), 1.02 (d, *J* = 6.7 Hz, 3H), 0.86 (t, *J* = 7.4 Hz, 3H).
^{13}C NMR (75 MHz, $CDCl_3$, 300 K): δ (ppm) = 167.4, 150.3, 145.4, 126.9, 119.4, 60.3, 38.9, 29.5, 19.7, 14.5, 11.8.
$[\alpha]^{22}_D$ = 44.8 (c = 2.0, CH_2Cl_2).

(S,2E,4E)-6-Methylocta-2,4-dienal (3)

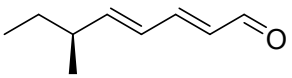

Chemical Formula: $C_9H_{14}O$
Molecular Weight: 138.21

1.40 g (7.68 mmol, 1.00 eq) ester were dissolved in THF (18 mL) and cooled to -78 °C. 16.1 mL (16.1 mmol, 1 M in THF, 2.10 eq) DIBAL-H were added dropwise and the solution stirred at -78 °C for 2 h. The reaction was quenched with MeOH (10 mL) and saturated K/Na tartrate solution (50 mL) and Et_2O (50 mL) were added. The biphasic mixture was stirred at rt o/n and the phase separated. The aqueous phase was reextracted with Et_2O (50 mL) and the combined organic fractions dried, filtered and the solvent evaporated. The crude product alcohol was directly used for the next step. The crude product was dissolved in hexane (20 mL) and 13.4 g (154 mmol, 20.0 eq) MnO_2 were added at 0 °C. After 3 h, TLC indicated full conversion. The mixture was filtered and the solvent removed. Purification via flash chromatography (hexanes/Et_2O 12:1) yielded 550 mg (4.00 mmol, 52% over two steps) aldehyde as a yellow oil.

$\boldsymbol{R_f}$ = 0.58 (hexanes/Et_2O 9:1)
^{1}H NMR (250 MHz, $CDCl_3$, 300 K): δ (ppm) = 9.54 (d, *J* = 8.0 Hz, 1H), 7.09 (dd, *J* = 15.3, 10.2 Hz, 1H), 6.39 – 6.00 (m, 3H), 2.23 (*virt.* hept, *J* = 6.8 Hz, 1H), 1.48 – 1.34 (m, 2H), 1.06 (d, *J* = 6.7 Hz, 3H), 0.89 (t, *J* = 7.4 Hz, 3H).
^{13}C NMR (63 MHz, $CDCl_3$, 300 K): δ (ppm) = 194.1, 153.2, 152.9, 130.3, 127.2, 39.2, 29.4, 19.5, 11.8.
$[\alpha]^{22}_D$ = 63.7 (c = 2.0, CH_2Cl_2).

(S,3E,5E,7E)-9-Methylundeca-3,5,7-trien-2-one (4)

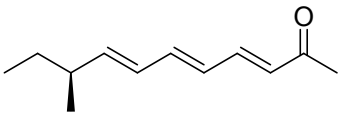

Chemical Formula: $C_{12}H_{18}O$
Molecular Weight: 178.28

To a solution of 460 mg (3.33 mmol, 1.00 eq) aldehyde in toluene (15 mL) were added 2.12 g (6.66 mmol, 2.00 eq) ylide and the mixture was heated up to 100 °C and stirred for 16 h. The brown red solution was allowed to cool to rt and hexane (30 mL) was added. The mixture was filtered and the solvent removed under reduced pressure. The residue was resuspended in hexane and filtered. After removal of the solvent, the crude product was purified via flash chromatography (hexanes/Et_2O 10:1 → 8:1) to yield 351 mg (1.97 mmol, 59%) ketone as a yellow oil.

$\boldsymbol{R_f}$ = 0.42 (hexanes/ Et_2O 8:1)
^{1}H NMR (250 MHz, $CDCl_3$, 300 K): δ (ppm) = 7.15 (dd, *J* = 15.5, 11.0 Hz, 1H), 6.58 (dd, *J* = 14.9, 10.6 Hz, 1H), 6.32 – 6.05 (m, 3H), 5.84 (dd, *J* = 15.2, 7.8 Hz, 1H), 2.27 (s, 3H), 2.15 (*virt.* p, *J* = 6.9 Hz, 1H), 1.45 – 1.28 (m, 2H), 1.02 (d, *J* = 6.7 Hz, 3H), 0.87 (t, *J* = 7.4 Hz, 3H).
^{13}C NMR (63 MHz, $CDCl_3$, 300 K): δ (ppm) = 198.6, 146.8, 143.9, 142.5, 129.5, 128.4, 38.9, 29.6, 27.4, 19.8, 11.9.
$[\alpha]^{22}_D$ = 58.2 (c = 0.17, $CHCl_3$).

(S,3Z,5E,7E,9E)-1,1,1-Trichloro-4-hydroxy-11-methyltrideca-3,5,7,9-tetraen-2-one

Neocarzilin A (NCA)

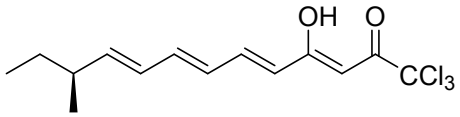

Chemical Formula: $C_{14}H_{17}Cl_3O_2$
Molecular Weight: 323.64

To a solution of 100 mg (0.56 mmol, 1.00 eq) ketone in 5 mL THF was added 617 µL (0.62 mmol, 1 M in THF, 1.10 eq) LiHMDS at -78 °C. The mixture was stirred for 1 h and then 346 mg (205 µL, 1.12 mmol, 2.00 eq) trichloroacetic anhydride were added. The mixture was stirred at -78 °C for 3 h and then quenched by addition of 50 mL PBS. After extraction with Et_2O (2 x 50 mL), the organic phase was dried, filtered and the solvent removed under reduced pressure. Purification via flash chromatography (hexanes/Et_2O 50:1 → 10:1) yielded 91.3 mg (28.2 mmol, 50%) neocarzilin A as an orange oil.

R_f = 0.66 (hexanes/Et_2O 10:1) [UV, $KMnO_4$]
RP-HPLC (analytical setup, method: gradient 2% D → 100% D over 20 min): t_R = 20.27 min
^{1}H NMR (360 MHz, $CDCl_3$, 300 K): δ (ppm) = 13.43 (s, 1H), 7.39 (ddd, *J* = 15.1, 11.4, 0.8 Hz, 1H), 6.70 – 6.58 (m, 1H), 6.33 – 6.26 (m, 1H), 6.23 – 6.13 (m, 2H), 6.02 (d, *J* = 15.0 Hz, 1H), 5.91 (dd, *J* = 15.2, 7.9 Hz, 1H), 2.29 – 2.07 (m, 1H), 1.44 – 1.35 (m, 2H), 1.05 (d, *J* = 6.7 Hz, 3H), 0.89 (t, *J* = 7.4 Hz, 4H).
^{13}C NMR (126 MHz, $CDCl_3$, 300 K): δ (ppm) = 186.1, 178.0, 147.7, 143.0, 142.8, 128.4, 128.4, 123.3, 95.2, 93.2, 38.9, 29.5, 19.7, 11.8.
HRMS ESI calcd. for $C_{14}H_{16}Cl_3O_2$ $[M-H]^-$: 321.0221, found: 321.0219.
$[\alpha]^{22}_D$ = 45.4 (c = 0.24, $CHCl_3$).

(S,3Z,5E,7E,9E)-1,1-Dichloro-4-hydroxy-11-methyltrideca-3,5,7,9-tetraen-2-one
Neocarzilin C (NCC)

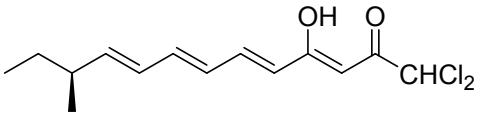

Chemical Formula: $C_{14}H_{18}Cl_2O_2$
Molecular Weight: 289.20

To a solution of 100 mg (0.56 mmol, 1.00 eq) ketone in 5 mL THF was added 617 µL (0.62 mmol, 1 M in THF, 1.10 eq) LiHMDS at -78 °C. The mixture was stirred for 1 h and then 266 mg (169 µL, 1.12 mmol, 2.00 eq) dichloroacetic anhydride were added. The mixture was stirred at -78 °C for 3 h and then quenched by addition of 50 mL PBS. After extraction with Et_2O (2 x 50 mL), the organic phase was dried, filtered and the solvent removed under reduced pressure. Purification via flash chromatography (hexanes/Et_2O 20:1 → 10:1) yielded 71.0 mg (0.25 mmol, 44%) neocarzilin C as an orange oil.

R_f = 0.51 (hexanes/Et_2O 10:1)
RP-HPLC (analytical setup, method: gradient 2% D → 100% D over 20 min): t_R = 18.80 min
^{1}H NMR (300 MHz, $CDCl_3$, 300 K): δ (ppm) = 13.96 (s, 1H), 7.34 (ddd, *J* = 15.1, 11.3, 0.8 Hz, 1H), 6.67 – 6.51 (m, 1H), 6.33 – 6.06 (m, 2H), 6.00 – 5.83 (m, 2H), 5.95 (s, 1H), 5.89 (s, 1H), 2.16 (*virt.* p, *J* = 6.9 Hz, 1H), 1.41 – 1.33 (m, 1H), 1.03 (d, *J* = 6.7 Hz, 3H), 0.87 (t, *J* = 7.4 Hz, 3H).
^{13}C NMR (75 MHz, $CDCl_3$, 300 K): δ (ppm) = 189.9, 178.5, 147.6, 142.7, 142.6, 128.6, 128.5, 123.6, 95.5, 69.0, 39.1, 29.6, 19.9, 11.9.
HRMS ESI calcd. for $C_{14}H_{17}Cl_2O_2$ $[M-H]^-$: 287.0611, found: 287.0614.
$[\alpha]^{22}_D$ = 43.0 (c = 0.14, $CHCl_3$)

(R)-4-benzyl-3-butyryloxazolidin-2-one (11)

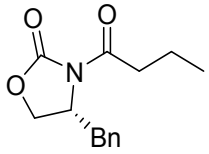

Chemical Formula: $C_{14}H_{17}NO_3$
Molecular Weight: 247.29

To a solution of 7.00 g (39.5 mmol, 1.00 eq) (R)-4-benzyloxazolidin-2-one in 86 mL dry THF, cooled to -78 °C, was added dropwise over 20 min a solution of 2.5 M *n*-BuLi (22.8 mL in hexanes, 56.9 mmol, 1.44 eq). The resulting mixture was stirred for 30 min and then 4.67 g butyryl chloride (4.54 mL, 43.9 mmol, 1.11 eq) was added. The mixture was stirred for 30 min at -78 °C and additional 30 min at room temperature. After this, the reaction was quenched by addition 75 mL of a saturated NH_4Cl solution. The aqueous phase was separated and extracted with DCM (3 x 50 mL). The combined organic extracts were subsequently washed with 40 mL 1 M NaOH solution and brine, dried over Na_2SO_4, filtered and the solvent evaporated under reduced pressure. Flash chromatography (hexanes/EtOAc 10:1 → 8:2) yielded 6.69 g (27.0 mmol, 68%) of the desired product as a slight yellow oil.

R_f = 0.19 (hexanes/Et_2O 10:1) [UV, $KMnO_4$].
^{1}H NMR (400 MHz, $CDCl_3$, 298 K): δ (ppm) = 7.33 (ddt, *J* = 8.0, 6.6, 1.2 Hz, 2H), 7.32 – 7.22 (m, 1H), 7.25 – 7.17 (m, 2H), 4.68 (ddt, *J* = 9.6, 7.4, 3.3 Hz, 1H), 4.24 – 4.12 (m, 2H), 3.30 (dd, *J* = 13.4, 3.4 Hz, 1H), 2.92 (qdd, *J* = 17.0, 7.8, 6.9 Hz, 2H), 2.77 (dd, *J* = 13.3, 9.6 Hz, 1H), 1.79 – 1.67 (m, 2H), 1.01 (t, *J* = 7.4 Hz, 3H).
^{13}C NMR (101 MHz, $CDCl_3$, 300 K): δ (ppm) = 173.4, 153.6, 135.5, 129.6, 129.1, 127.5, 66.3, 55.3, 38.1, 37.5, 17.9, 13.8.

(R)-4-benzyl-3-((R)-2-methylbutanoyl)oxazolidin-2-one (12)

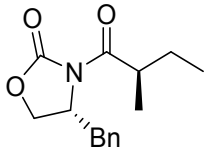

Chemical Formula: $C_{15}H_{19}NO_3$
Molecular Weight: 261.32

To a solution of 5.70 g (23.1 mmol, 1.00 eq) (R)-4-benzyl-3-butyryloxazolidin-2-one in 33 mL dry THF was added a solution of 13.8 mL (27.7 mmol, 2 M in THF, 1.20 eq) NaHMDS at -78 °C. After stirring for 1 h at -78 °C 8.18 g (3.6 mL, 57.6 mmol, 2.50 eq) methyl iodide were added dropwise and the resulting solution was stirred for additional 3 h at -78 °C. The reaction mixture was warmed to room temperature and quenched with 20 mL brine. The aqueous phase was separated and extracted with DCM (3 x 20 mL). The combined organic phases were dried, filtered and the solvent was evaporated under reduced pressure. Purification via flash chromatography (hexanes/EtOAc 15:1) yielded 4.66 g (17.8 mmol, 77%) of the desired product as a slightly yellow oil.
R_f = 0.37 (hexanes/EtOAc 10:1) [UV, $KMnO_4$].
^{1}H NMR (400 MHz, $CDCl_3$, 298 K): δ (ppm) = 7.36 – 7.31 (m, 2H), 7.32 – 7.22 (m, 1H), 7.24 – 7.19 (m, 2H), 4.68 (ddt, *J* = 9.6, 7.2, 3.2 Hz, 1H), 4.23 – 4.14 (m, 2H), 3.64 (*virt.* h, *J* = 6.8 Hz, 1H), 3.27 (dd, *J* = 13.3, 3.3 Hz, 1H), 2.77 (dd, *J* = 13.4, 9.6 Hz, 1H), 1.81 – 1.71 (m, 1H), 1.53 – 1.42 (m, 1H), 1.22 (d, *J* = 6.9 Hz, 3H), 0.93 (t, *J* = 7.4 Hz, 3H).
^{13}C NMR (101 MHz, $CDCl_3$, 300 K): δ (ppm) = 11.8, 17.0, 26.6, 38.1, 39.3, 55.5, 66.2, 127.5, 129.1, 129.6, 135.5, 153.2, 177.3.

((R)-2-methylbutan-1-ol (13)

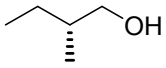

Chemical Formula: $C_5H_{12}O$
Molecular Weight: 88.15

To a solution of 4.65 g (17.8 mmol, 1.00 eq) (R)-4-benzyl-3-((R)-2-methylbutanoyl)oxazolidin-2-one in 31 mL Et_2O under an inert atmosphere was added 1.2 mL MeOH and the colorless solution was cooled to -20 °C. 271 mg (12.5 mmol, 0.70 eq) lithium borohydride were added portionwise and the mixture was stirred for 5 h at 0 °C. After this time, the reaction was quenched by addition of 10 mL 1 M $NaOH_{aq}$ and stirred for 30 min at room temperature. The white precipitate was removed by filtration and the aqueous phase was separated and extracted with Et_2O (2 x 20 mL). The combined organic fractions were dried, filtered and the solvent was removed under reduced pressure with a water bath temperature not higher than 20 °C (pressure not lower than 200 mbar). Purification by flash chromatography (pentane/Et_2O 3:1) afforded 1.04 g (11.8 mmol, 66%) alcohol as a colorless liquid. 2.33 g (13.1 mmol, 74%) of Evans auxiliary could be isolated as white solid.

R_f = 0.28 (pentane/Et_2O 3:1) [UV, $KMnO_4$].
^{1}H NMR (500 MHz, $CDCl_3$, 298 K): δ (ppm) = 3.51 (ddd, *J* = 10.5, 5.8, 1.1 Hz, 1H), 3.43 (ddd, *J* = 10.5, 6.4, 1.2 Hz, 1H), 1.54 (dq, *J* = 12.5, 6.3 Hz, 1H), 1.50 – 1.40 (m, 1H), 1.37 (s, 1H), 1.15 (dt, *J* = 13.9, 7.5 Hz, 1H), 0.91 (d, *J* = 6.7 Hz, 3H), 0.91 (t, *J* = 7.5 Hz, 3H).
^{13}C NMR (101 MHz, $CDCl_3$, 300 K): δ (ppm) = 68.2, 37.5, 25.9, 16.3, 11.5.

(R)-2-methylbutanal (14)

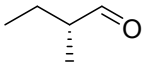

Chemical Formula: $C_5H_{10}O$
Molecular Weight: 86.13

To a solution of 1.47 mL (2.18 g, 17.1 mmol, 1.50 eq) oxalyl chloride in 13 mL dry DCM under an inert atmosphere at -78 °C was added dropwise over 15 min a solution of 2.02 mL (2.23 g, 28.5 mmol, 2.50 eq) dimethyl sulfoxide in 3 mL dry DCM. The resulting solution was stirred for 30 min at -78 °C before a solution of 1.01 mL (11.4 mmol, 1.00 eq) ((R)-2-methylbutan-1-ol in 7 mL dry DCM was added. After additional stirring for 1.5 h at -78 °C 7.9 mL (5.78 g, 57.0 mmol, 5.00 eq) triethylamine were added and the mixture was again stirred for 30 min at -78 °C. Afterwards the reaction mixture was thawed and stirred for 2 h at room temperature, then quenched with 40 mL H_2O and extracted with DCM (2 x 20 mL). The combined organic extracts were subsequently washed with aqueous 1 M HCl (2 x 30 mL), H_2O (30 mL), saturated $NaHCO_3$ solution (30 mL) and brine (30 mL), dried over Na_2SO_4, filtered and the solvent was removed under reduced pressure (max. water bath temperature 27 °C, pressure not lower than 200 mbar) yielding 551 mg (6.39 mmol, 56%) aldehyde as a brown oil which was used without further purification in the next step.

R_f = 0.44 (hexanes/EtOAc 25:1) [UV, $KMnO_4$].
^{1}H NMR (500 MHz, $CDCl_3$, 298 K): δ (ppm) = 9.62 (d, *J* = 1.7 Hz, 1H), 2.65 (s, 1H), 2.33 – 2.22 (m, 1H), 1.75 (*virt.* dp, *J* = 14.5, 7.3 Hz, 1H), 1.44 (*virt.* dp, *J* = 14.6, 7.4 Hz, 1H), 1.09 (d, *J* = 7.0 Hz, 3H), 0.95 (t, *J* = 7.5 Hz, 2H).

Ethyl (R,2E,4E)-6-methylocta-2,4-dienoate (15)

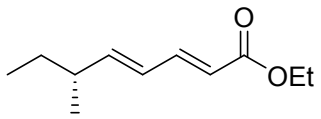

Chemical Formula: $C_{11}H_{18}O_2$
Molecular Weight: 182.26

To a solution of 2.40 g (9.59 mmol, 1.50 eq) ethyl (E)-4-(diethoxyphosphoryl)but-2-enoate in 7 mL THF under an inert atmosphere at -78 °C was added over 10 min 9.59 mL (9.59 mmol , 1 M in THF, 1.50 eq) LiHMDS to yield an orange solution which was stirred for 1 h at -78 °C. Afterwards 551 mg (6.40 mmol, 1.50 eq) aldehyde in 3 mL THF was added and the resulting mixture was stirred at -40 °C for 4.5 h. After warming to room temperature, the reaction was quenched by addition of 20 mL saturated NH_4Cl solution. The aqueous phase was separated, extracted with Et_2O (2 x 20 mL) and the combined organic fraction s were washed with brine (30 mL), dried over Na_2SO_4, filtered and the organic solvent was removed under reduced pressure. The brown crude product was purified by flash chromatography (hexanes/EtOAc 40:1) to yield 346 mg (1.90 mmol, 30%) ester as a pale yellow oil.

R_f = 0.33 (hexanes/EtOAc 25:1) [UV, $KMnO_4$].
^{1}H NMR (300 MHz, $CDCl_3$, 298 K): δ (ppm) = 7.26 (dd, *J* = 15.4, 10.5 Hz, 2H), 6.14 (ddt, *J* = 15.2, 10.4, 0.7 Hz, 1H), 6.00 (dd, *J* = 15.2, 7.5 Hz, 1H), 5.79 (dd, *J* = 15.4, 0.6 Hz, 1H), 4.20 (q, J = 7.1 Hz, 3H), 2.17 (hept, *J* = 6.8 Hz, 1H), 1.37 (dq, *J* = 7.6, 7.0 Hz, 3H), 1.29 (t, *J* = 7.1 Hz, 4H), 1.02 (d, *J* = 6.7 Hz, 4H), 0.87 (t, *J* = 7.4 Hz, 4H).

(R,2E,4E)-6-methylocta-2,4-dienal (16)

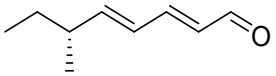

Chemical Formula: $C_9H_{14}O$
Molecular Weight: 138.21

In an inert atmosphere 346 mg (1.90 mmol, 1.00 eq) ester was diluted in 4 mL dry THF and cooled to -78 °C. 4.75 mL (4.75 mmol, 1.1 M in cyclohexane, 2.50 eq) DIBAL-H was added dropwise and the mixture as stirred for 2.5 h at -78 °C. The reaction was quenched by addition of 2.5 mL MeOH. 10 mL of a saturated Na/K-tartrate solution was added and the turbid mixture was stirred for 1 h until it went clear again. The aqueous phase was separated and washed with Et_2O (2 x 20 mL). The combined organic extracts were washed with brine (25 mL), dried and the solvent was removed under reduced pressure to yield 259 mg alcohol which was taken up in 10 mL hexanes for oxidation without further purification. 3.30 g (38.0 mmol, 20.0 eq) MnO_2 were added portionwise and the resulting suspension was stirred for 3 h at room temperature. After this time, the mixture was filtered over a short plug of silica using 40 mL hexanes to elute the product. The organic solvent was removed under reduced pressure yielding 206 mg (1.49 mmol, 78%) aldehyde as a yellow oil.

R_f = 0.29 (hexanes/EtOAc 20:1) [UV, $KMnO_4$].
^{1}H NMR (400 MHz, $CDCl_3$, 298 K): δ (ppm) = 9.53 (d, *J* = 8.0 Hz, 1H), 7.08 (dd, *J* = 15.3, 10.6 Hz, 1H), 6.29 (ddt, *J* = 15.3, 10.6, 0.8 Hz, 1H), 6.16 (dd, *J* = 15.2, 7.7 Hz, 1H), 6.09 (dd, *J* = 15.3, 8.0 Hz, 1H), 2.22 (h, *J* = 6.9 Hz, 1H), 1.40 (p, *J* = 7.4 Hz, 2H), 1.05 (d, *J* = 6.7 Hz, 3H), 0.88 (t, *J* = 7.4 Hz, 3H).
^{13}C-NMR (101 MHz, $CDCl_3$, 298 K): δ (ppm) = 11.8, 19.5, 29.4, 39.2, 127.2, 130.3, 152.9, 153.2, 194.1.
HRMS APCI calcd. for $C_9H_{14}O$ $[M+H]^+$: 139.1117, found: 139.1117.

(R,3E,5E,7E)-9-methylundeca-3,5,7-trien-2-one (17)

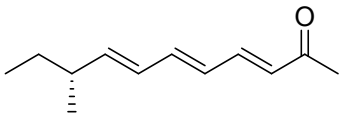

Chemical Formula: $C_{12}H_{18}O$
Molecular Weight: 178.28

206 mg (1.49 mmol, 1.00 eq) aldehyde were diluted in 7.5 ml toluene, 961 mg (2.99 mmol, 2.00 eq) 1-triphenylphosphoranylidene-2-propanone were added and the mixture was stirred for 18 h at 100 °C. Afterwards, the reaction mixture was allowed to cool to room temperature and 10 mL hexane was added to precipitate phosphorous side products. The white precipitate was filtered off and the resulting filtrate was reduced and again diluted with 10 mL hexane. After stirring for 30 min the precipitate was again filtered off and the solvent of filtrate was removed under reduced pressure. Flash chromatography (hexanes/EtOAc 20:1) yielded 206 mg (1.15 mmol, 77%) ketone as a bright yellow oil.

R_f = 0.19 (hexane/EtOAc 20:1) [UV, $KMnO_4$].
^{1}H NMR (400 MHz, $CDCl_3$, 298 K): δ (ppm) = 7.14 (ddd, *J* = 15.5, 11.1, 0.7 Hz, 1H), 6.58 (ddd, *J* = 14.9, 10.8, 0.8 Hz, 1H), 6.24 (ddd, *J* = 14.9, 11.1, 0.8 Hz, 1H), 6.14 (dt, *J* = 15.2, 0.9 Hz, 1H), 6.11 (d, *J* = 15.5 Hz, 2H), 5.84 (dd, *J* = 15.2, 7.9 Hz, 1H), 2.27 (s, 3H), 2.15 (p, *J* = 6.8 Hz, 1H), 1.36 (pd, *J* = 7.4, 1.1 Hz, 2H), 1.02 (d, *J* = 6.8 Hz, 3H), 0.87 (t, *J* = 7.4 Hz, 3H).
^{13}C-NMR (101 MHz, $CDCl_3$, 300 K): δ (ppm) = 198.6, 146.9, 143.9, 142.5, 129.5, 128.4, 38.9, 29.6, 27.4, 19.8, 11.9.
HRMS APCI calcd. for $C_{12}H_{18}O$ $[M+H]^+$: 179.1430, found: 179.1430.

(R,3Z,5E,7E,9E)-1,1,1-trichloro-4-hydroxy-11-methyltrideca-3,5,7,9-tetraen-2-one (NCA')

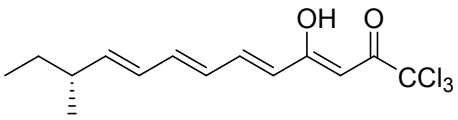

Chemical Formula: $C_{14}H_{17}Cl_3O_2$
Molecular Weight: 323.64

To a solution of 80.0 mg (448.7 µmol, 1.00 eq) in 4 mL dry THF under an inert atmosphere at -78 °C was added 494 µL (494 µmol, 1 M in THF, 1.10 eq) LiHMDS. The resulting orange mixture was stirred for 1 h at -78 °C. Then 173 µL (292 mg, 898 µmol, 2.00 eq) trichloroacetic acid were added over 10 min and the reaction mixture was stirred for 2.5 h at -78 °C. Then, the mixture was allowed to warm to room temperature, was quenched with 10 mL PBS, the aqueous phase was separated and extracted with 10 mL Et_2O. The combined organic extracts were dried over Na_2SO_4 and the solvent was removed under reduced pressure. The green crude product was purified via reversed phase HPLC (gradient 50% → 98% CH_3CN, λ = 388 nm) resulting in 87.5 mg (270 µmol, 60%) trichloride as a bright yellow solid.

R_f = 0.45 (hexanes/EtOAc 20:1) [UV, $KMnO_4$].
RP-HPLC (analytical setup, method: gradient 2% D → 100% D over 20 min): t_R = 19.41 min
^{1}H NMR (300 MHz, $CDCl_3$, 300 K): δ (ppm) = 13.41 (s, 1H), 7.37 (dd, *J* = 14.9, 11.3 Hz, 1H), 6.62 (dd, *J* = 14.7, 10.7 Hz, 1H), 6.28 (dd, *J* = 14.8, 11.3 Hz, 1H), 6.16 (dd, *J* = 14.8, 11.1 Hz, 1H), 6.15 (s, 1H), 6.00 (d, *J* = 15.0 Hz, 1H), 5.89 (dd, *J* = 15.2, 7.8 Hz, 1H), 2.17 (h, *J* = 7.0 Hz, 1H), 1.38 (p, *J* = 7.4 Hz, 2H), 1.03 (d, *J* = 6.7 Hz, 3H), 0.88 (t, *J* = 7.4 Hz, 3H).
^{13}C-NMR (126 MHz, $CDCl_3$, 300 K): δ (ppm) = 186.2, 178.1, 147.8, 143.1, 142.9, 128.6, 128.5, 123.4, 95.3, 93.3, 39.1, 29.6, 19.8, 11.9.
HRMS APCI calcd. for $C_{14}H_{17}Cl_3O_2$ $[M+H]^+$: 323.0367, found: 323.0366.

Ethyl (2E,4E)-6-methylhepta-2,4-dienoate (5)

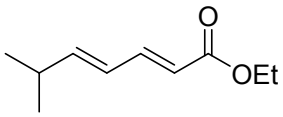

Chemical Formula: $C_{10}H_{16}O_2$
Molecular Weight: 168.24

To a solution of 7.51 g (30.0 mmol, 1.50 eq) ethyl (E)-4-(diethoxyphosphoryl)but-2-enoate in 25 mL THF was added 30.0 mL (30.0 mmol, 1 M in THF, 1.50 eq) LiHMDS at -78 °C. The solution was stirred at that temperature for 1 h and then 1.44 g (20.0 mmol, 1.00 eq) isobutanal in 10 mL THF were added. The mixture was stirred for 1h at -78 °C and then at -40 °C for 3h. The reaction was quenched by addition of saturated NH_4Cl solution (30 mL) and the mixture extracted with Et_2O (2 x 50 mL). The combined organic fractions were dried, filtered and the solvent evaporated under reduced pressure. Purification via flash chromatography (hexanes/Et_2O 15:1 → 5:1) yielded 1.71 g (10.2 mmol, 51%) ester as a yellow oil.

R_f = 0.76 (hexanes/Et_2O 6:1) [UV, $KMnO_4$].
^{1}H NMR (360 MHz, $CDCl_3$, 300 K): δ (ppm) = 7.32 – 7.20 (m, 2H), 6.24 – 6.02 (m, 2H), 5.80 (d, *J* = 15.4 Hz, 1H), 4.19 (q, *J* = 7.1 Hz, 2H), 2.52 – 2.29 (m, 1H), 1.29 (t, *J* = 7.1 Hz, 3H), 1.04 (d, *J* = 6.8 Hz, 6H).
^{13}C NMR (91 MHz, $CDCl_3$, 300 K): δ (ppm) = 167.4, 151.3, 145.4, 125.6, 119.5, 60.3, 31.7, 22.0, 14.5.

(2E,4E)-6-Methylhepta-2,4-dienal (6)

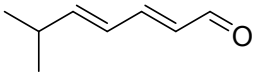

Chemical Formula: $C_8H_{12}O$
Molecular Weight: 124.18

3.60 g (21.4 mmol, 1.00 eq) ester were dissolved in THF (25 mL) and 37.4 mL (44.9 mmol, 1.2 M in toluene, 2.10 eq) DIBAL-H were added at -78 °C. The reaction was stirred at -78 °C for 4 h and was quenched with sat. K/Na tartrate solution at -78 °C. The mixture was stirred overnight and the phases separated. The aqueous phase was reextracted with Et_2O (2 x 30 mL), the combined organic fractions dried, filtered and the solvent evaporated. The crude alcohol was dissolved in Et_2O (50 mL) and 27.9 g (321 mmol, 15.0 eq) MnO_2 were added. The mixture was stirred for 3 h after which the TLC indicated complete consumption of starting material. The reaction mixture was filtered and the solvent evaporated. The crude product was purified by flash chromatography (hexanes/Et_2O 10:1 → 5:1) to yield 2.20 g (17.7 mmol, 83% over two steps) aldehyde as a yellow oil.

R_f = 0.63 (hexanes/Et_2O 6:1) [UV, $KMnO_4$]
^{1}H NMR (360 MHz, $CDCl_3$, 300 K): δ (ppm) = 9.54 (d, *J* = 8.0 Hz, 1H), 7.20 – 7.02 (m, 1H), 6.38 – 6.16 (m, 2H), 6.09 (dd, *J* = 15.4, 8.1 Hz, 1H), 2.61 – 2.38 (m, 1H), 1.08 (d, *J* = 6.8 Hz, 6H).
^{13}C NMR (91 MHz, $CDCl_3$, 300 K): δ (ppm) = 194.1, 153.9, 153.3, 130.4, 126.0, 31.9, 21.8.

(3E,5E,7E)-9-Methyldeca-3,5,7-trien-2-one (7)

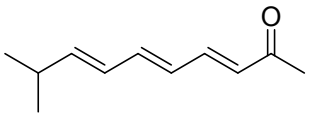

Chemical Formula: $C_{11}H_{16}O$
Molecular Weight: 164.25

To a solution of 1.00 g (8.05 mmol, 1.00 eq) aldehyde in toluene (30 mL) were added 5.13 g (16.1 mmol, 2.00 eq) ylide and the mixture was heated up to 100 °C and stirred for 16 h. The brown red solution was allowed to cool to rt and hexane (30 mL) was added. The triphenylphosphine oxide was removed by filtration and the solvent removed *in vacuo*. The residue was resuspended in hexane and filtered. After removal of the solvent, the crude product was purified via flash chromatography (hexanes/Et_2O 5:1) to yield 866 mg (5.27 mmol, 65%) ketone as a yellow oil.

R_f = 0.40 (hexanes/ Et_2O 10:1)
^{1}H NMR (360 MHz, $CDCl_3$, 300 K): δ (ppm) = 7.14 (ddd, *J* = 15.5, 11.1, 0.7 Hz, 1H), 6.57 (dd, *J* = 14.9, 10.6 Hz, 1H), 6.24 (*virt.* ddt, *J* = 14.9, 11.1, 0.7 Hz, 1H), 6.18 – 6.05 (m, 2H), 5.93 (dd, *J* = 15.2, 6.7 Hz, 1H), 2.47 – 2.35 (m, 1H), 2.26 (s, 3H), 1.03 (d, *J* = 6.8 Hz, 6H).
^{13}C NMR (91 MHz, $CDCl_3$, 300 K): δ (ppm) = 198.6, 147.9, 143.9, 142.5, 129.5, 128.5, 127.1, 31.6, 27.4, 22.1.
HRMS APCI calcd. for $C_{11}H_{17}O$ $[M+H]^+$: 165.1273, found: 165.1273.

(3Z,5E,7E,9E)-1,1,1-Trichloro-4-hydroxy-11-methyldodeca-3,5,7,9-tetraen-2-one

Neocarzilin B (NCB)

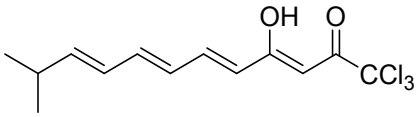

Chemical Formula: $C_{13}H_{15}Cl_3O_2$
Molecular Weight: 309.61

To a solution of 500 mg (3.04 mmol, 1.00 eq) ketone in anhydrous THF (25 mL) were added 3.34 mL (3.34 mmol, 1 M in THF, 1.10 eq) LiHMDS at -78 °C. The mixture was stirred for 1 h and then 1.88 g (1.11 mL, 6.09 mmol, 2.00 eq) trichloroacetic anhydride were added. The mixture was stirred at -78 °C for 3 h and then quenched by addition of 50 mL PBS. After extraction with Et_2O (2 x 50 mL), the organic phase was dried, filtered and the solvent removed under reduced pressure. Purification via flash chromatography (hexanes/Et_2O 50:1 → 10:1) yielded 745 mg (2.41 mmol, 79%) neocarzilin B as an orange solid.

R_f = 0.46 (hexanes/Et_2O 10:1)
RP-HPLC (analytical setup, method: gradient 2% B → 100% B over 20 min): t_R = 19.55 min
^{1}H NMR (250 MHz, $CDCl_3$, 300 K): δ (ppm) = 13.41 (s, 1H), 7.36 (dd, *J* = 15.0, 11.4 Hz, 1H), 6.61 (dd, *J* = 14.8, 10.5 Hz, 1H), 6.28 (dd, *J* = 14.8, 11.3 Hz, 1H), 6.15 (s, 1H), 6.21 – 6.09 (m, 2H), 6.04 – 5.90 (m, 2H), 2.51 – 2.34 (m, 1H), 1.05 (d, *J* = 6.7 Hz, 6H).
^{13}C NMR (63 MHz, $CDCl_3$, 300 K): δ (ppm) = 186.2, 178.1, 148.8, 143.1, 142.9, 128.6, 127.3, 123.4, 95.3, 93.3, 31.7, 22.1.
HRMS ESI calcd. for $C_{13}H_{14}Cl_3O_2$ $[M-H]^-$: 307.0065, found 307.0065.

Ethyl (2E,4E)-deca-2,4-dien-9-ynoate (8)

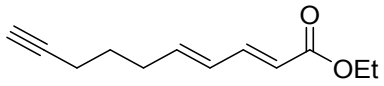

Chemical Formula: $C_{12}H_{16}O_2$
Molecular Weight: 192.26

To a solution of 4.55 g (18.2 mmol, 1.00 eq) ethyl (E)-4-(diethoxyphosphoryl)but-2-enoate in THF (36 mL) at -78 °C were added 8.00 mL (20.0 mmol, 2.5 M in hexane, 1.10 eq) nBuLi. The solution was stirred at this temperature for 15 min and 1.75 g (18.2 mmol, purity ca. 90%, 1.00 eq) 5-hexynal were added. After 15 min, the mixture was warmed up to rt and stirred for 1 h. The reaction mixture was quenched by addition of sat. NH_4Cl solution and extracted with Et_2O (3 x 40 mL). After filtration over Na_2SO_4, the solvent was removed under reduced pressure and the crude product subjected to flash chromatography (hexanes/ Et_2O 15:1). 1.88 g (9.87 mmol, 54%, E/Z = 5:1) ester were isolated as a yellow oil.

$\boldsymbol{R_f}$ = 0.63 (hexanes/ Et_2O 6:1) [UV, $KMnO_4$]
^{1}H NMR (250 MHz, $CDCl_3$, 300 K): δ (ppm) = 7.34 – 7.16 (m, 1H), 6.27 – 6.02 (m, 2H), 5.80 (dt, *J* = 15.4, 0.6 Hz, 1H), 4.20 (q, *J* = 7.1 Hz, 2H), 2.39 – 2.12 (m, 4H), 1.97 (t, *J* = 2.6 Hz, 1H), 1.74 – 1.58 (m, 2H), 1.29 (t, *J* = 7.1 Hz, 3H).
^{13}C NMR (63 MHz, $CDCl_3$, 300 K): δ (ppm) = 167.3, 144.8, 143.0, 129.3, 119.9, 83.9, 69.0, 60.4, 31.9, 27.6, 18.0, 14.5.

(2E,4E)-Deca-2,4-dien-9-ynal (9)

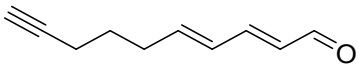

Chemical Formula: $C_{10}H_{12}O$
Molecular Weight: 148.21

To a solution of 3.02 g (15.8 mmol, 1.00 eq) ester in THF (60 mL), 27.2 mL (31.5 mmol, 25 wt-% in hexane, 2.00 eq) DIBAL-H were added under argon atmosphere at -78 °C. After stirring for 1.5 h at -78 °C, the mixture was allowed to warm up to room temperature. Then dry methanol (30 mL) and saturated sodium potassium tartrate solution (60 mL) were added slowly. Stirring was continued for another h, water (60 mL) was added and the resulting mixture was extracted with ether (3 × 60 mL). The organic layer was washed with brine (1 × 60 mL), dried over sodium sulfate and concentrated under reduced pressure. After a suspension of 11.6 g MnO2 (133 mmol, 20 eq) in Hexane (25 mL) was cooled to 0 °C, 1.00 g (6.67 mmol, 1.00 eq) of the crude product was added. The mixture was stirred for 4 h at rt after which TLC indicated full conversion. The MnO_2 was filtered off and the filtrate was concentrated on the rotary evaporator. Column chromatography (hexanes/Et_2O 5:1 → 3:1) provided 664 mg (4.48 mmol, 67%) of the product.

$\boldsymbol{R_f}$ = 0.67 (hexanes/Et_2O 6:1) [UV, $KMnO_4$]
^{1}H NMR (360 MHz, $CDCl_3$, 300 K): δ (ppm) = 9.56 (d, *J* = 8.0 Hz, 1H), 7.10 (dd, *J* = 15.3, 10.4 Hz, 1H), 6.43 – 6.22 (m, 2H), 6.11 (dd, *J* = 15.3, 8.0 Hz, 1H), 2.37 (q, *J* = 7.3 Hz, 2H), 2.25 (td, *J* = 7.0, 2.7 Hz, 2H), 2.00 (t, *J* = 2.6 Hz, 1H), 1.72 (p, *J* = 7.2 Hz, 2H).
^{13}C NMR (91 MHz, $CDCl_3$, 300 K): δ (ppm) = 194.0, 152.4, 145.6, 130.6, 129.6, 83.7, 69.1, 32.1, 27.4, 18.0.

(3E,5E,7E)-Trideca-3,5,7-trien-12-yn-2-one (10)

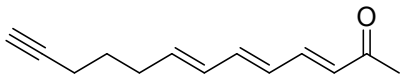

Chemical Formula: $C_{13}H_{16}O$
Molecular Weight: 188.27

To a solution of 664 mg (4.48 mmol, 1.00 eq) aldehyde in toluene (17 mL), 2.83 g (8.96 mmol, 2.00 eq) 1-(triphenylphosphoranylidene)-2-propanone were added at 0 °C and the solution was allowed to warm up to room temperature. The reaction mixture was heated up to 100 °C and was stirred for 16 h. After the solution had cooled down, brine was added and the mixture extracted with ethyl acetate (3 x 25 mL). The organic layer was washed with brine (1 x 25 mL), dried over Na_2SO_4 and concentrated on the rotary evaporator. Column chromatography (hexanes/ Et_2O 9:1) provided 452 mg (2.40 mmol, 54%) ketone as a yellow oil.

R_f = 0.58 (hexanes/ Et_2O 9:1) [UV, $KMnO_4$]
^{1}H NMR (250 MHz, $CDCl_3$, 300 K): δ (ppm) = 7.22 – 7.06 (m, 1H), 6.66 – 6.49 (m, 1H), 6.32 – 6.07 (m, 3H), 5.93 (dt, *J* = 14.7, 7.0 Hz, 1H), 2.34 – 2.16 (m, 4H), 2.27 (s, 3H), 1.97 (t, *J* = 2.7 Hz, 1H), 1.73 – 1.59 (m, 2H).
^{13}C NMR (63 MHz, $CDCl_3$, 300 K): δ (ppm) = 198.5, 143.7, 141.8, 139.4, 130.9, 129.8, 128.8, 84.0, 68.9, 31.9, 27.8, 27.5, 18.0.
HRMS APCI calcd. for $C_{13}H_{17}O$ $[M+H]^+$:189.1273, found: 189.1273.

(3Z,5E,7E,9E)-1,1,1-trichloro-4-hydroxypentadeca-3,5,7,9-tetraen-14-yn-2-one (NC-1)

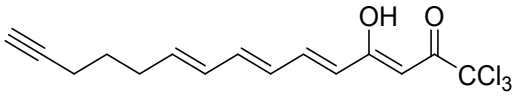

Chemical Formula: $C_{15}H_{15}Cl_3O_2$
Molecular Weight: 333.63

To a solution of 120.0 mg (0.64 mmol, 1.00 eq) ketone in 10 mL THF was added 1.31 mL (1.31 mmol, 1 M in THF, 2.05 eq) LiHMDS at -78 °C. The mixture was stirred for 1 h and then 196 mg (116 µL, 0.64 mmol, 1.00 eq) trichloroacetic anhydride were added. The reaction mixture was stirred for 2 h and then quenched with water. The phases were separated, aqueous phase extracted with Et_2O (20 mL) and the combined organic fractions dried, filtered and the solvent evaporated. Purification via HPLC (gradient 80% → 95 % CH_3CN) yielded 54 mg (0.16 mmol, 25%) trichloride as a yellow oil.

R_f = 0.71 (hexanes/Et_2O 10:1) [UV, $KMnO_4$]
RP-HPLC (analytical setup, method: gradient 2% B → 100% B over 20 min): t_R = 18.59 min
^{1}H NMR (360 MHz, $CDCl_3$, 300 K): δ (ppm) = 13.38 (s, 1H), 7.36 (dd, *J* = 15.0, 11.3 Hz, 1H), 6.61 (dd, *J* = 14.9, 10.7 Hz, 1H), 6.35 – 6.13 (m, 2H) 6.15 (s, 1H), 6.11 – 5.91 (m, 2H), 2.30 (q, *J* = 7.3 Hz, 2H), 2.22 (td, *J* = 7.0, 2.7 Hz, 3H), 1.97 (t, *J* = 2.7 Hz, 1H), 1.69 – 1.63 (m, 2H).
^{13}C NMR (91 MHz, $CDCl_3$, 300 K): δ (ppm) = 186.3, 178.0, 142.7, 142.4, 140.3, 131.0, 128.9, 123.8, 95.3, 93.4, 84.0, 68.9, 32.0, 27.8, 18.0.
HRMS ESI calcd. for $C_{15}H_{16}Cl_3O_2$ $[M-H]^-$: 331.0065, found: 331.0066.

6. NMR spectra

^{1}H-, ^{13}C-NMR-Spectra

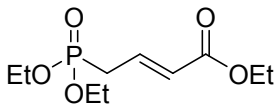

Chemical Formula: $C_{10}H_{19}O_5P$
Molecular Weight: 250.23

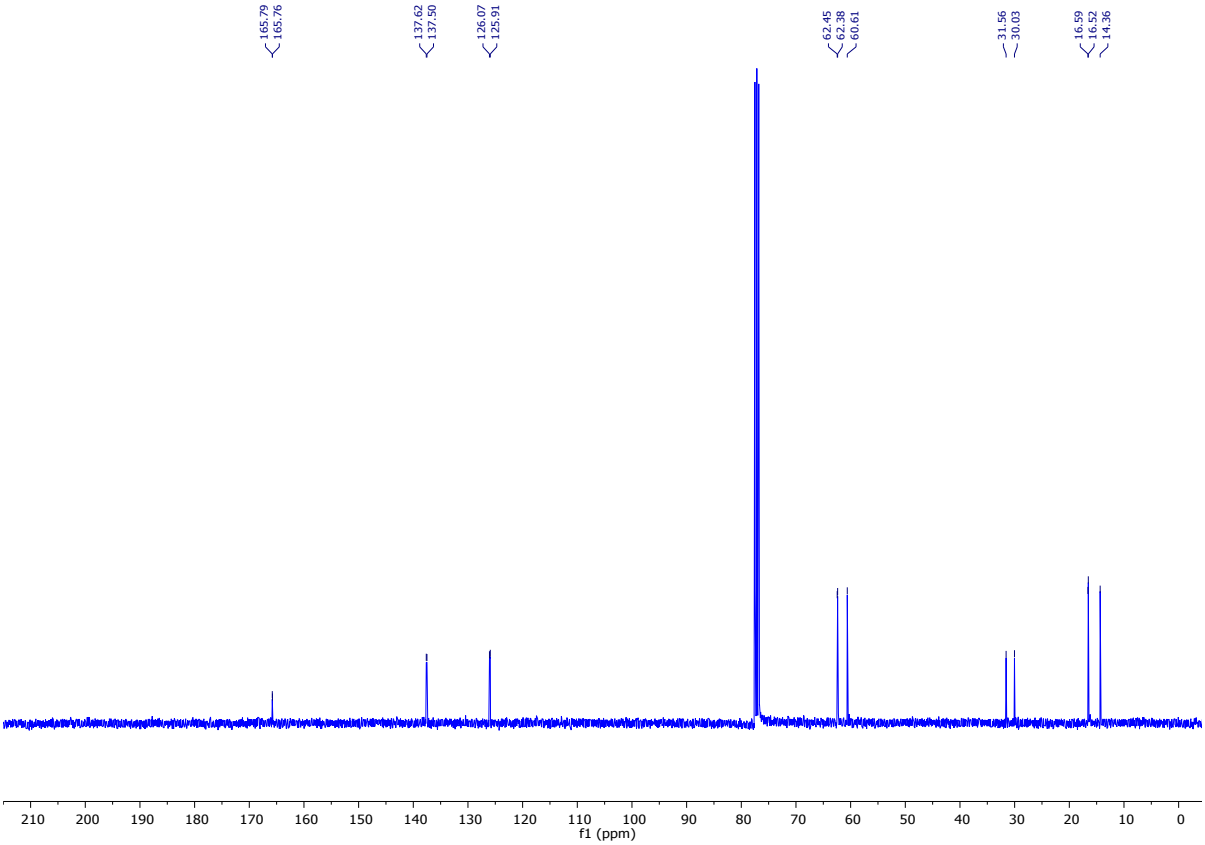

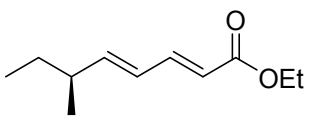

Chemical Formula: $C_{11}H_{18}O_2$
Molecular Weight: 182.26

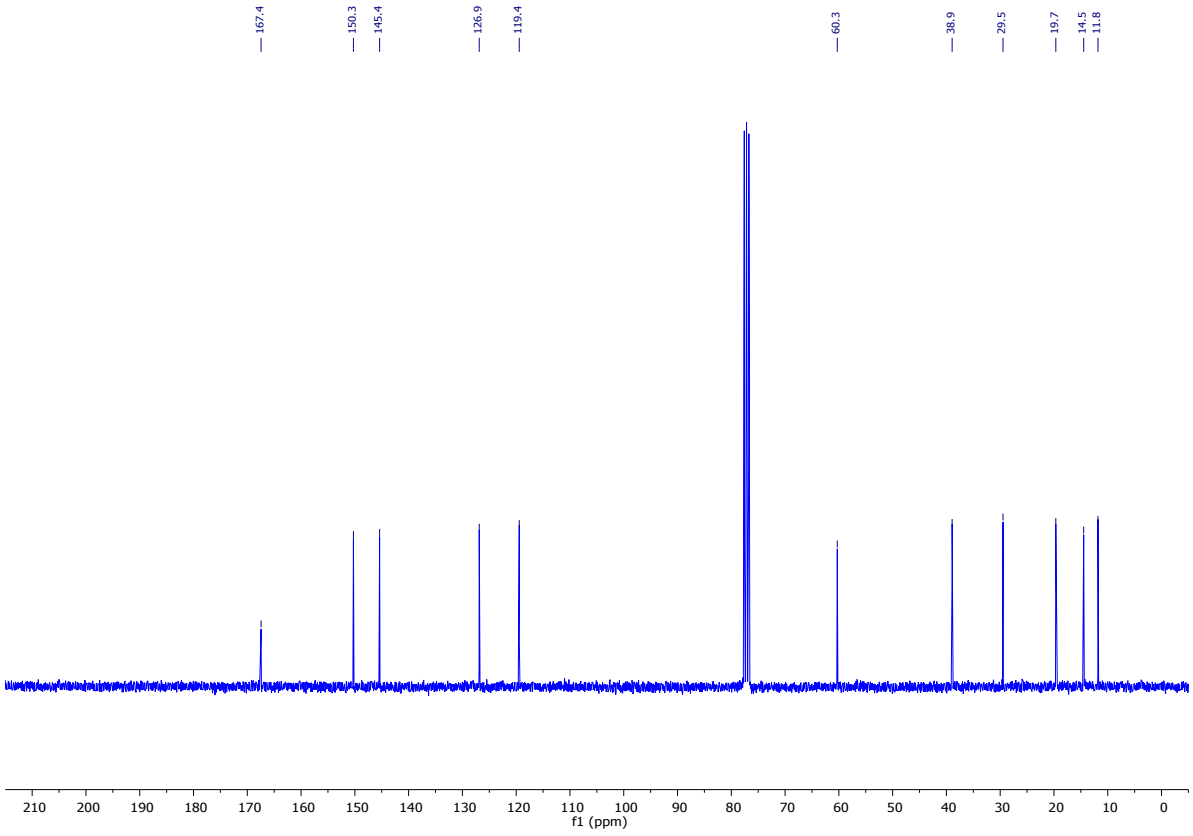

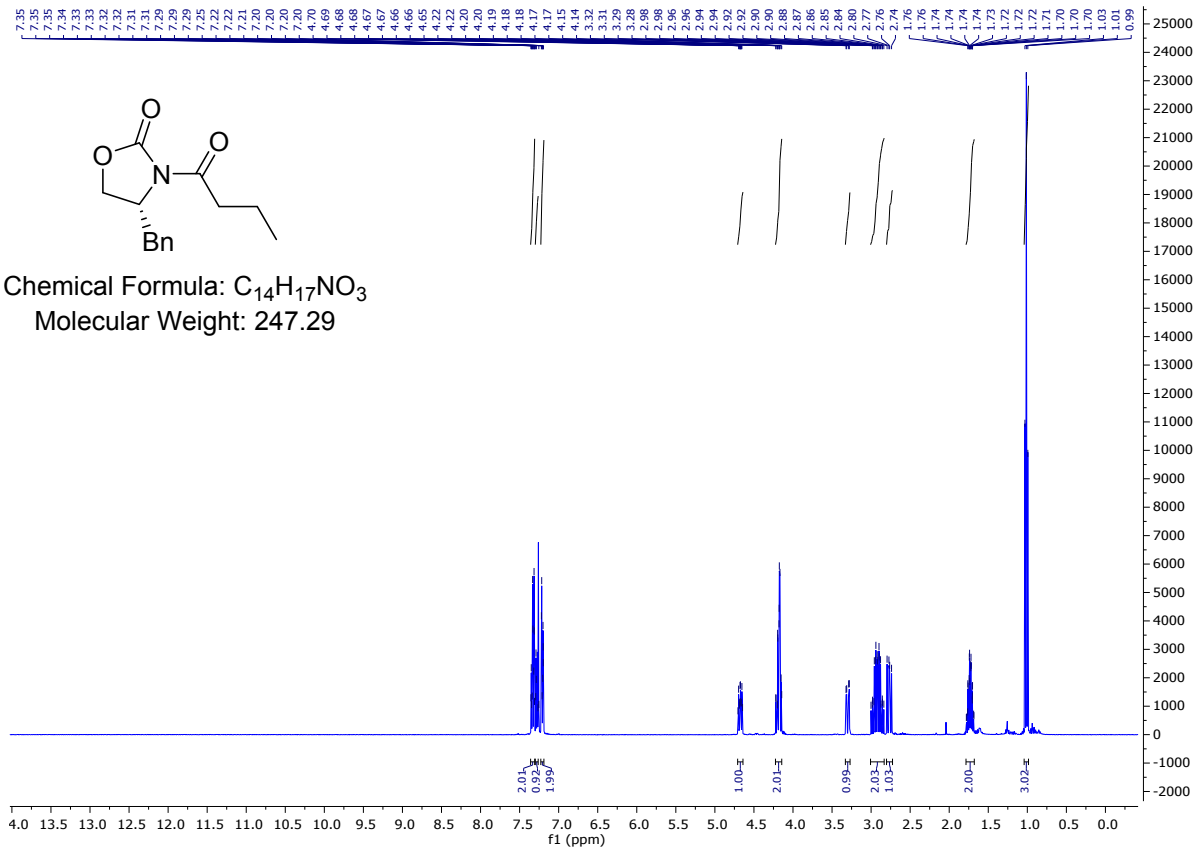

Chemical Formula: $C_{14}H_{17}NO_3$
Molecular Weight: 247.29

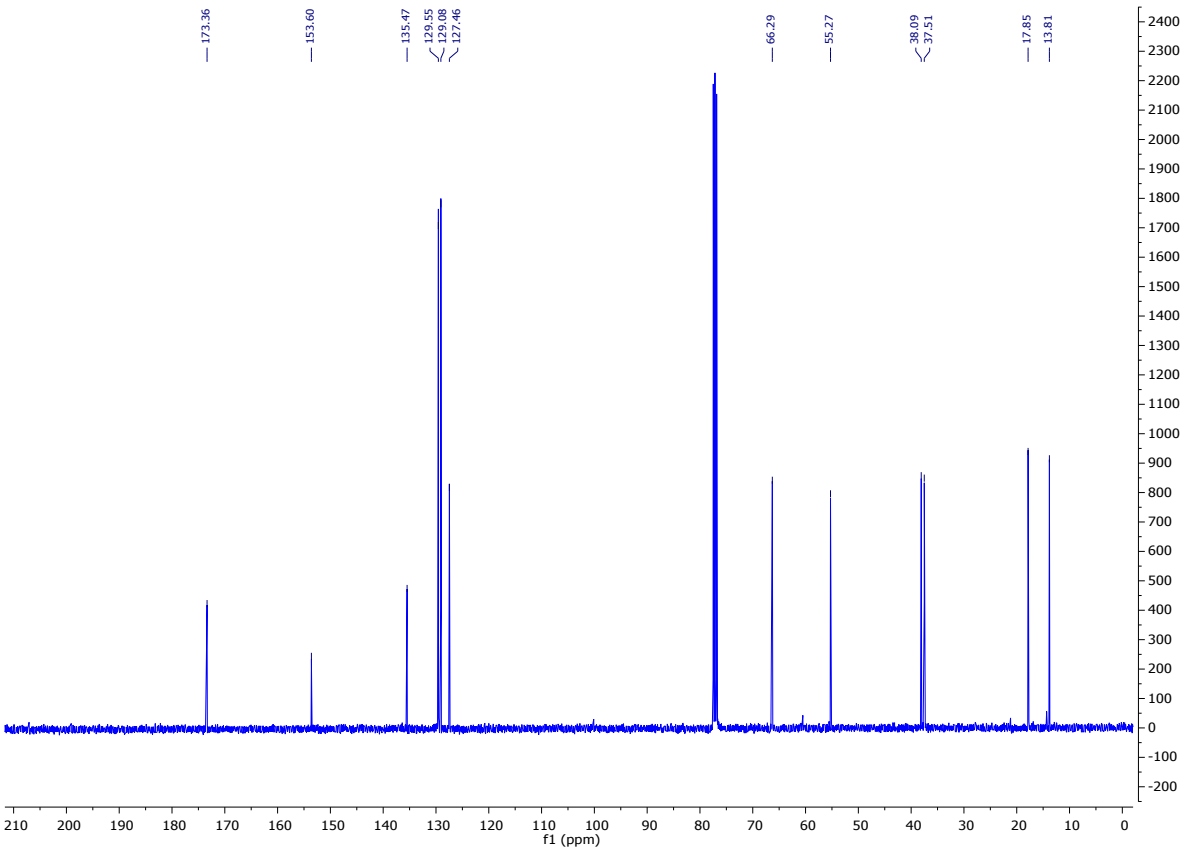

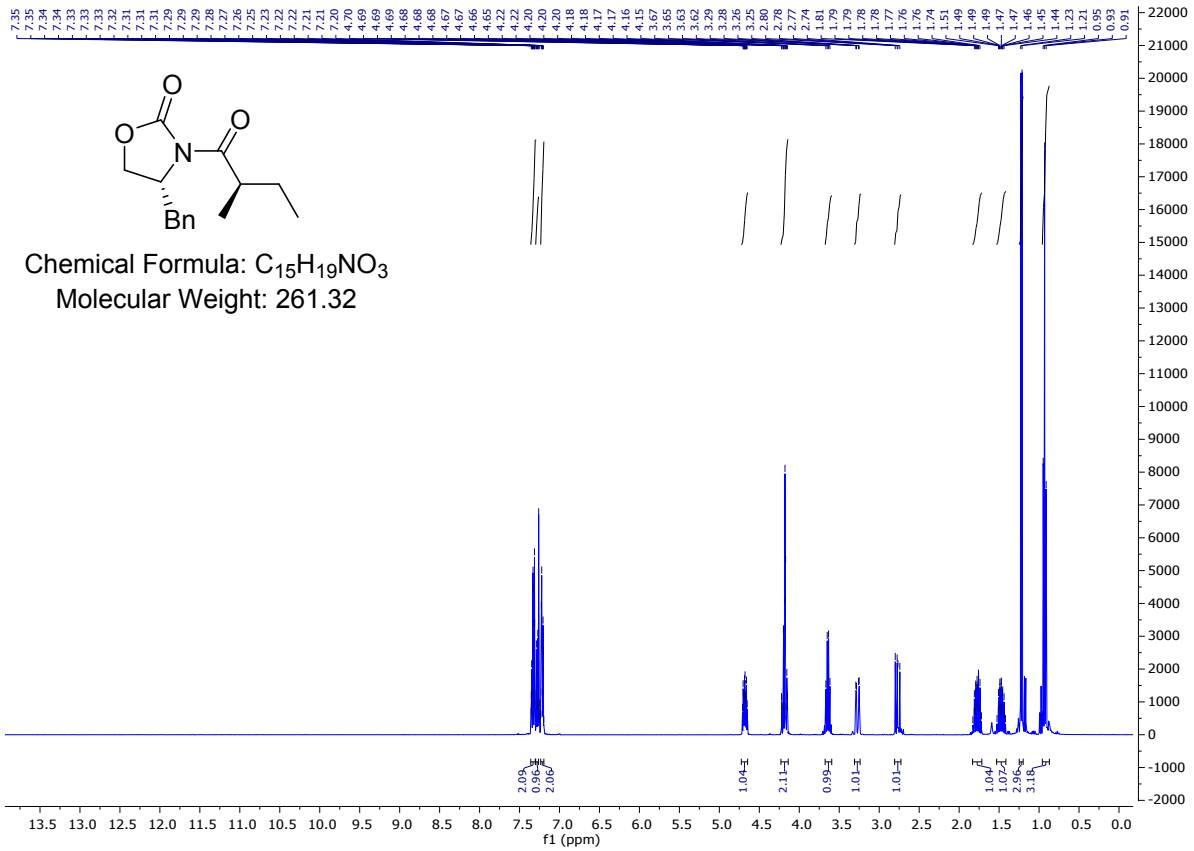

Chemical Formula: $C_{15}H_{19}NO_3$
Molecular Weight: 261.32

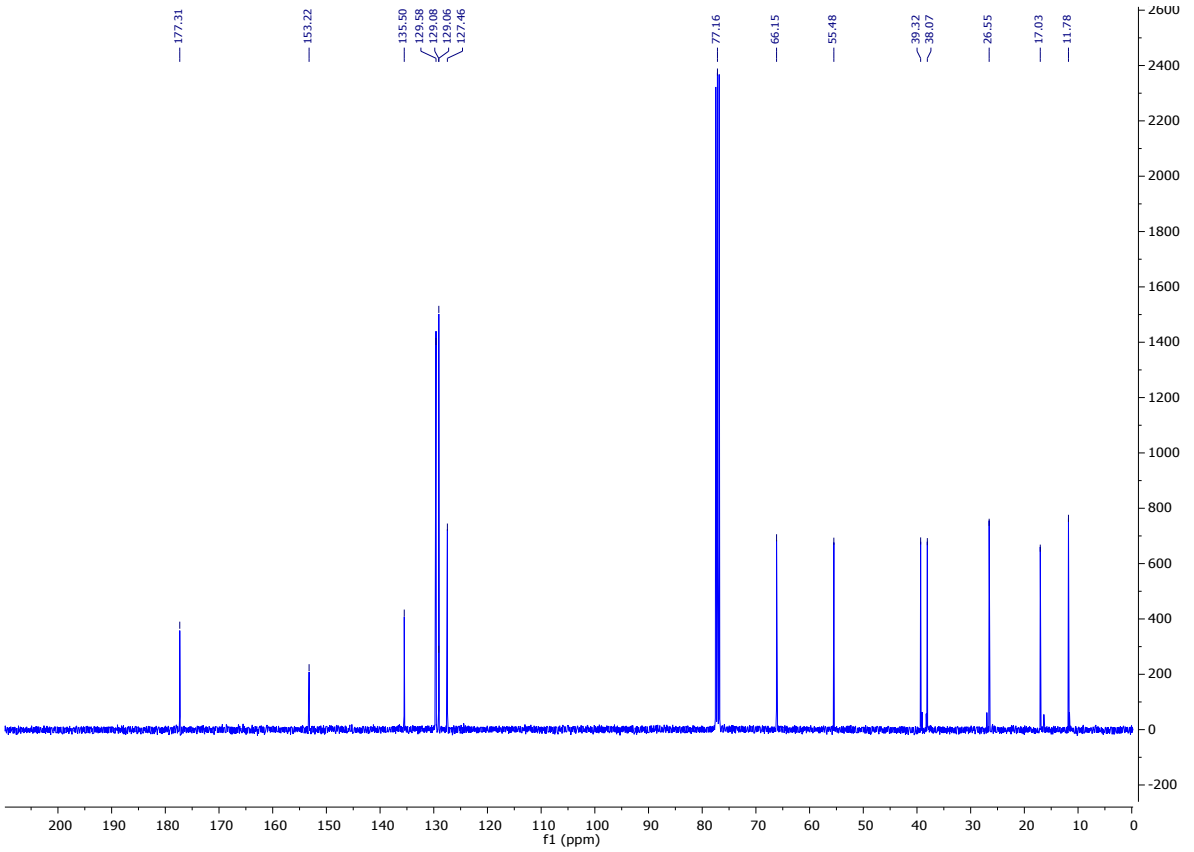

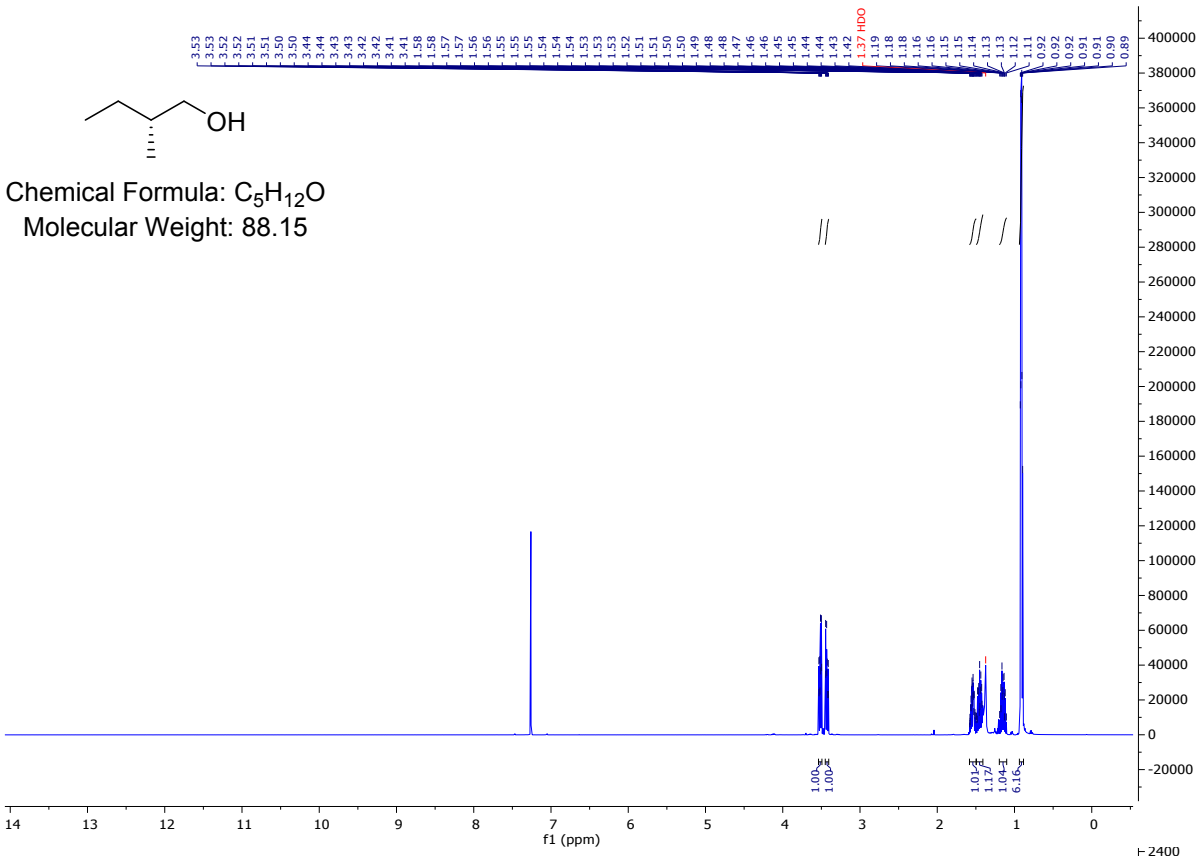

Chemical Formula: $C_5H_{12}O$
Molecular Weight: 88.15

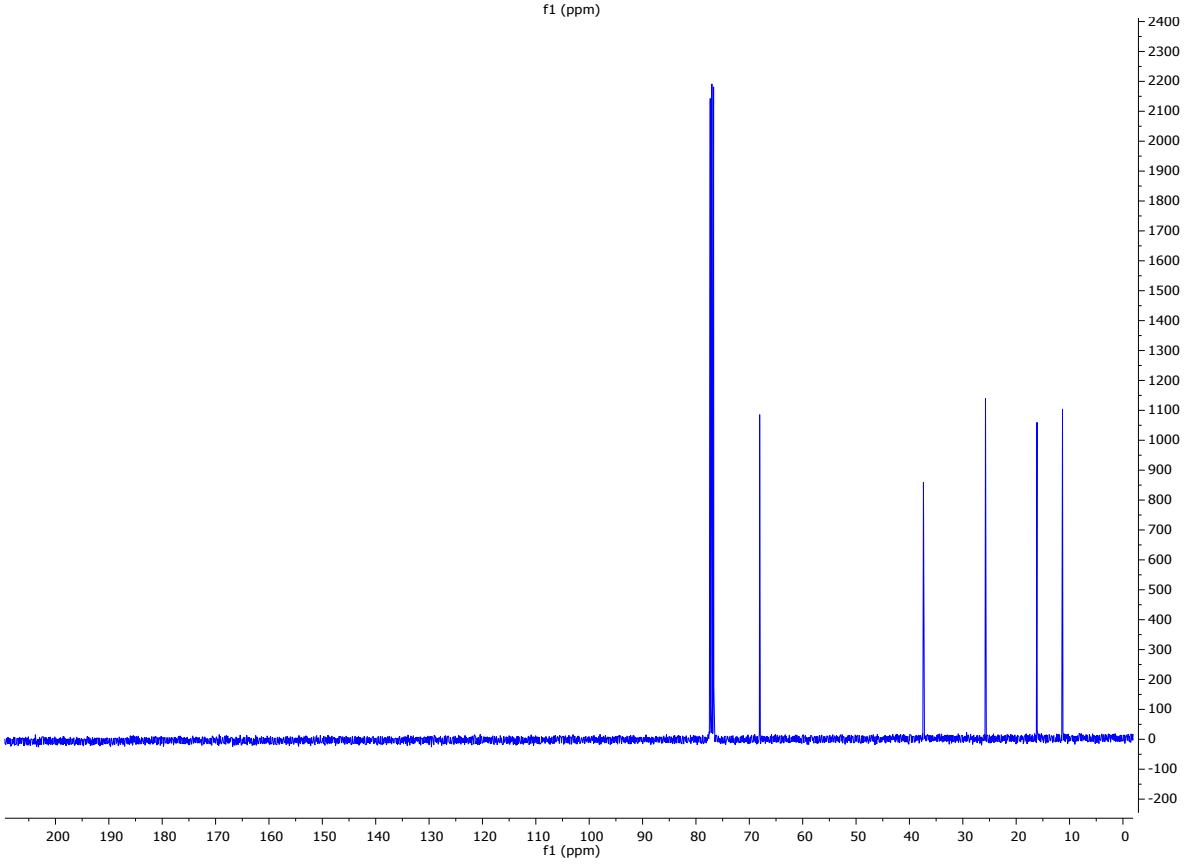

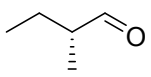

Chemical Formula: $C_5H_{10}O$
Molecular Weight: 86.13

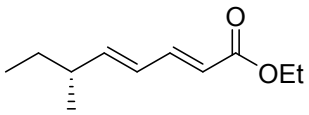

Chemical Formula: $C_{11}H_{18}O_2$
Molecular Weight: 182.26

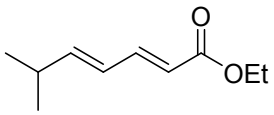

Chemical Formula: $C_{10}H_{16}O_2$
Molecular Weight: 168.24

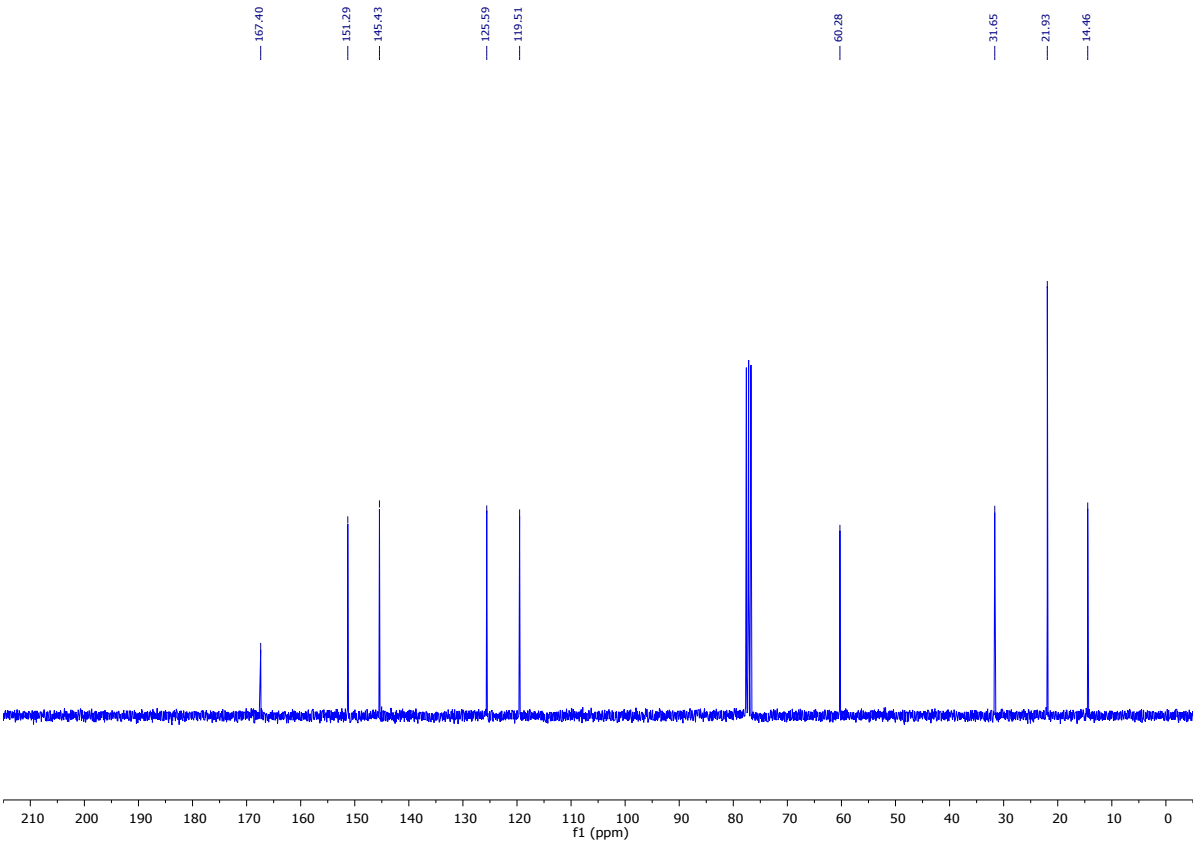

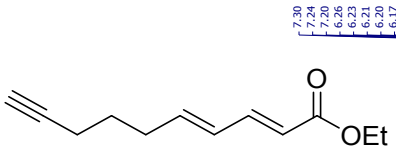

Chemical Formula: $C_{12}H_{16}O_2$
Molecular Weight: 192.26

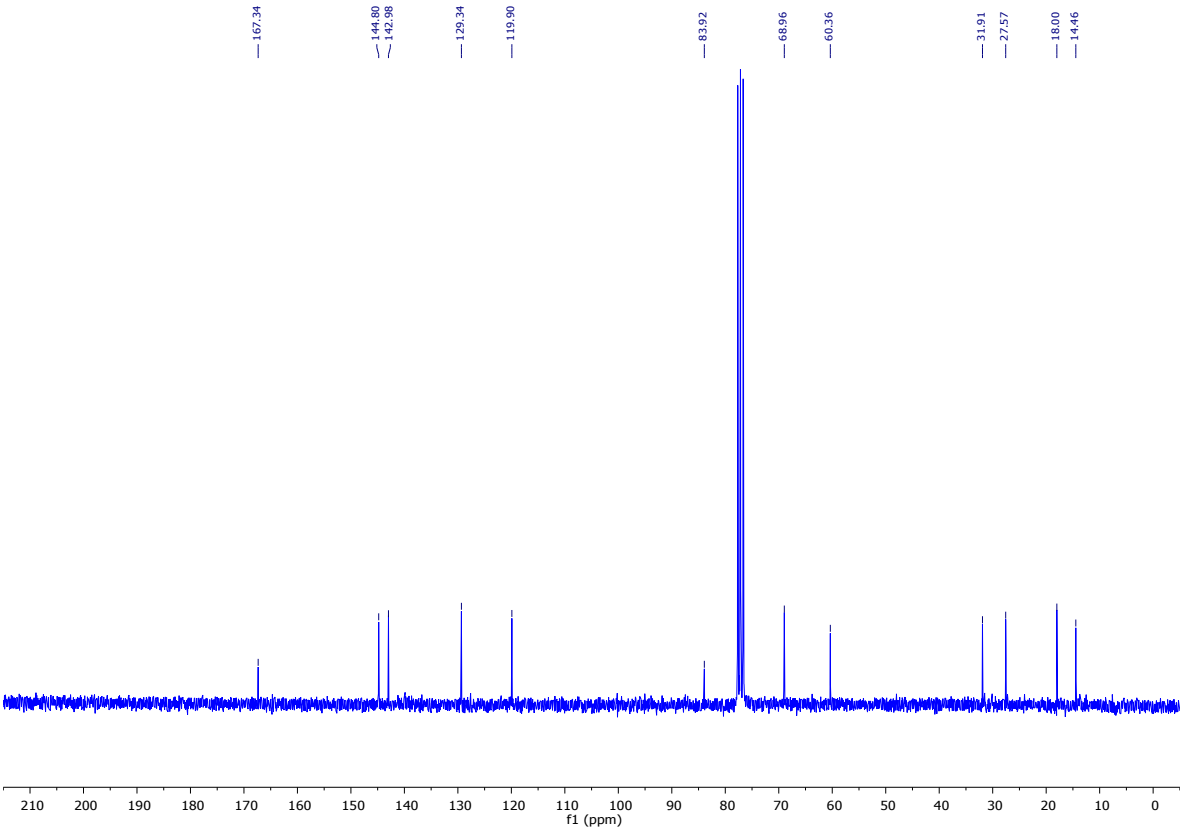

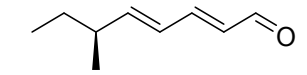

Chemical Formula: $C_9H_{14}O$
Molecular Weight: 138.21

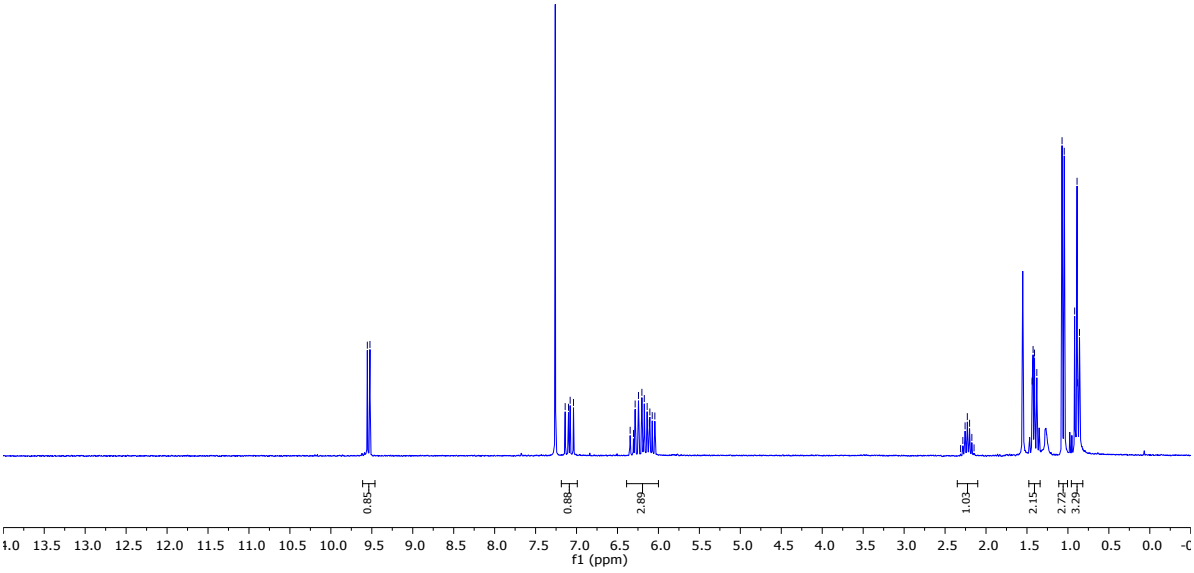

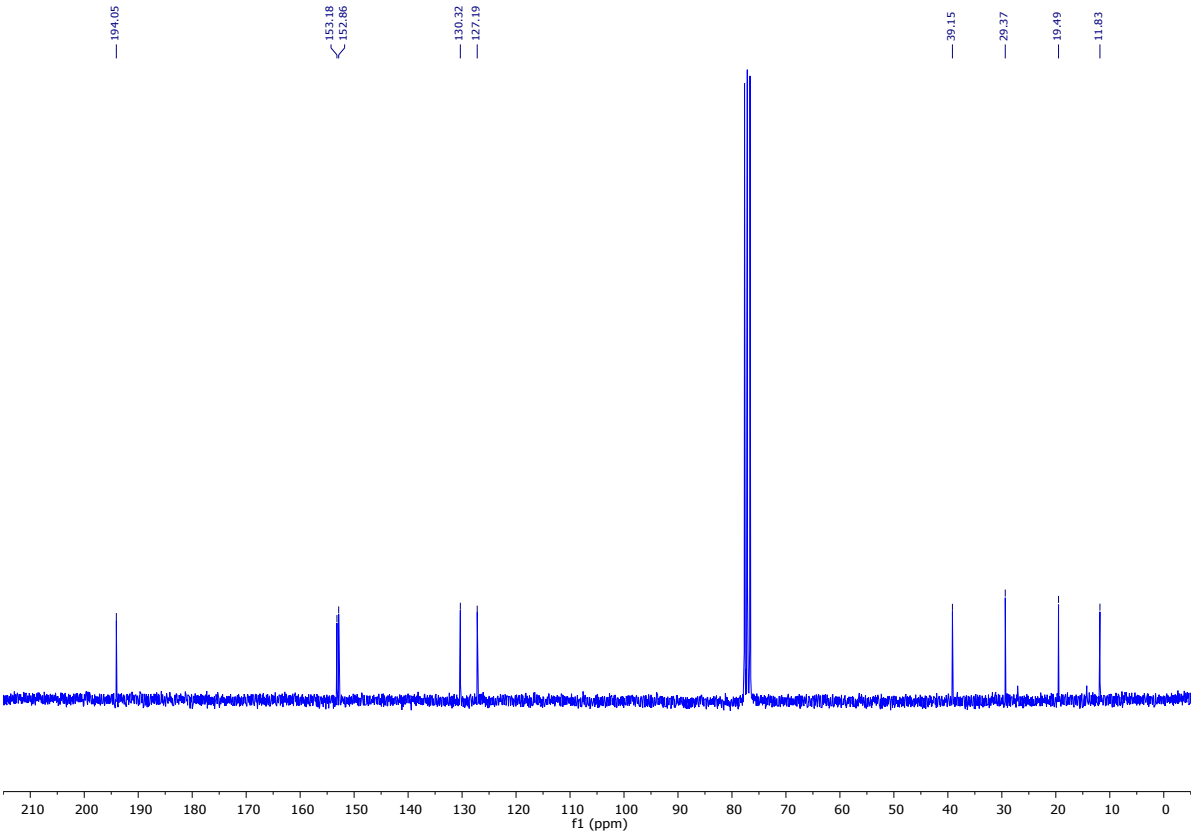

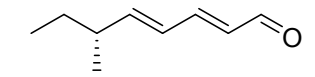

Chemical Formula: $C_9H_{14}O$
Molecular Weight: 138.21

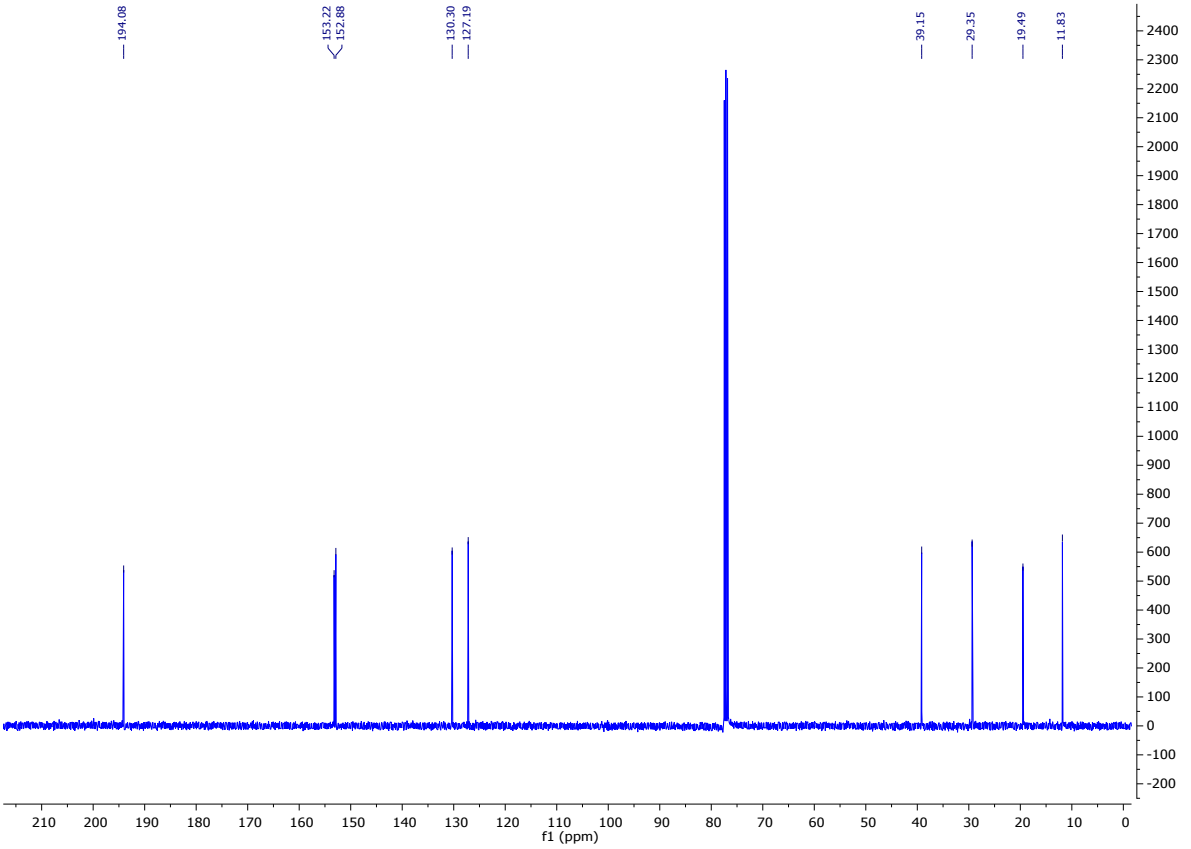

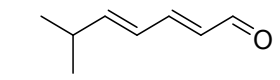

Chemical Formula: $C_8H_{12}O$
Molecular Weight: 124.18

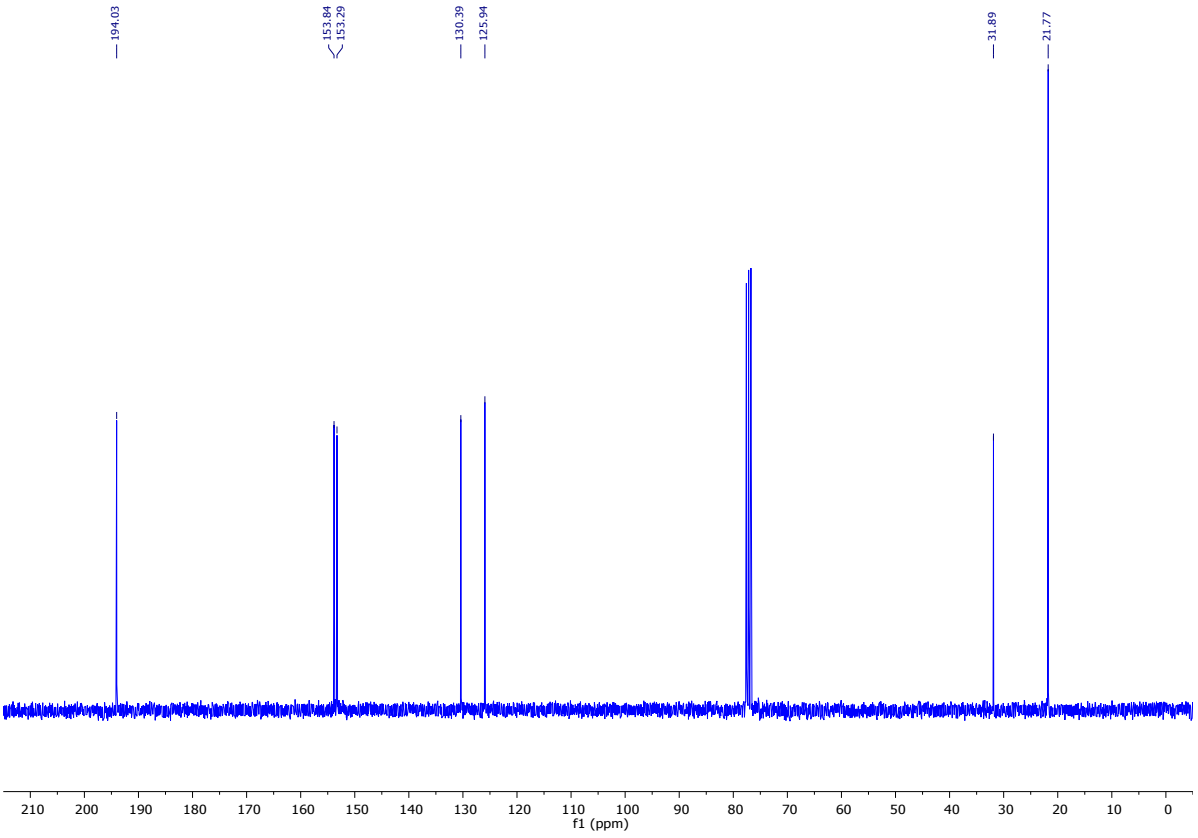

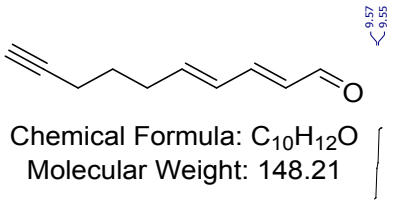

Chemical Formula: $C_{10}H_{12}O$
Molecular Weight: 148.21

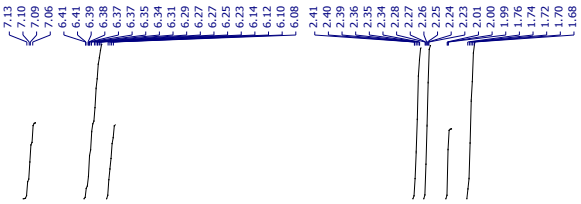

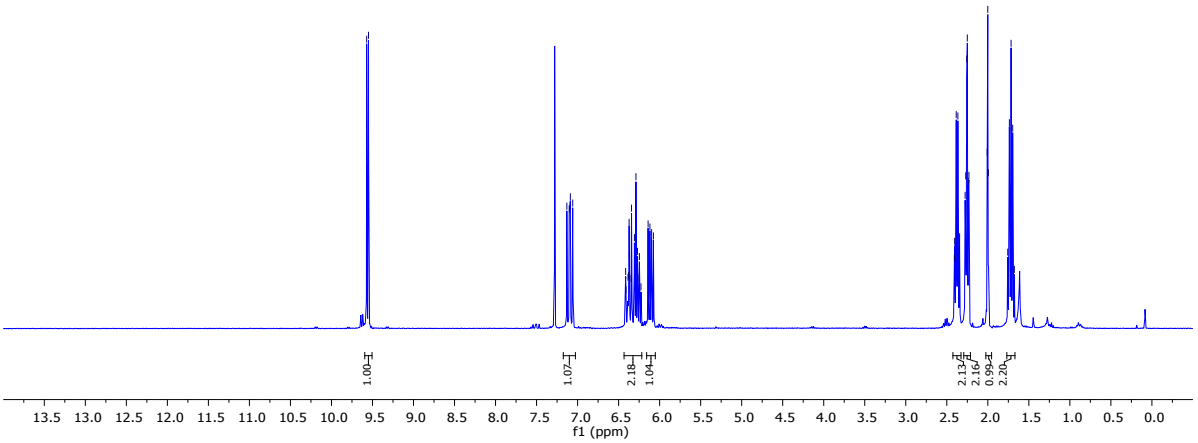

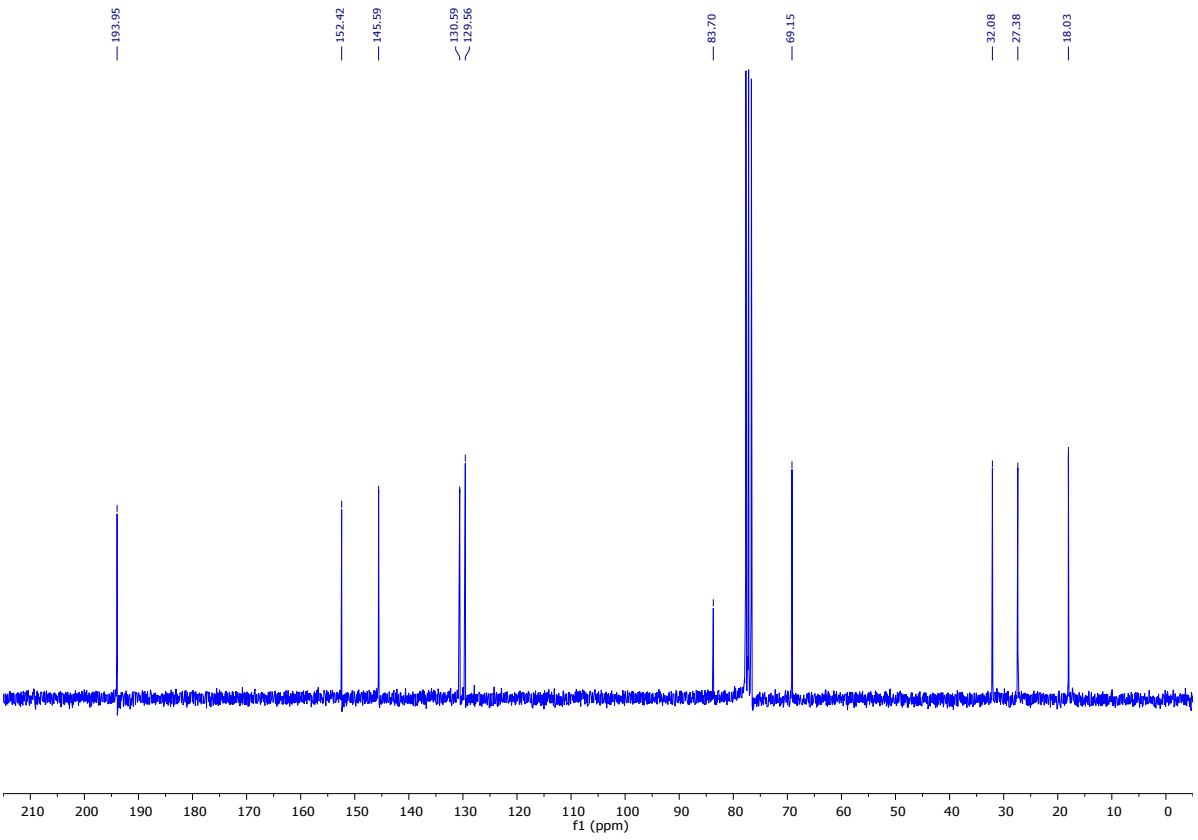

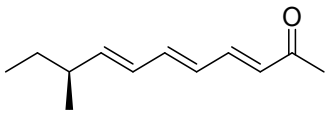

Chemical Formula: $C_{12}H_{18}O$
Molecular Weight: 178.28

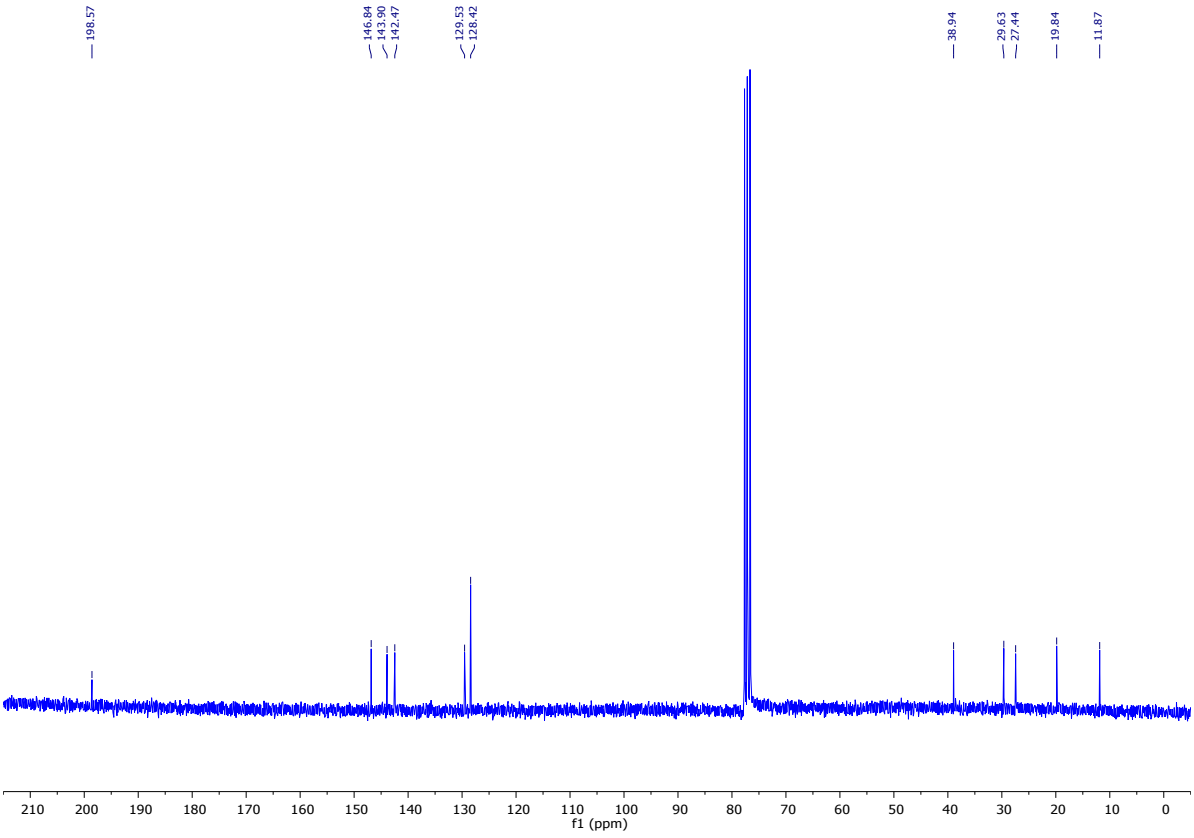

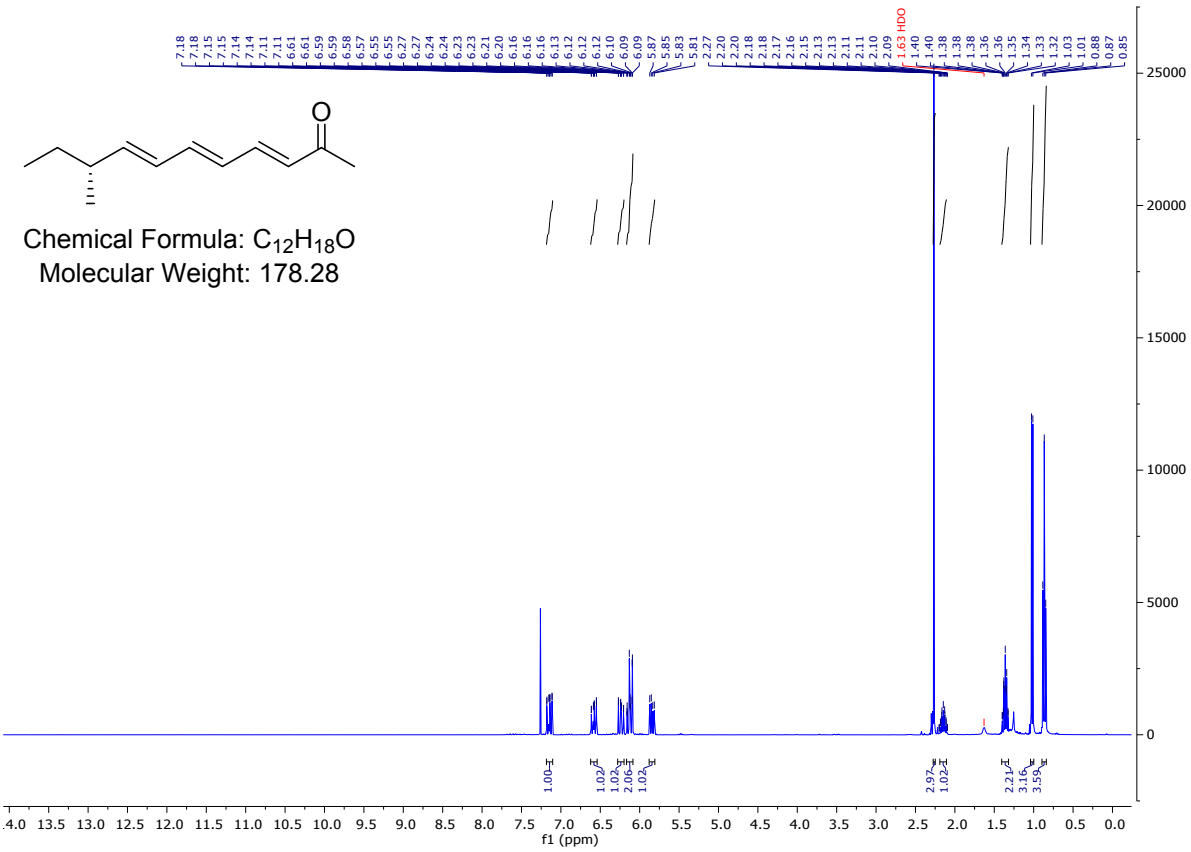
O
Chemical Formula: $C_{12}H_{18}O$
Molecular Weight: 178.28
1.63 HDO
f1 (ppm)

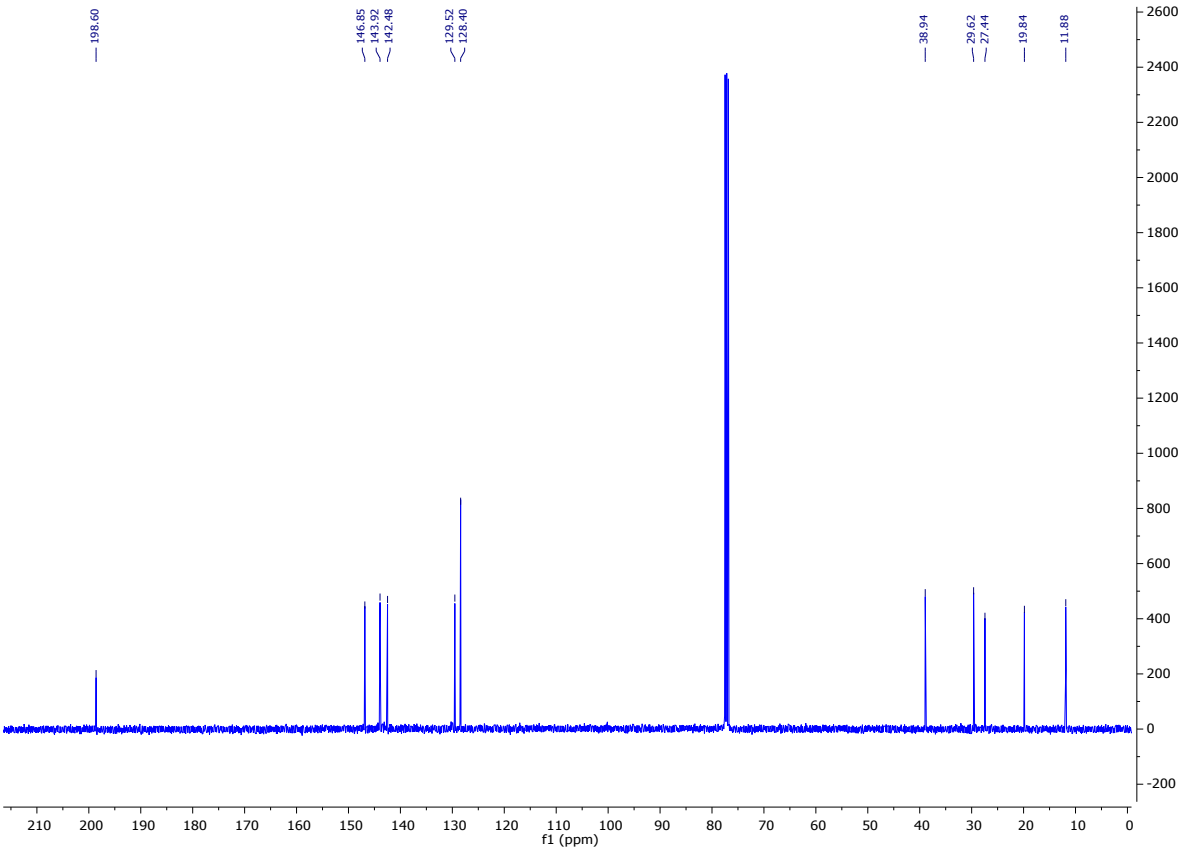
198.60
146.85
143.92
142.48
129.52
128.40
38.94
29.62
27.44
19.84
11.88
f1 (ppm)

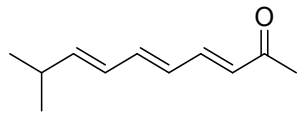

Chemical Formula: $C_{11}H_{16}O$
Molecular Weight: 164.25

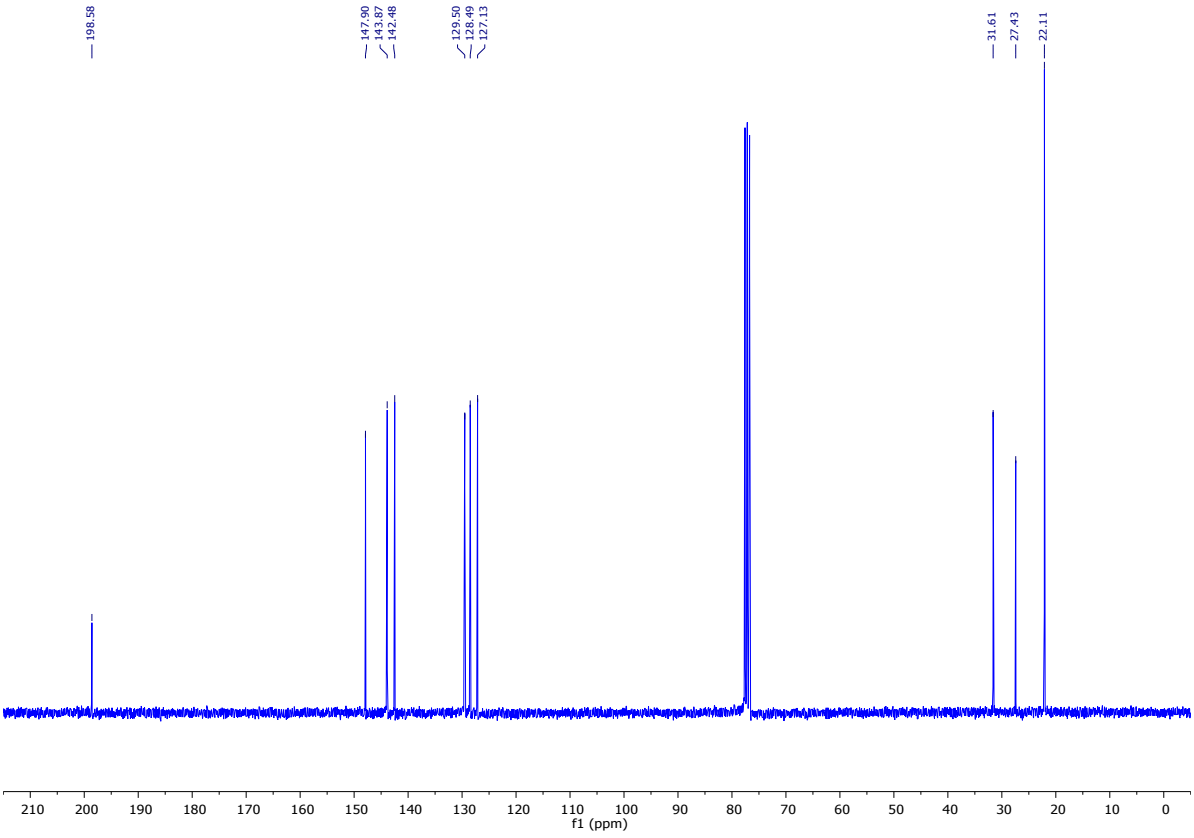

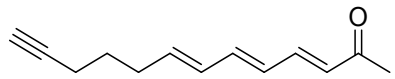

Chemical Formula: $C_{13}H_{16}O$
Molecular Weight: 188.27

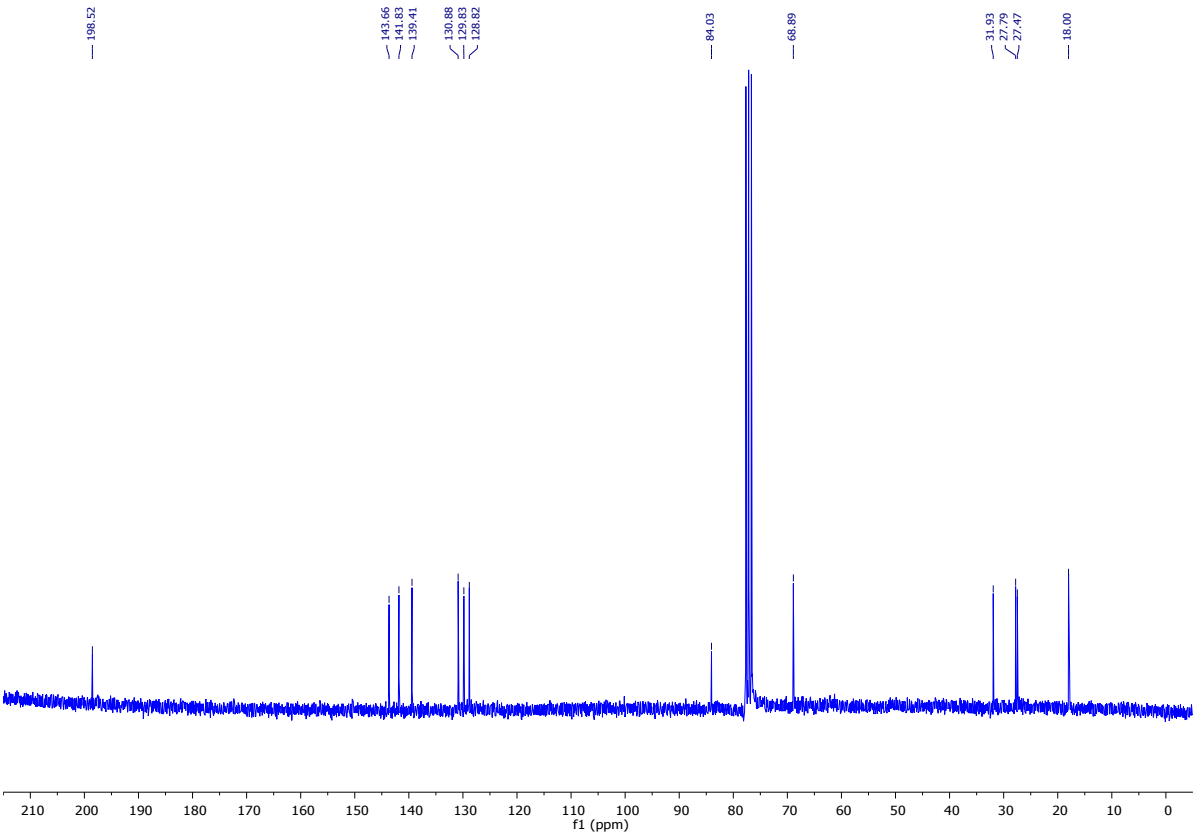

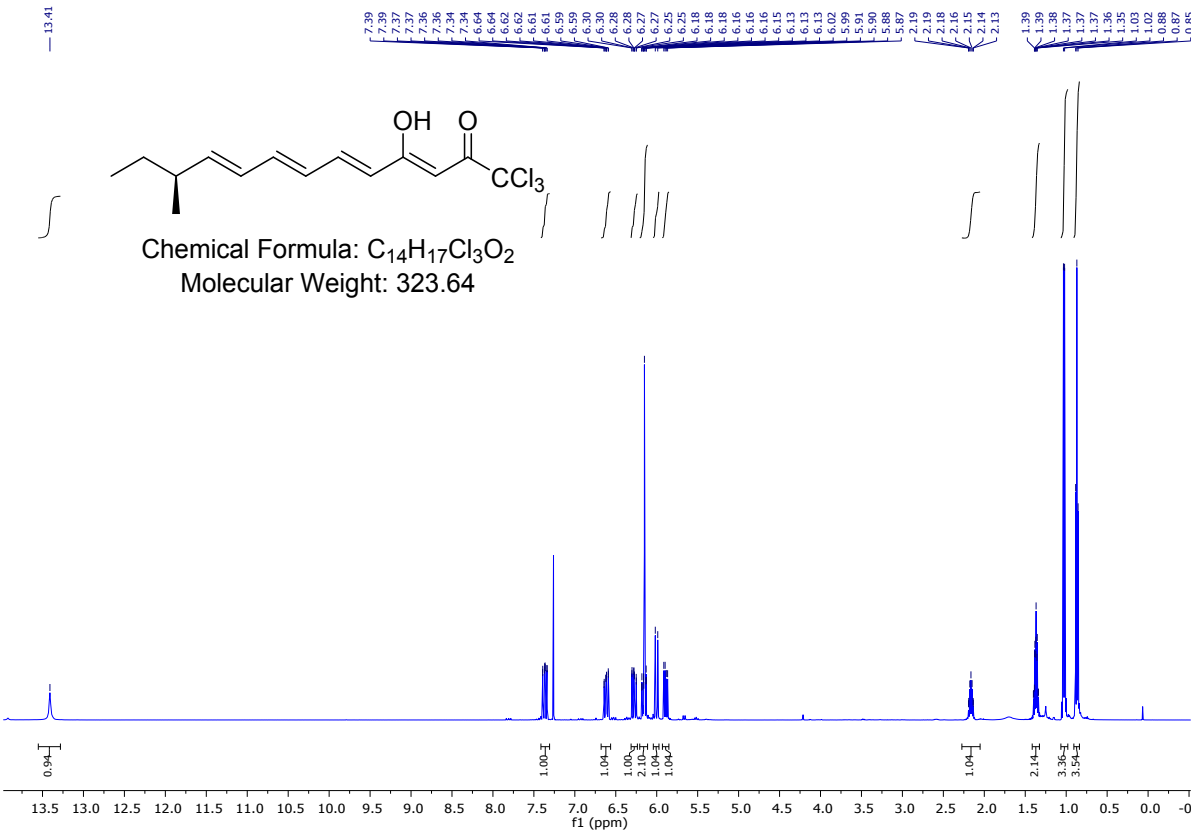

Chemical Formula: $C_{14}H_{17}Cl_3O_2$
Molecular Weight: 323.64

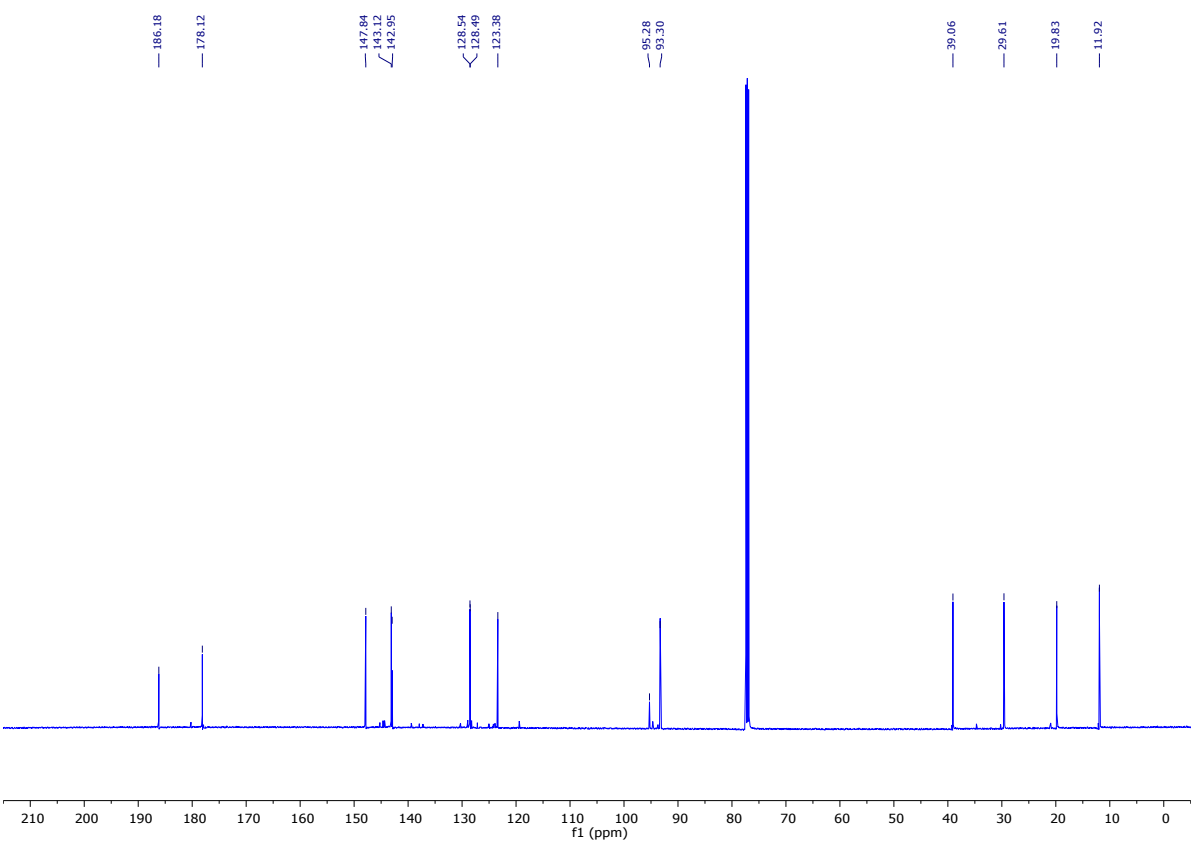

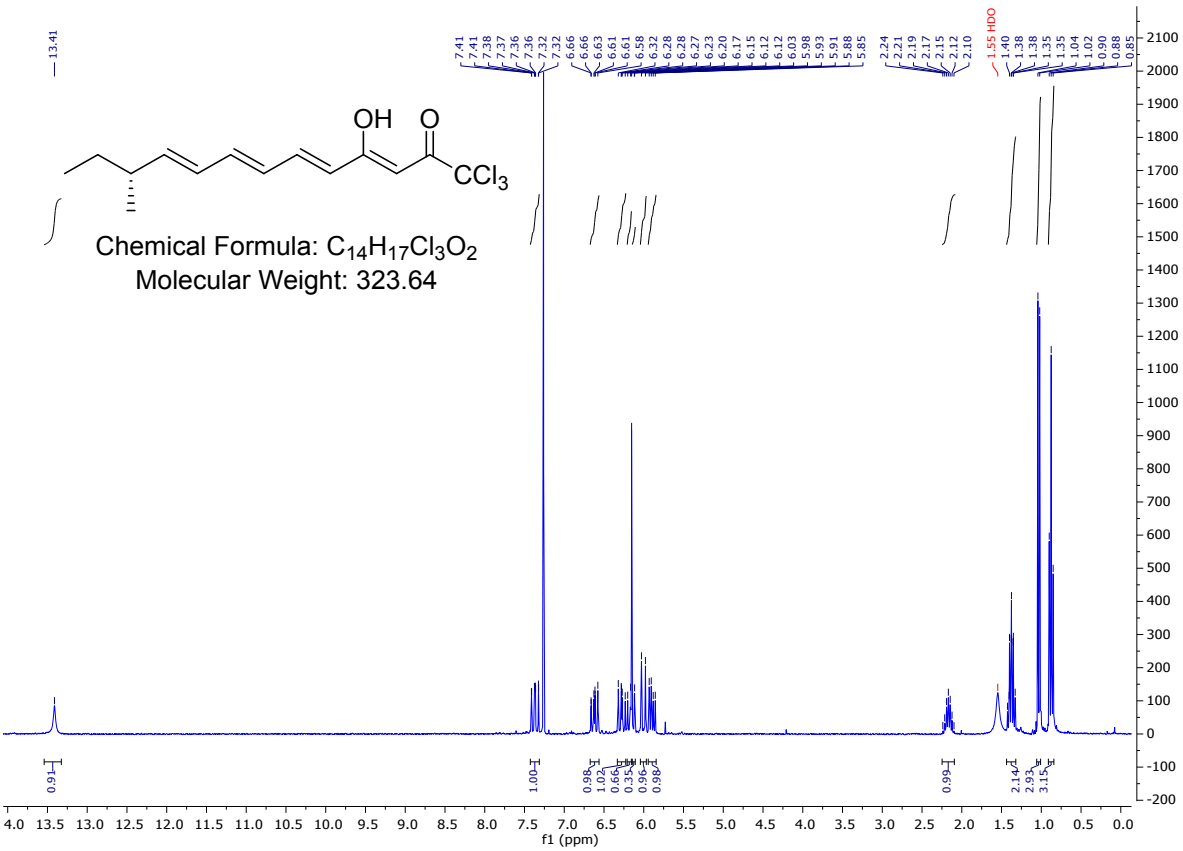
OH
O
CCl3
Chemical Formula: C14H17Cl3O2
Molecular Weight: 323.64
f1 (ppm)

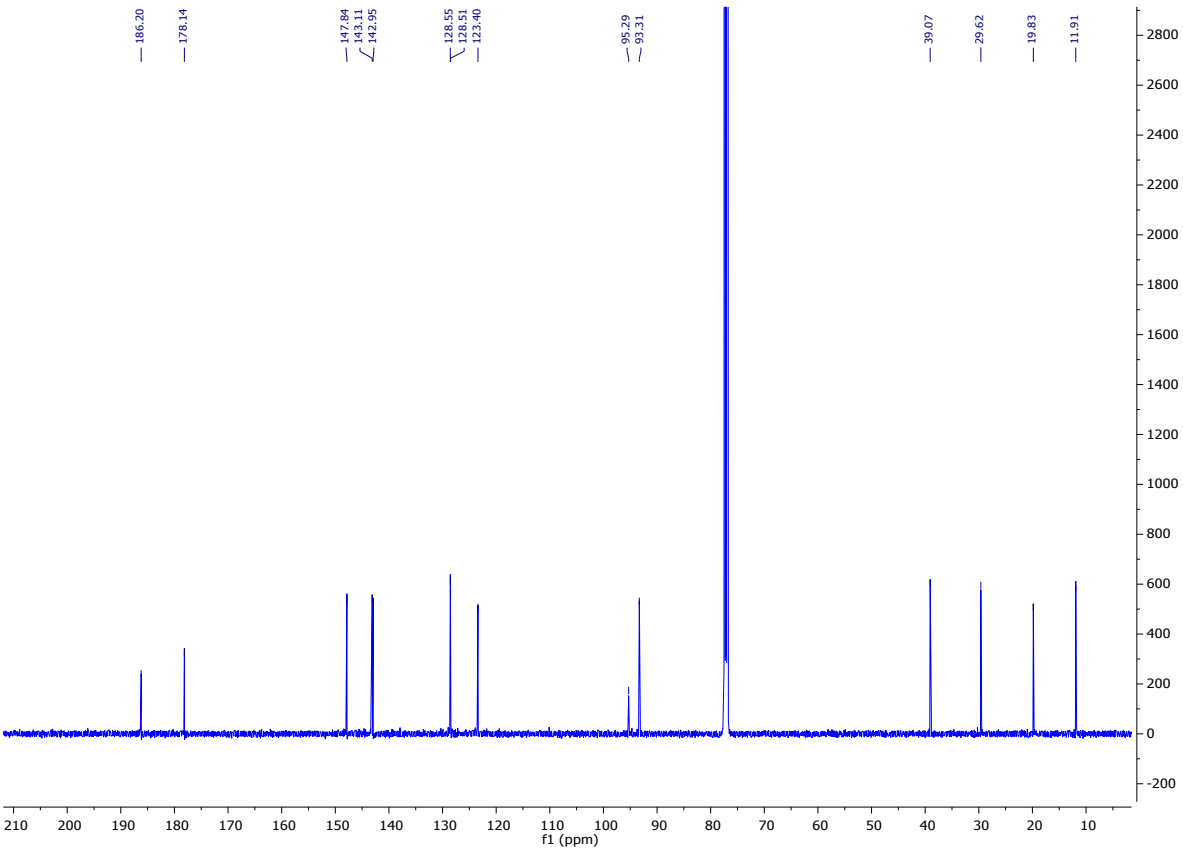
f1 (ppm)

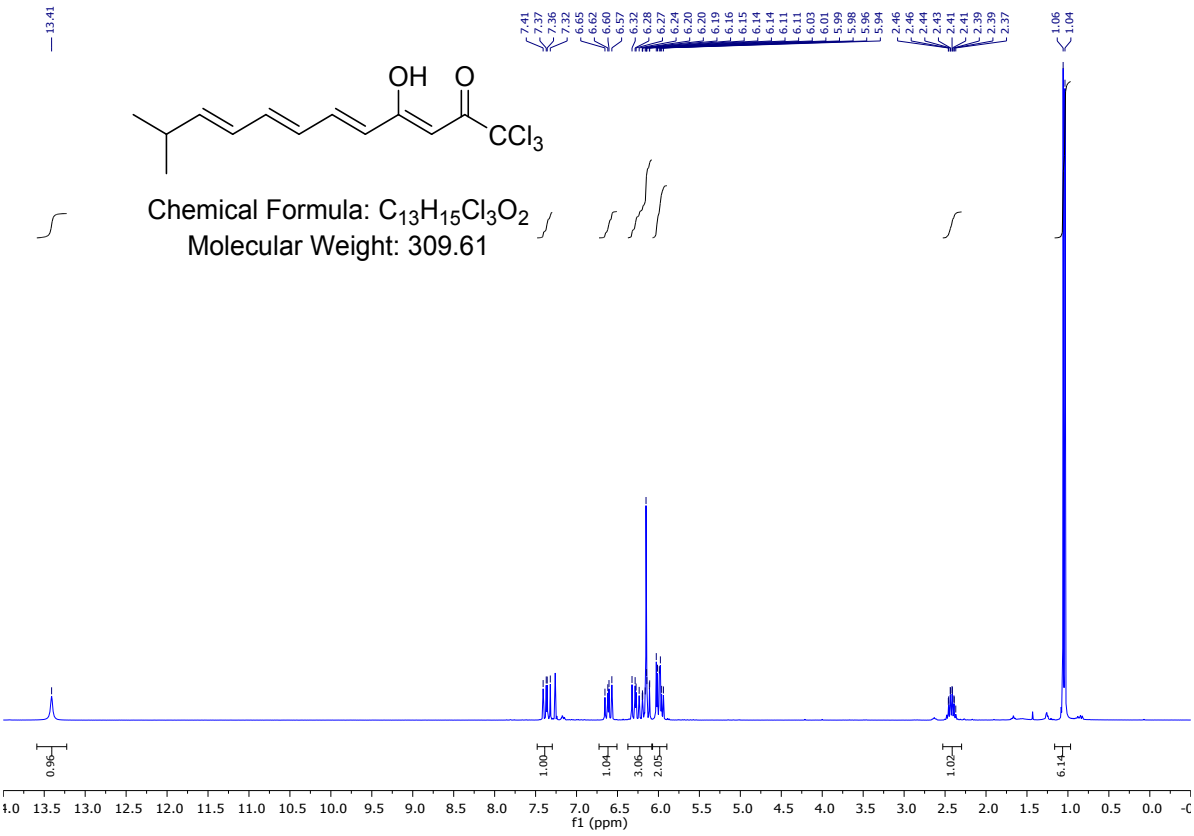
OH
O
CCl3
Chemical Formula: C13H15Cl3O2
Molecular Weight: 309.61
f1 (ppm)

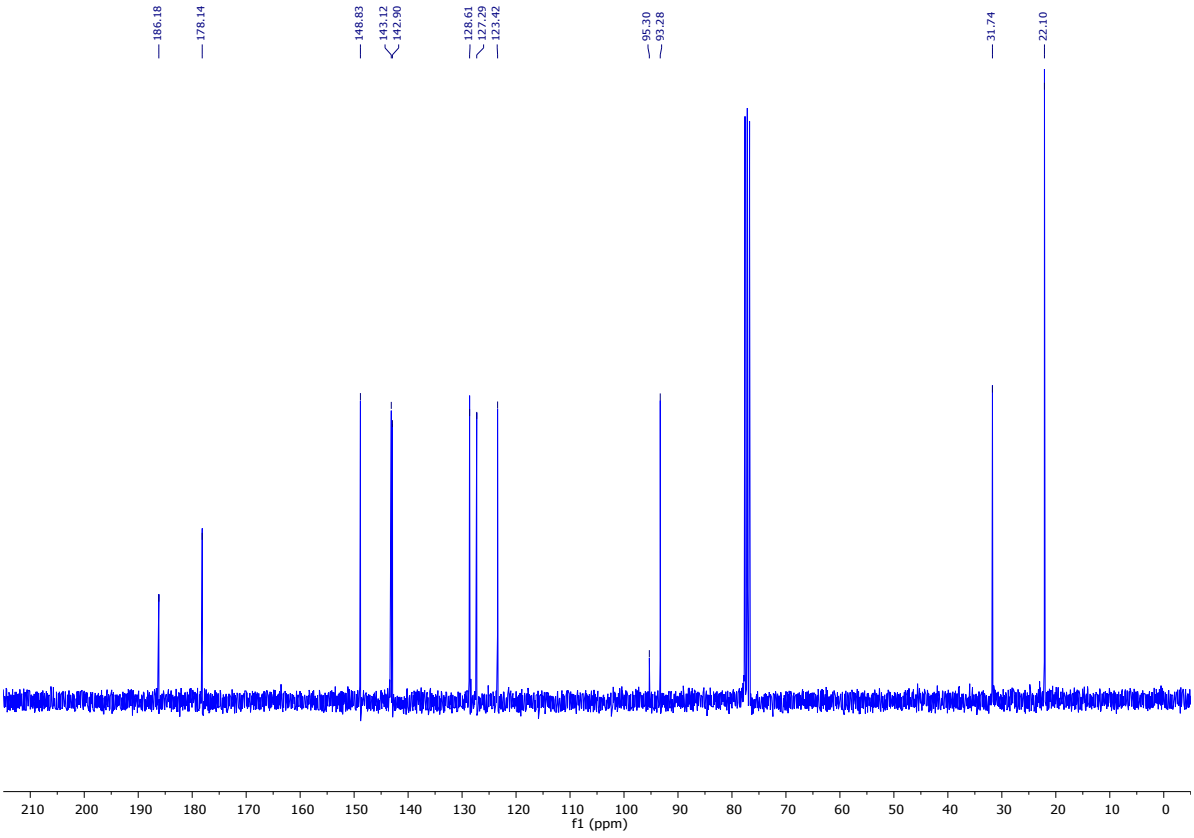
f1 (ppm)

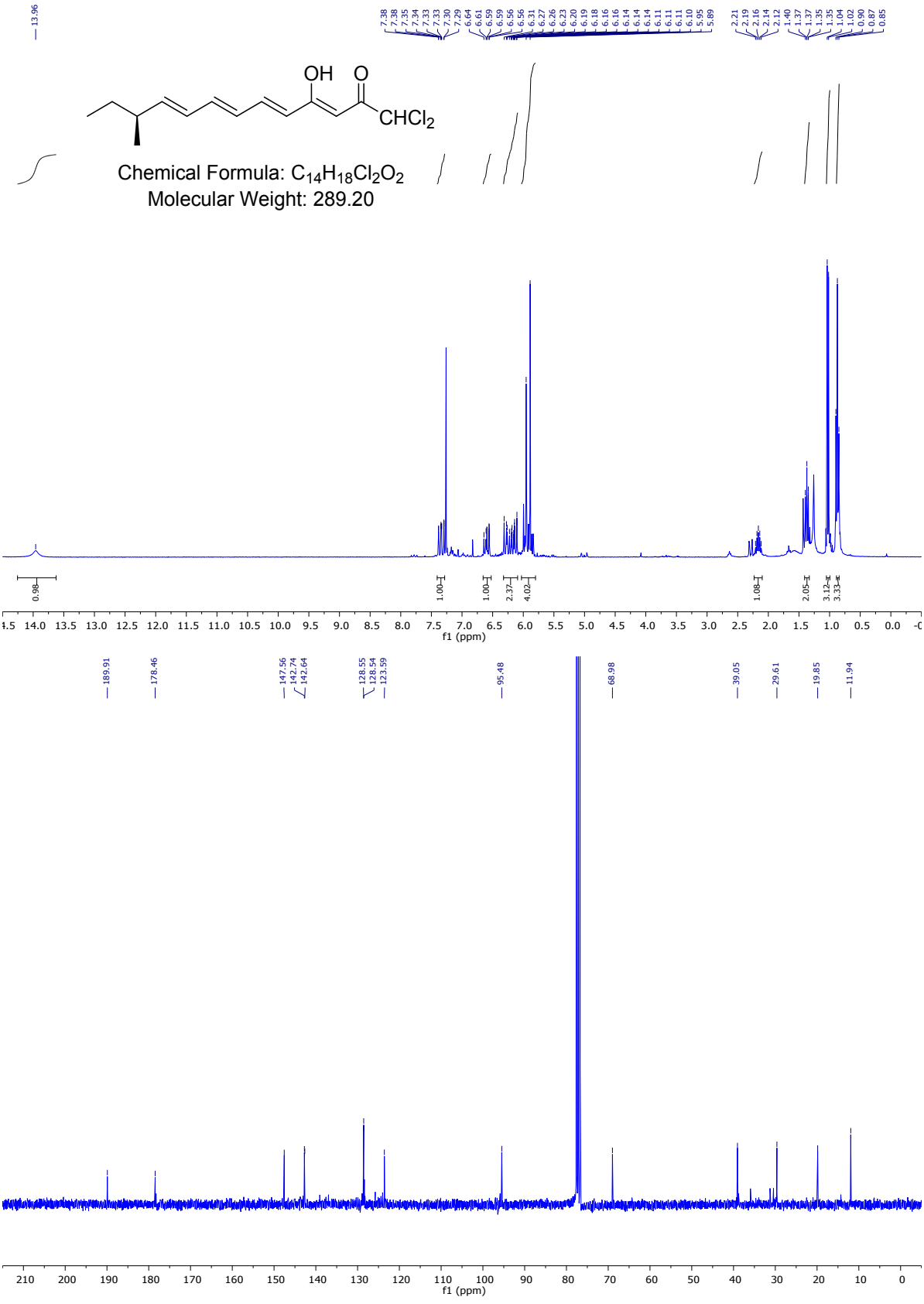
OH
O
CHCl2
Chemical Formula: C14H18Cl2O2
Molecular Weight: 289.20
f1 (ppm)
f1 (ppm)

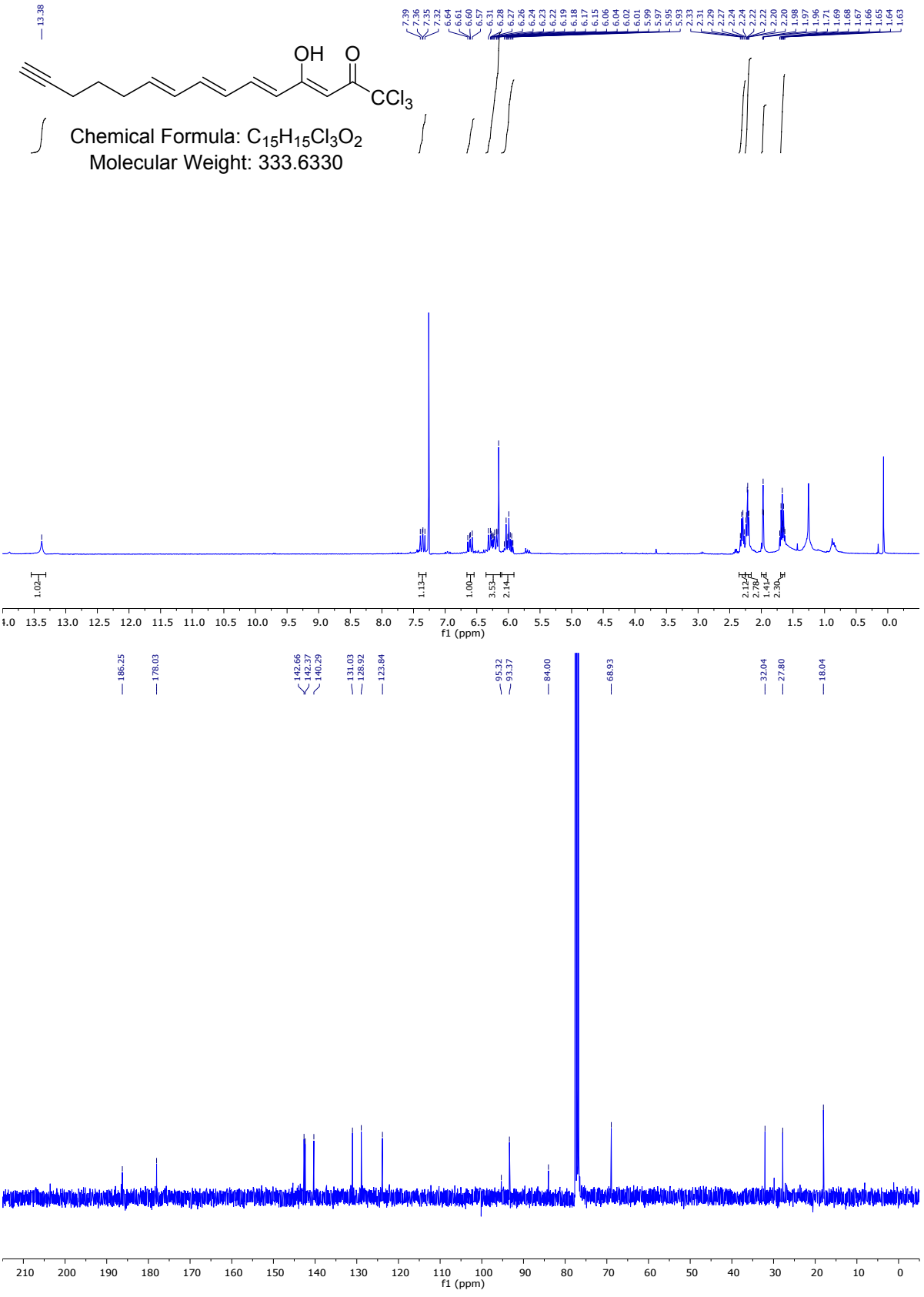
OH
O
CCl3
Chemical Formula: C15H15Cl3O2
Molecular Weight: 333.6330
f1 (ppm)
f1 (ppm)

7. Safety statement

All operations conducted were performed according to standard laboratory safety rules. No unexpected or unusually high safety hazards were encountered.

8. Supplementary references

1. Riccardi, C.; Nicoletti, I., Analysis of apoptosis by propidium iodide staining and flow cytometry. *Nat. Protoc.* **2006,** *1* (3), 1458-1461.
2. Kleiner, P.; Heydenreuter, W.; Stahl, M.; Korotkov, V. S.; Sieber, S. A., A whole proteome inventory of background photocrosslinker binding. *Angew. Chem. Int. Ed. Engl.* **2017,** *56* (5), 1396-1401.
3. Keilhauer, E. C.; Hein, M. Y.; Mann, M., Accurate protein complex retrieval by affinity enrichment mass spectrometry (AE-MS) rather than affinity purification mass spectrometry (AP-MS). *Mol. Cell. Proteomics* **2015,** *14* (1), 120-135.
4. Fux, A.; Korotkov, V. S.; Schneider, M.; Antes, I.; Sieber, S. A., Chemical cross-linking enables drafting ClpXP proximity maps and taking snapshots of in situ interaction networks. *Cell Chem. Biol.* **2019,** *26* (1), 48-59 e7.
5. Rappsilber, J.; Mann, M.; Ishihama, Y., Protocol for micro-purification, enrichment, pre-fractionation and storage of peptides for proteomics using StageTips. *Nat. Protoc.* **2007,** *2* (8), 1896-1906.
6. Cox, J.; Neuhauser, N.; Michalski, A.; Scheltema, R. A.; Olsen, J. V.; Mann, M., Andromeda: a peptide search engine integrated into the MaxQuant environment. *J. Proteome Res.* **2011,** *10* (4), 1794-1805.
7. Cox, J.; Hein, M. Y.; Luber, C. A.; Paron, I.; Nagaraj, N.; Mann, M., Accurate proteome-wide label-free quantification by delayed normalization and maximal peptide ratio extraction, termed MaxLFQ. *Mol. Cell. Proteomics* **2014,** *13* (9), 2513-2526.
8. Vizcaino, J. A.; Deutsch, E. W.; Wang, R.; Csordas, A.; Reisinger, F.; Rios, D.; Dianes, J. A.; Sun, Z.; Farrah, T.; Bandeira, N.; Binz, P. A.; Xenarios, I.; Eisenacher, M.; Mayer, G.; Gatto, L.; Campos, A.; Chalkley, R. J.; Kraus, H. J.; Albar, J. P.; Martinez-Bartolome, S.; Apweiler, R.; Omenn, G. S.; Martens, L.; Jones, A. R.; Hermjakob, H., ProteomeXchange provides globally coordinated proteomics data submission and dissemination. *Nat. Biotechnol.* **2014,** *32* (3), 223-226.
9. Vizcaino, J. A.; Csordas, A.; Del-Toro, N.; Dianes, J. A.; Griss, J.; Lavidas, I.; Mayer, G.; Perez-Riverol, Y.; Reisinger, F.; Ternent, T.; Xu, Q. W.; Wang, R.; Hermjakob, H., 2016 update of the PRIDE database and its related tools. *Nucleic Acids Res.* **2016,** *44* (22), 11033.
10. Tyanova, S.; Temu, T.; Sinitcyn, P.; Carlson, A.; Hein, M. Y.; Geiger, T.; Mann, M.; Cox, J., The Perseus computational platform for comprehensive analysis of (prote)omics data. *Nat. Methods* **2016,** *13* (9), 731-740.
11. Shannon, P.; Markiel, A.; Ozier, O.; Baliga, N. S.; Wang, J. T.; Ramage, D.; Amin, N.; Schwikowski, B.; Ideker, T., Cytoscape: a software environment for integrated models of biomolecular interaction networks. *Genome Res.* **2003,** *13* (11), 2498-2504.
12. Maere, S.; Heymans, K.; Kuiper, M., BiNGO: a Cytoscape plugin to assess overrepresentation of gene ontology categories in biological networks. *Bioinformatics* **2005,** *21* (16), 3448-3449.
13. Braig, S.; Bischoff, F.; Abhari, B. A.; Meijer, L.; Fulda, S.; Skaltsounis, L.; Vollmar, A. M., The pleiotropic profile of the indirubin derivative 6BIO overcomes TRAIL resistance in cancer. *Biochem. Pharmacol.* **2014,** *91* (2), 157-167.
14. Ran, F. A.; Hsu, P. D.; Wright, J.; Agarwala, V.; Scott, D. A.; Zhang, F., Genome engineering using the CRISPR-Cas9 system. *Nat. Protoc.* **2013,** *8* (11), 2281-2308.
15. Haeussler, M.; Schonig, K.; Eckert, H.; Eschstruth, A.; Mianne, J.; Renaud, J. B.; Schneider-Maunoury, S.; Shkumatava, A.; Teboul, L.; Kent, J.; Joly, J. S.; Concordet, J. P., Evaluation of off-target and on-target scoring algorithms and integration into the guide RNA selection tool CRISPOR. *Genome Biol.* **2016,** *17* (1), 148.